HITIT JOURNAL OF SCIENCE

HİTİT JOURNAL OF SCIENCE

LANGUAGE OF PUBLICATION
English

HAKEM KURULU | REFEREE BOARD

Hitit Medical Journal Dergisi, çift taraflı kör hakemlik sistemi kullanmaktadır. Hakem isimleri gizli tutulmakta ve yayımlanmamaktadır.

Hitit Medical Journal uses a double-blind review. Referee names are kept strictly confidential.

BOARD OF EDITORS

Editörden

Değerli Okuyucular;

Hitit Journal of Science ilk sayısı ile sizlerle buluşmaktan büyük bir mutluluk duyuyoruz. Dergimize olan ilgi ve destek için teşekkür ederiz.

Dergimizde, Temel Bilimler (Fizik, Kimya, Biyoloji ve Matematik) alanında kapsamlı ve çeşitli makaleler yayımlamaya özen gösteriyoruz. Bu sayıda da bilim dünyasına katkı sağlayacak 4'ü araştırma makalesi olmak üzere toplam 5 makaleyi siz değerli okuyucularımızla paylaşmanın gururunu yaşıyoruz.

Tüm okuyucularımıza keyili ve verimli okumalar diliyoruz.

Saygılarımızla,

Prof. Dr. Dursun Ali KÖSE
HJS Editöryal Kurul adına

From the Editor

Dear Readers;
We are very pleased to meet you with the first issue of Hitit Journal of Science. Thank you for your interest and support to our magazine.
In our journal, we take care to publish comprehensive and diverse articles in the field of Basic Sciences (Physics, Chemistry, Biology and Mathematics). In this issue, we are proud to share with you, our valued readers, a total of 5 articles, 4 of which are research articles, that will contribute to the world of science. We wish all our readers a pleasant and productive reading experience.
Regards,

Prof. Dr. Dursun Ali KÖSE
On behalf of the HJS Editorial Board

INDEX

HİTİT JOURNAL OF SCIENCE

Monoazo Dyes: Coupling Reactions between Indanone Compounds and Heterocyclic Aminothiophene-Containing Spiro Group

Naki ÇOLAK[1],[*] | Gülnihal ERTEN[1] | Aynur İZANCI[2] | Umut SANCUR[2]

[1]Department of Chemistry, Hitit University, 19030, Corum, Türkiye.
[2]Department of Molecular Biology and Genetic, Hitit University, 19030, Corum, Türkiye.

Corresponding Author
Naki ÇOLAK
E-mail: nakicolak@hitit.edu.tr Phone: +90 364 227 7000 (1634)
RORID: ror.org/01x8m3269

Cite As
Çolak N, et al. Monoazo Dyes: Coupling Reactions between Indanone Compounds and Heterocyclic Aminothiophene-Containing Spiro Group. Hitit journal of Science. 2024;1(1):1-7.

Peer Review: Evaluated by independent reviewers working in at least two different institutions appointed by the field editor.
Ethical Statement: Not available.
Plagiarism Checks: Yes - iThenticate
Conflict of Interest: Authors approve that to the best of their knowledge, there is not any conflict of interest or common interest with an institution/organization or a person that may affect the review process of the paper.

CRedit Author Statement
1st Author: Conceptualization, Methodology, Software, Validation, Writing-original draft. **2nd Author:** Data curation, Visualization, Investigation.

Monoazo Dyes: Coupling Reactions between Indanone Compounds and Heterocyclic Aminothiophene-Containing Spiro Group

Naki ÇOLAK1,* | Gülnihal ERTEN[1] | Aynur İZANCI[2] | Umut SANCUR[2]
[1]Department of Chemistry, Hitit University, 19030, Corum, Türkiye.
[2]Department of Molecular Biology and Genetic, Hitit University, 19030, Corum, Türkiye.

Abstract

In this study, 2-amino-spiro[benzo]thiophene derivatives were prepared using the Gewald method. Subsequently, monoazo dyes were synthesized via conventional diazotization method, with 2-indanone or 1,3-indandione compounds as preferred coupling components. The chemical structures of the monoazo dyes have been characterized using several spectroscopic methods (FT-IR, 1H-NMR, 13C-APT NMR). The tautomeric forms of the dyes were discussed, and it was concluded that the hydrazo form is the dominant tautomer.

Keywords: 2-Aminothiophene, Spiro[benzo]thiophene, Azo dyes, Heterocyclic components

INTRODUCTION

Primary aromatic amine compounds are used in the synthesis of diazonium compounds. Several different methods can be applied for the synthesis of aromatic diazonium compounds. The selection of the method to be applied is influenced by the solubility or basic character of primary amines. Additionally, a strong acidic environment is preferred during the reaction to prevent the formation of by-products (such as triazines, etc.)[1]. Due to the azo chromophore group in their structure, diazonium compounds are colorful compounds and are mostly referred to as azo dyes. In fact, azo dyes constitute the largest class of synthetic dyes. The incorporation of a heterocyclic component in the diazo or coupling moiety of dyes positively affects their fastness properties. Some research suggests that azo dyes modified with heterocyclic structures exhibit bioactive properties[2-4]. In the literature, many different azo dyes containing various heterocyclic structures have been reported, such as thiophene[5], pyrazole[6], thiazole[7], pyrimidine[8], coumarin[9], indole[10], barbituric acid[11], etc. It has been reported that, in addition to their beneficial uses in various fields[12-14], azo compounds containing heterocyclic components exhibit toxicological and mutagenic properties, posing a risk to health[15].

Thiophene-based azo dyes, with a history spanning approximately 70 years, have been obtained in a wide range of colors with the presence of various chromophore groups[16]. Studies have shown that the durability properties of thiophene-based azo dyes are superior to many carbocyclic azo dyes. The observed changes with the addition of different substituents to the thiophene skeleton have been quite valuable for understanding the structure-activity relationship[17].

When we examine studies on thiophene-based azo compounds, we realize their potential applications in various fields such as heat- and light-resistant dyes[18-21], diverse biological activities[22-24], solar cells and non-linear optics[25-26], corrosion inhibitors[27-28], and more. Therefore, in this study, we synthesized two new azo compounds by diazotizing 2-aminothiophene derivatives and coupling them with 2-indanone and 1,3-indandione compounds. In the further stages of our research, the applications of the newly synthesized azo compounds will be investigated, with a priority given to their biological activities, and their evaluation as useful products will be ensured.

MATERIAL AND METHODS

For the determination of melting points, a capillary tube was used, and the Gallenkamp apparatus (without any adjustments) was employed. Infrared spectra (4000-400 cm-1) were acquired utilizing a Thermo Nicolet 6700 FT-IR spectrometer equipped with Attenuated Total Reflectance. For nuclear magnetic resonance spectra, the Bruker AVANCE III instrument (400 MHz for ^{1}H-NMR; 100 MHz for ^{13}C-NMR) and TMS as an internal standard were used. All reagents (Sigma-Aldrich) employed without additional purification.

2.1 Synthesis of amine compounds (1,2).

2-amino-4,7-dihydro-5H-spiro[benzo[b]thiophene-6,2'-[1,3]dioxolane]-3-carbonitrile (1) and methyl 2-amino-4,7-dihydro-5H-spiro[benzo[b]thiophene-6,2'-[1,3]dioxolane]-3-carboxylate (2) were synthesized based on the method outlined in the literature[29-34]. In this reaction, malononitrile (0.66 g, 0.01 mol) was used for compound 1, while methylcyanoacetate (1.00 g, 0.01 mol) for compound 2. Additionally, 1,4-dioxaspiro[4.5]decan-8-one, sulfur and morpholine were added in equimolar amounts. The reaction mixture was stirred at room temperature in absolute ethanol (15 ml). Due to the exothermic nature of the reaction, the temperature increased to 50°C. The reaction ended after 72 hours with the formation of a thick precipitate. The product formed after pouring the reaction mixture into water was collected by filtration. It was then purified by recrystallization (via EtOH) (Scheme 1).
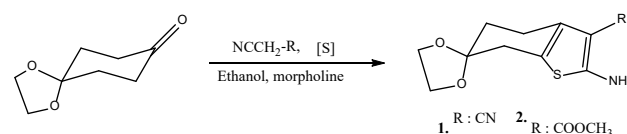
Scheme 1. Synthesis demonstration of amine compounds (1: 2-amino-4,7-dihydro-5H-spiro[benzo[b]thiophene-6,2'-[1,3]dioxolane]-3-carbonitrile; 2: methyl 2-amino-4,7-dihydro-5H-spiro[benzo[b]thiophene-6,2'-[1,3]dioxolane]-3-carboxlate).

2.2 Diazotization procedure

While dry $NaNO_2$ (0.138g, 0.002 mol) was added gradually to concentrated H_2SO_4 (1.1 ml), the reaction temperature rose to 65°C. Then, it was cooled to around 5°C, and with continuous stirring, CH_3COOH (20 ml) was added dropwise. Throughout this process, care was taken to ensure that the temperature did not exceed 15°C. Then, the reaction mixture (0-5°C) was added dropwise with compound 1 (0.472 g, 0.002 mol) or

compound 2 (0.538 g, 0.002 mol) and continued to stir at same temperature for 2 h, thereby ensuring the formation of diazonium salt. The excess nitric acid was removed from the solution using urea. Diazonium salt solutions can only remain stable for short periods and at low temperatures. Therefore, immediate coupling reaction should be ensured following the synthesis. The reaction scheme for this experimental stage is illustrated in Scheme 2.

2.3 Coupling procedure

For coupling solution, 2-indanone (0.266 g, 0.002 mol) (or 1,3-indandione (0.292 g, 0.002)) was dissolved in a mixture containing CH_3COOH (10 ml), H_2O (5 ml) and CH_3COONa (5 g). The temperature was lowered by an ice-bath and then was slowly dripped in to the diazonium solution with vigorous stirring. The pH was modified using an aqueous 10% CH_3COONa. The reaction was terminated after 2 h, and the temperature was allowed reach to ambient temperature. The crude coupling product was separated and purified by recrystallization (DMF-water)[35] (Scheme 2).

The physical and spectral data of obtained compounds were shown in Table 1.

Additional, the spectrum graphics of compounds (S1-S12) are given in Supplementary Material.
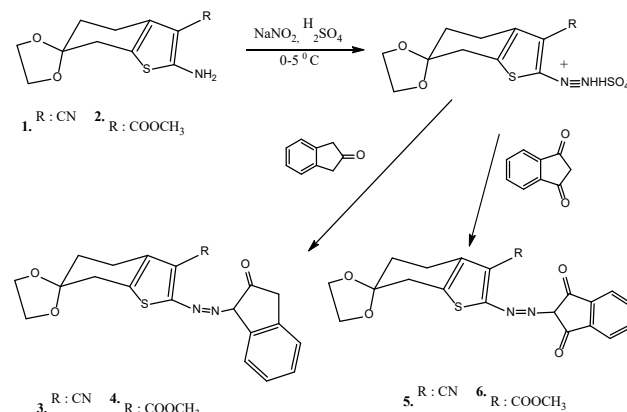
Scheme 2. Synthesis demontstration of diazonium compounds (**3-6**).

Table1. Physical and spectral data of diazonium compounds (**3-6**)

Compound number, Yield, Color, m.p. (°C)	FT-IR (ῡ, cm⁻¹)	¹H-NMR (λ, ppm)	¹³C-APT (λ, ppm)
3 68% Yellow 250-252	3257 (N-H) 3085 (Ar-H) 2962-2895 (Aliph. C-H) 2221 (C≡N) 1662 (C=O)	9.65 (s, 1H, NH) 7.98-7.94 (d, 1H, J= 7.40, Hz, Ar-H) 7.52 (d, 1H, Ar-H) 7.47-7.43 (m, j= 7.40 Hz, 2H, Ar-H) 4.09 (s, 4H, CH₂) 3.79 (s, 2H, CH₂) 2.91 (s, 2H, CH₂) 2.87-2.84 (t, 2H, j= 6.38 Hz, CH₂) 2.01-1.98 (t, 2H, J= 6.38 Hz, CH₂)	Pozitive amplitude : 161.96, 147.50, 131.41, 127.89, 126.06, 113.69, 107.50, 94.47, 64.80, 34.29, 30.58, 23.14 Negative amplitude : 132.84, 132.06, 129.77, 129.77
4 60% Dark yellow 204-205	3177 (N-H) 3082 (Ar-H) 2987-2903 (aliph. C-H) 1676 and 1658 (2 C=O)	12.34 (s, 1H, NH) 7.86 (t, 1H, Ar-H) 7.58-7.48 (m, 3H, Ar-H) 4.06 (s, 4H, CH₂) 3.94 (s, 3H, CH₃) 3.76 (s, 2H, CH₂) 3.06-3.02 (t, 2H, J= 6.38 Hz, CH₂) 2.93 (s, 2H, CH₂) 1.99-1.96 (t, 2H, J=6.38 Hz, CH₂)	Pozitive amplitude : 166.81, 163.81, 148.30, 134.01, 131.60, 130.13, 125.01, 112.24, 108.41, 64.84, 38.83, 35.01, 31.72, 25.23 Negative amplitude : 132.76, 131.12, 126.99, 51.44
5 55% Pale brown 238-240	3201 (N-H) 3084 (Ar-H) 2962-2899 (aliph. C-H) 2212 (C≡N) 1679 and 1621 (2C=O)	12.39 (s, 1H, NH) 8.27-8.22 (t, 1H, J= 7.20 Hz, Ar-H) 7.94-7.89 (t, 1H, J= 7.20 Hz, Ar-H) 7.84-7.75 (dt, 2H, Ar-H) 3.99 (s, 4H, CH₂) 2.83 (s, 2H, CH₂) 2.64 (t, 2H, CH₂) 1.87 (t, 2H, CH₂)	Pozitive amplitude: 165.60, 148.00, 146.80, 131.06, 130,11, 125.70, 113.76, 107.46, 94.09, 63.70, 33.60, 30.31, 22.31. Negative amplitude : 134.64, 131.35, 129.27, 124.19
6 58% Brown 125-127	3349 (N-H) 3082 (Ar-H) 2960-2878 (aliph. C-H) 1716, 1667 and 1615 (3C=O).	11.93 (s, 1H, NH) 7.82 (t, 1H, Ar-H) 7.49-7.38 (m, 3H, Ar-H) 4.06 (s, 4H, CH₂) 3.86 (s, 3H, CH₃) 3.05-3.02 (t, 2H, J= 6.42 Hz, CH₂) 2.87 (s, 2H, CH₂) 1.98-1.95 (t, 2H, J=6.42 Hz, CH₂)	Pozitive amplitude: 166.99, 162.90, 148.29, 133.68, 131.72, 124.36, 130.20, 111.93, 107.85, 38.75, 35.09, 31.98, 25.23. Negative amplitude : 132.12,130.01, 127.63

³ 2-((2-oxo-2,3-dihydro-1H-inden-1-yl)diazenyl)-4,7-dihydro-5H-spiro[benzo[b]thiophene-6,2'-[1,3]dioxolane]-3-carbonitrile

⁴ Methyl 2-((2-oxo-2,3-dihydro-1H-inden-1-yl)diazenyl)-4,7-dihydro-5H-spiro[benzo[b]thiophene-6,2'-[1,3]dioxolane]-3-carboxylate

⁵ 2-((1,3-dioxo-2,3-dihydro-1H-inden-2-yl)diazenyl)-4,7-dihydro-5H-spiro[benzo[b] thiophene-6,2'-[1,3]dioxolane]-3-carbonitrile

⁶ Methyl 2-((1,3-dioxo-2,3-dihydro-1H-inden-2-yl)diazenyl)-4,7-dihydro-5H-spiro[benzo[b] thiophene-6,2'-[1,3]dioxolane]-3-carboxylate
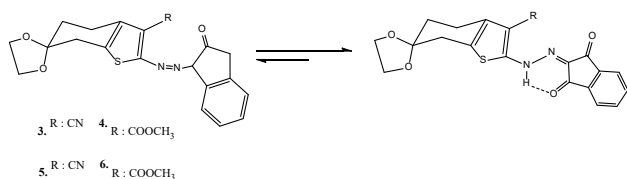
Scheme 3. Tautomeric form of diazo compounds.

CONCLUSION

Amine compounds were synthesized by the Gewald's method, based on the ketone compounds 1,4-dioxaspiro[4.5] decan-8-one. The preparation of diazonium compounds of amino thiophene compounds differs considerably from aniline-derived compounds. For this reason, it is necessary to be extremely careful when preparing diazonium salts of these compounds. Synthesis of compounds with high yields is possible when the relevant literature is followed. It was observed that the compounds obtained as a result of the interlocking of 1 and 2 amine compounds with 2-indanone and 1,3-indandione preferred the hydrazo form due to the low area of the NH groups (Scheme 3).

The fact that the NH peak in the docked compounds is at (3-6), 9.65, 12.34, 12.39, 11.93 ppm, respectively, indicates that the compounds are in the form of hydrazo. The aromatic peaks of the compounds were detected in the range of 7.98-7.43 ppm for compound no. 3, and in the range of 7.86-7.48 ppm for compound no. 4, in the range of 8.27-7.75 ppm for compound no. 5, in the range of 7.82-7.38 ppm for compound no. 6. The CH_2 group between the two oxygens of the compounds was observed as a singlet of 4.09, 4.06, 3.99 and 4.06 ppm, respectively. Additionally, the CH_3 group belonging to the ester group was observed 3.94 ppm for substance 4 and 3.86 ppm for substance 6. It was observed that the CH_2 group, which was not hydrogen in its neighbor in the aliphatic ring structure, was divided into triplets at (3-6), 3.79 ppm, 2.93 ppm, 2.83 ppm, 2.87 ppm, respectively, and the neighboring CH_2 groups were split into triplets at 2.86 ppm, 3.04 ppm, 2.64 ppm, 3.02 ppm, and the other CH_2 group was at 1.99 ppm, 1.98 ppm, 1.87 ppm, 1.97 ppm.

The compounds are present in the hydrazo tautomer on the ^{13}C-APT NMR spectrum.

In the ^{13}C-APT NMR spectrum of the compounds, it was observed that the carbon peaks of the non-hydrogen C and CH_2 groups with two hydrogen atoms on them came out at positive amplitude. Carbons in the indanone ring and with hydrogen atom on it have been observed in the spectrum ^{13}C-APT at negative amplitude and in the range of 134.64 to 124.19 ppm.

ACKNOWLEDGEMENT

References

1. Christie RM. Colour Chemistry. 2nd ed. Cambridge: The Royal Society of Chemistry; 2015. Chapter 3, Azo Dyes and Pigments; p. 72-98.
2. Mishra VR, Ghanovatkar CN, Sekar N. UV protective heterocyclic disperse azo dyes: Spectral properties, dyeing, potent antibacterial activity on dyed fabric and comparative computational study. Spectrochim Acta A: Mol Biomol Spectrosc. 2019;223:117353. doi:10.1016/j.saa.2019.117353
3. Mohammadi A, Khalili B, Tahavar M. Novel push-pull heterocyclic azo disperse dyes containing piperazine moiety: Synthesis, spectral properties, antioxidant activity and dyeing performance on polyester fibers. Spectrochim Acta A: Mol Biomol Spectrosc. 2015;150:799-805. doi:10.1016/j.saa.2015.06.024
4. Manjunatha B, Bodke YD, Nagaraja O, Lohith TN, Nagaraju G, Sridhar MA. Coumarin-Benzothiazole based azo dyes: Synthesis, characterization, computational, photophysical and biological studies. J Mol Struct. 2021;1246:131170. doi: 10.1016/j.molstruc.2021.131170
5. Sujamol MS, Athira CJ, Sindhu Y, Mohanan K. Synthesis, spectroscopic characterization, dyeing performance and corrosion inhibition study of transition metal complexes of a novel azo derivative formed from 2-aminothiophene. Chem Data Coll. 2021;31:100634. doi: 10.1016/j.cdc.2020.100634
6. Karcı F, Bakan E. New disazo pyrazole disperse dyes: synthesis, spectroscopic studies and tautomeric structures. J Mol Liq. 2015;206:309-315. doi: 10.1016/j.molliq.2015.02.032
7. Khedr AM, El-Ghamry H, Kassem MA, Saad FA, El-Guesmi N. Novel series of nanosized mono- and homobi-nuclear metal complexes of sulfathiazole azo dye ligand: Synthesis, characterization, DNA-binding affinity and anticancer activity. Inorg Chem Commun. 2019;108:107496. doi:10.1016/j.inoche.2019.107496
8. Mughal EU, Raja QA, Alzahrani AYA, Naeem N, Sadiq A, Bozkurt E. Pyrimidine-based azo dyes: Synthesis, photophysical investigations, solvatochromism explorations and anti-bacteral activity. Dyes Pigm. 2023;220:111762. doi:10.1016/j.dyepig.2023.111762
9. Yıldırım F, Demirçalı A, Karcı F, Bayrakdar A, Taşlı PT, Kart, HH. New coumarin-based disperse disazo dyes: synthesis, spectroscopic properties and theoretical calculations. J Mol Liq. 2016;223:557-565. doi:10.1016/j.molliq.2016.08.008
10. Karabacak Ç, Dilek Ö. Synthesis, solvatochromic properties and theoretical calculation of some novel disazo indole deys. J Mol Liq. 2014;199:227-236. doi:10.1016/j.molliq.2014.09.019
11. Harisha S, Keshavayya J, Kumara Swamsy BE, Viswanath CC. Synthesis, characterization and electrochemical studies of azo dyes derived from barbituric acid. Dyes Pigm. 2017 Jan;136:742-753. doi:10.1016/j.dyepig.2016.09.004
12. Erten G, Karcı F, Demirçalı A, Söyleyici S. 1H-pyrazole-azomethine based novel diazo derivative chemosensor for the detection of Ni2+. J Mol Struct. 2020 Apr 15;1206:127713. doi:10.1016/j.molstruc.2020.127713
13. Derkowksa-Zielinska B, Skowronski L, Biitseva A,

Grabowski A, Naparty MK, Smokal V, Kysil A, Krupka O. Optical characterization of heterocyclic azo dyes containing polymers thin films. Appl Surf Sci. 2017;421(B):361-366. doi: 10.1016/j.apsusc.2016.12.080

14. Ayare NN, Sharma S, Sonigara KK, Prasad J, Soni SS, Sekar N. Synthesis and computational study of coumarin thiophene-based-π-A azo bridge colorants for DSSC and NLOphoric application. J Photochem Photobiol A. 2020;394:112466. doi: 10.1016/j.jphotochem.2020.112466

15. Karabulut YK, Gürkan YY. Investigation of some azo dyes by QSAR method and acute toxicity test with Daphnia Magna. J Ins Sci Tech. 2023;13(2):1110-1119. doi:10.21597/jist.1214772

16. Karcı F, Karcı F. Synthesis and tautomeric structures of some novel thiophene-based bis-heterocyclic monoazo dyes. J Mol Struct. 2012;1024:117-122. doi: 10.1016/j.molstruc.2012.05.021

17. Singh MV, Tiwari AK, Sharma YK, Chauhan MS, Sethi M, Guo Z. Synthetic procedures, properties, and applications of thiophene-based azo scaffolds. ES Food Agrofor. 2023;12:887. doi: 10.30919/esfaf887

18. Abdou MM. Thiophene-based azo dyes and their applications in dyes chemistry. Am.J. Chem. 2013;3(5):126-135. doi:10.5923/j.chemistry.20130305.02

19. Nassar HS. New azo disperse dyes with thiophene moiety for dyeing polyester fibers. Int. J. Text. Sci. 2015;4(5):102-112. doi: 10.5923/j.textile.20150405.02

20. Sharma SJ, Khan ZN, Zambare AA, Bagal MS, Barshi AS, Rindle SM, Sekar N. Synthesis, spectroscopic, DFT, TD-DFT, and dyeing studies of 2-amino-3-cyano thiophene-based azo dyes on wool and nylon. Dyes Pigm. 2024;228:112209. doi: 10.1016/j.dyepig.2024.112209

21. Sing MV, Tiwari AK, Sharma YK, Chauhan MS, Sethi M, Guo Z. Synthetic procedures, properties, and applications of thiophene-based azo scaffolds. ES Food. Agrof. 2023;12:887. doi: 10.30919/esfaf887

22. Mezgebe K, Mulugeta E. Synthesis and pharmacological activities of azo dye derivatives incorporating heterocyclic scaffolds: a rewiev. RSC Adv. 2022;12(40):25932-25946. doi: 10.1039%2Fd2ra04934a

23. Gouda MA, Eldien HF, Girges MM, Berghot MA. Synthesis and antitumor evaluation of thiophene based azo dyes incorporating pyrazolone moiety. J. Saudi Chem. Soc. 2016;20(2):151-157. doi:10.1016/j.jscs.2012.06.004

24. Al-Azmi A, John E. Synthesis of 4-arylazo-2-(N-pyrazolylcarboxamido)thiophene disperse dyes for dyeing of polyester and their antibacterial evaluation. Text. Res. J. 2020;90(23-24):1-11. doi: 10.1177/0040517520931476

25. Ayare NN, Sharma S, Sonigara KK, Prasad J, Soni SS, Sekar N. Synthesis and computational study of coumarin thiophene-based D-π-A azo bridge colorants for DSSC and NLOphoric application. J. Photochem. Photobiol. A Chem. 2020;394:112466. doi: 10.1016/j.jphotochem.2020.112466

26. Sharma SJ, Sekar N. Exploration of 4-substituted thiophene-based azo dyes for dye-senditized solar cells and non-linear optical materials: synthesis and an in silico approach. Phys. Chem. Chem. Phys. 2024; Advance article. doi: 10.1039/D4CP00918E

27. El-Haddad MN, Fouda AS, Mostafa HA. Corrosion inhibition of carbon steel by new thiophene azo dye derivatives in acidic solution. J. Materi. Eng. Perform. 2013; 22:2277-2287. doi: 10.1007/s11665-013-0508-0

28. Gadow HS, Fawzy A, Khairy M, Sanad MMS, Toghan A. Experimental and theoretical approaches to the inhibition of carbon steel corrosion by thiophene derivative in 1 M HCl. Int. J. Electrochem. Sci. 2023;18(7):100174. doi: 10.1016/j.ijoes.2023.100174

29. Peet NP, Sunder S, Barbuch RJ, Vinogradoff AP. Mechanistic observations in the Gewald syntheses of 2-aminothiophenes. J Heterocycl Chem. 1986;23(1):129–134. doi: 10.1002/jhet.5570230126

30. Gewald K. Methods for the synthesis of 2-aminothiophenes and their reactions (review). Chem Hetrocycl Compd. 1976;12:1077-1090. doi: 10.1007/BF00945583

31. Gewald K, Schinke E, Bottcher H. Heterocyclen aus CH-aciden Nitrilen, VIII. 2-Amino-thiophene aus methylenaktiven Nitrilen, Carbonylverbindungen und Schwefel. Chem Ber. 1966;99(1): 94-100. doi: 10.1002/cber.19660990116

32. Buldurun K, Turan N, Savci A, Alan Y, Colak N. Synthesis, characterization, X-ray diffraction analysis of a tridentate Schiff base ligand and its complexes with Co (II), Fe (II), Pd (II) and Ru (II): Bioactivity studies. Iran J Chem Chem. Eng. 2022;41(8):2635-2649. doi: 10.30492/ijcce.2021.531629.4775

33. Çolak N, Gündüzalp AB, Mamaş S, Akkaya D, Kaya K. Synthesis, spectroscopic studies and electrochemical properties of Schiff bases derived from 5-chloro-2-hydroxybenzaldehyde with methyl 2-amino-6-methyl-4, 5, 6, 7-tetrahydrobenzo [b] thiophene-3-carboxylate. Bulg Chem Commun. 2016;48(Special C):20-26.

34. Çolak N, Altıner S, Şahin ZS, Gündüzalp AB. Synthesis, Spectroscopic and Computational Studies of (E)-2-(2,3-dihydroxy)-benzylidene)amino)-6-methyl-4,5,6,7-tetrahydrobenzo[b]thiophene-3-carbonitrile. Gazi University Journal of Science. 2017;30(3):245 – 254.

35. Maradiya HR. Synthesis of azobenzo[b]thiophene derivatives and their dyeing performance on polyester fibre. Turk J Chem. 2001;25(4):441-450.

Supplementary Material
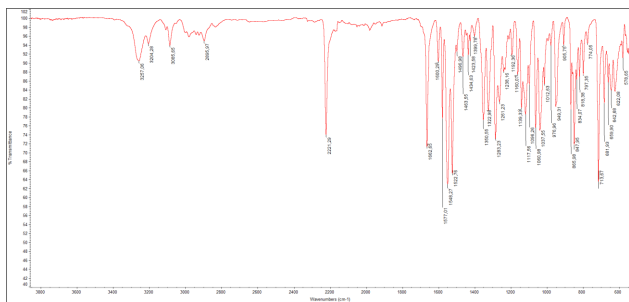
Figure S1. FT-IR spectrum of compound 3
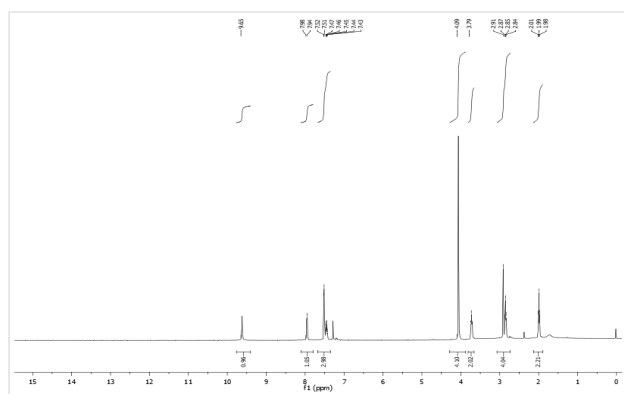
Figure S2. ¹H-NMR spectrum of compound 3
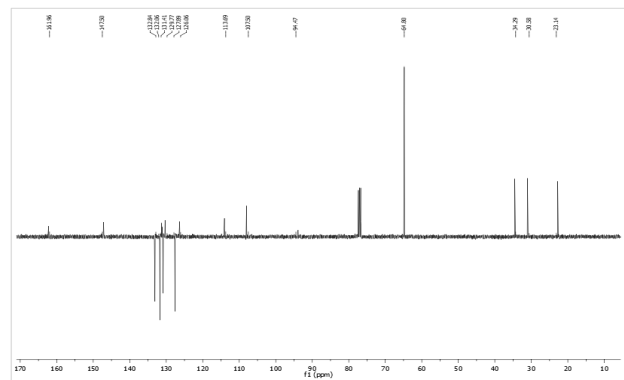
Figure S3. ¹³C-NMR APT spectrum of compound 3
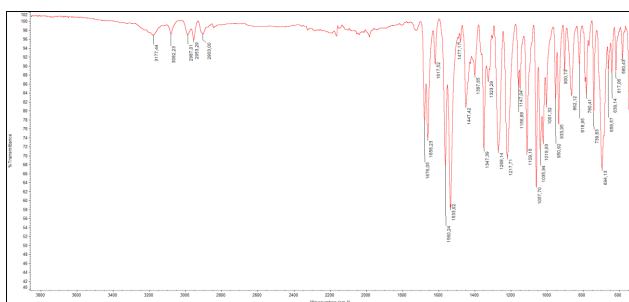
Figure S4. FT-IR spectrum of compound 4
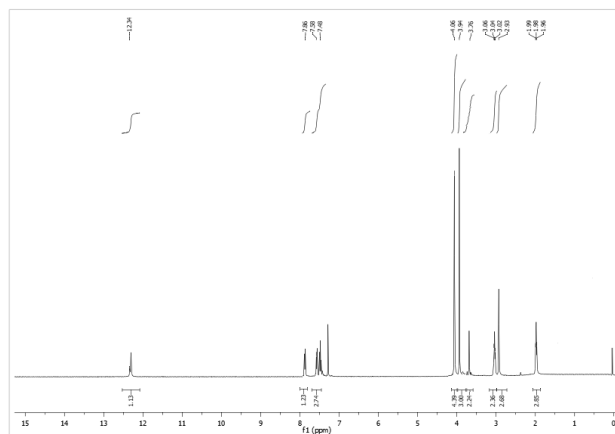
Figure S5. ¹H-NMR spectrum of compound 4
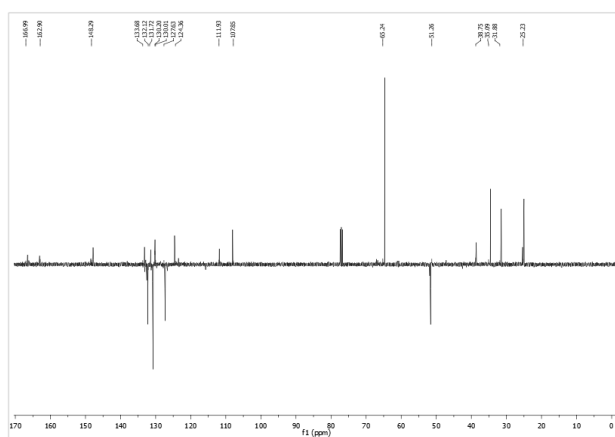
Figure S6. ¹³C-NMR APT spectrum of compound 4
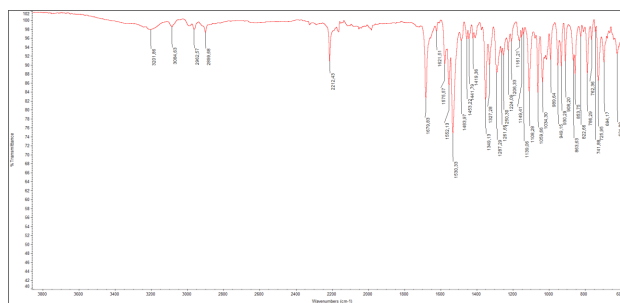
Figure S7. FT-IR spectrum of compound 5
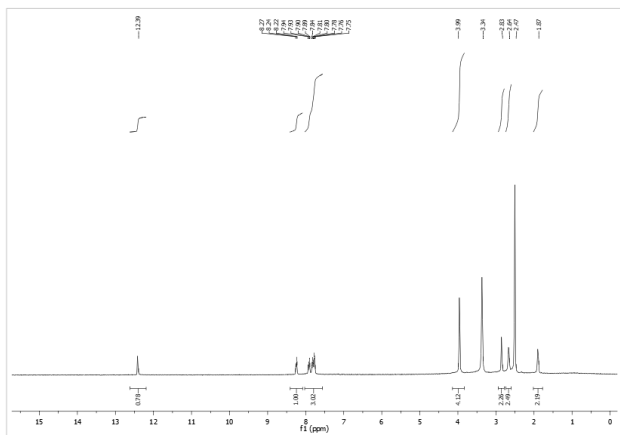
Figure S8. ¹H-NMR spectrum of compound 5
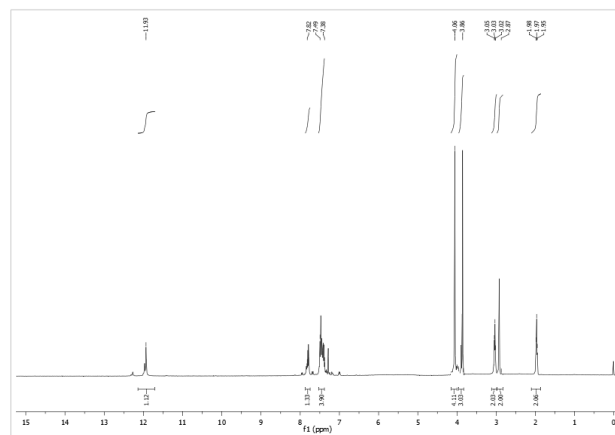
Figure S11. ¹H-NMR spectrum of compound 6
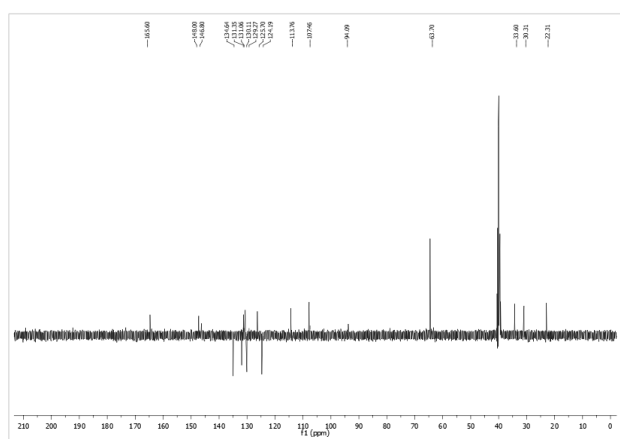
Figure S9. ¹³C-NMR APT spectrum of compound 5
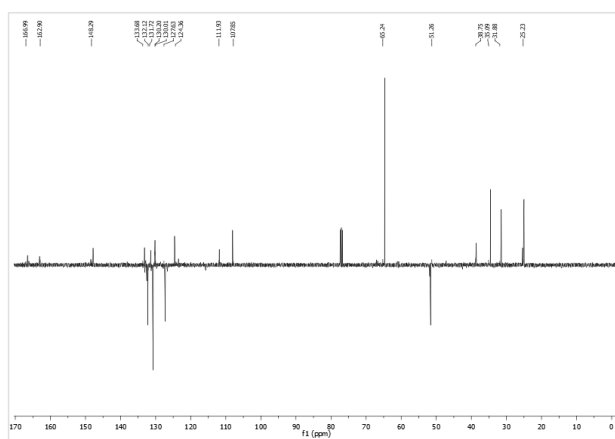
Figure S12. ¹³C-NMR APT spectrum of compound 6
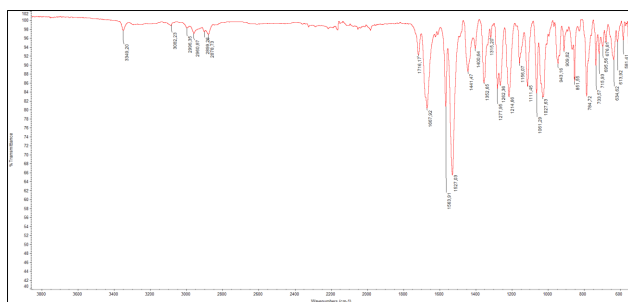
Figure S10. FT-IR spectrum of compound 6

Artificial Intelligence-assisted Drug Development

Irmak Sevval TOPCU[1,*] ⓘD | Orcun AVSAR[1] ⓘD

[1]Hitit University, Faculty of Art and Sciences, Department of Molecular Biology and Genetics, 19040, Corum, Türkiye.

Corresponding Author
Irmak Sevval TOPCU
E-mail: irmaktopcu00@gmail.com Phone: +90 553 546 3671
RORID: ror.org/01x8m3269

Cite As
Topçu I.S, Avşar O. Artificial Intelligence-assisted Drug Development. Hitit journal of Science. 2024;1(1):8-21

Artificial Intelligence-assisted Drug Development

Irmak Sevval TOPCU[1,*] | Orcun AVSAR[1]

[1]Hitit University, Faculty of Art and Sciences, Department of Molecular Biology and Genetics, 19040, Corum, Türkiye.

Abstract

Deep learning and machine learning algorithms, two types of artificial intelligence, have come to light as potential solutions to issues and roadblocks in the drug design and discovery process. Both in vitro and in silico techniques have the potential to significantly lower drug development costs when compared to conventional animal models. Early on in the drug research and development process, drug candidates with relevant therapeutic activities can be identified, unsuitable compounds with unwanted side effects can be excluded, and in vitro and in silico techniques can be used to limit the number of drug poisonings. Drug discovery procedures, illness modeling, target identification, artificial intelligence, drug screening, and molecular design can all be completed far more quickly and affordably than with conventional techniques.

Keywords: Artificial Intelligence, In silico approaches, Target identification, Target verification, Target interactions.

OVERVIEW

The multi-step process of drug research and development includes clinical testing, manufacturing approval, and drug discovery. It is costly, time-consuming, complex, and has a high attrition rate (Waring M.J. et al. 2015). Clinical trial drug attrition results in a significant loss of resources (Fleming N. 2018). Chemical and biological scientists have faced a significant problem over the past 20 years: creating effective and sophisticated systems for the targeted administration of therapeutic substances with maximum efficiency and minimal danger (Lipinski CF., 2019). Another obstacle in the process of designing and developing new drugs is the expense and duration involved in creating novel therapeutic agents (Hamet P., Tremblay J., 2017). Researchers all over the world have resorted to computational techniques like virtual screening (VS) and molecular docking, also referred to as traditional approaches, to try and minimize these difficulties and barriers; however, these methods have also introduced problems like inaccuracy and inefficiency (Hassanzadeh P. et al., 2019). Long and intricate processes like target identification and validation, therapeutic screening, lead compound optimization, preclinical and clinical trials, and manufacturing applications are all part of the drug research and design process. The process of identifying the medication that works best to treat a condition is further complicated by all these procedures. Consequently, controlling process speed and cost is the largest issue facing pharmaceutical businesses (Zhang L. et al., 2017). By providing straightforward, scientific solutions to all of these issues, artificial intelligence shortens the process's time and expense (Jordan A.M., 2018).

Machine intelligence, another name for artificial intelligence, is the capacity of computer systems to learn from inputs or past data. When a machine simulates cognitive behavior linked to learning and problem-solving in the human brain, it is said to be artificial intelligence (Goel AK, Davies J (2019) Artificial intelligence. In: Cambridge Handbook of Intelligence. Cambridge). The fields of logic, statistics, cognitive psychology, decision theory, cybernetics, computer engineering, neuroscience, and linguistics are the foundations of artificial intelligence (AI). A better understanding of AI will help to mitigate its negative effects on worker safety, health, and welfare as well as its opportunities and challenges for the future of work (Russell S.J.; Norvig, P., 2016).

1. THE EMERGENCE OF ARTIFICIAL INTELLIGENCE

Robotics is widely acknowledged as the source of artificial intelligence. The Czech word "robota," which means "robot," was originally used in the science fiction drama "Rossum's Universal Robots" by author Karel Capek in 1921. The term "robot" was made famous by Isaac Asimov in the middle of the 20th century while compiling a collection of contemporary science fiction short stories. But the earliest record of a humanoid automaton dates back to the third century in China, when Yan Shi, a mechanical expert, gave the Zhou Emperor Mu a handcrafted, humanoid mechanical figure composed of wood, leather, and synthetic materials (Hamet P, Tremblay J., 2017). Al-Jazari, a Muslim philosopher from the Golden Age, invented a humanoid robot that could strike cymbals in the 12th century. Leonardo da Vinci studied human anatomy in great detail throughout the Renaissance in order to construct his humanoid robot. Only in the 1950s were his 1495 sketches unearthed. Driven by pulleys and wires, Leonardo's robot was a knight-like device that could sit, stand, swing its arms, and move its head and jaw.

From Charles Babbage, who created the first mechanical computer in 1850, to the question "can machines think?" in 1950, computer scientists and science fiction authors were captivated by the notion of machine intelligence comparable to human intelligence. Alan Turing proposed a machine intelligence test in 1950. This test, often known as the Turing test, assesses a machine's capacity for intelligent behavior that is on par with or identical to that of a human. If "a human interrogator, after some written questions have been posted, cannot tell whether the written answers come from a human or a machine," then the computer passes the test. In order to pass the Turing test, a computer needs to be able to recognize speech, store information from what it hears or knows (knowledge representation), utilize that information to answer questions and make inferences (automatic reasoning), and recognize new patterns in order to adapt to changing conditions (ML). The computer will meet the requirements of the so-called Total Turing test if it is equipped with two more capabilities: computer vision and physical interaction. The primary focuses of AI research and development at the moment are represented by these six capabilities (Howard J., 2019).

When Arthur L. Samuel created an IBM checkers software in 1952, he popularized the phrase "machine learning." "The science and engineering of making intelligent machines" is how John McCarthy defined artificial intelligence (AI) when he first used the word in 1955. He had a significant impact on

AI's early development. He and his colleagues created the field of artificial intelligence during a 1956 conference held at Dartmouth College. This event gave rise to the term that became a new field of study spanning multiple disciplines and served as the conceptual foundation for all ensuing computer-related research and development projects (Hamet P., Tremblay J., 2017). Frank Rosenblatt created the perceptron in 1957 with the purpose of recognizing images (Rosenblatt F., 1957). The continuous back-propagation model was created by Henry J. Kelley in 1960, and Stuart Dreyfus created a more straightforward version in 1962 based solely on the chain rule (Kelley H.J., 2012; Dreyfus S., 1962). The first functional deep learning networks were created in 1965 by Ivakhnenko and Lapa (Gupta R., et al., 2021). Around 1980, Kunihiko Fukushima created the first convolutional neural network (CNN), which was modeled after the structure of an animal's visual cortex (Fukushima K., 1988).

1.1. SYSTEMATIC LEARNING

Machine learning (ML) is a subfield of artificial intelligence that allows computers to learn from data. It has become popular for using computers to make predictions, acquire cognitive insights, and assist in decision-making (Jordan M.I., Mitchell T.M., 2015). ML is a break from earlier artificial intelligence techniques, which worked by hand-coding a full set of logic rules into software in an effort to foresee every scenario that could arise. With machine learning (ML), computers can use cutting-edge software techniques to extract their own rules (Haugeland J. Artificial Intelligence: The Very Idea. Cambridge).

1.1.2. GUIDED EXPERIENCE

Using a training dataset that has been precisely labeled by a human expert, supervised learning looks for patterns and makes predictions (Maini V. et al., 2019). A radiographic data image classification algorithm can learn the correct relationship between an input image (X-ray, for example) and an output label (lung cancer) using a supervised learning training dataset. It can then use this relationship to classify unlabeled images that the computer has never seen before (Choy G. et al., 2018).

1.1.3.UNSUPERVISED LEARNING

There is no usage of a preset training dataset. The learning algorithm receives unlabeled data; without human assistance, it then finds the data's hidden structure and groups the data into clusters (Hinton G., Sejnowski T.J., 1999; James G. et al., 2017).

1.1.4.SEMI-SUPERVISED LEARNING

It's a machine learning technique for better comprehending a dataset's structure. Currently, a variety of industry sectors are producing large volumes of unlabeled data from text, audio, and images (Chapelle O. et al., 2006).

1.1.5. LEARNING REINFORCEMENT

Reinforcement learning is a type of computer experimentation that is derived from basic learning theory in psychology. It is a training approach that is based on rewarding good behaviors and penalizing undesired ones (Thorndike E., 1932, Varian H., 2019). With reinforcement learning, a machine may be taught the right answers by applying incentives and penalties in the same way that humans learn by making mistakes (Sutton RS, Barto AG., 2018). Reinforcement learning can be utilized in conjunction with neural networks to train a robot to grasp objects it has never seen before or to operate autonomous vehicles (Knight W., 2017).

1.1.6. DEEP NEURAL NETWORKS

Neural networks that are fully connected and have several hidden layers. There are several nonlinear processing units in each hidden layer. DNNs use several neurons in numerous layers to automatically extract features at hierarchical levels (D'Souza S., et al., 2020).

1.1.7.DEEP LEARNING

According to Goodfellow, Bengio, and Courville (2016), deep learning is a subtype of neural networks that recognizes patterns using many processing layers of coupled neurons between input and output layers. In the areas of speech recognition, image identification, and natural language understanding, deep learning algorithms have made great progress (Krizhevsky A., et al, 2012; Hinton G., et al, 2012; Hirschberg J., et al, 2015).

2.GENERAL USAGE AREAS OF ARTIFICIAL INTELLIGENCE
2.1. ELECTRONIC DEVICES

Functional sensors are not as valuable as advanced or smart sensors. To monitor various parameters, these smart sensors can be surgically implanted in the body, fastened to safety gear, or fastened to any item (Nag A., et al., 2017; Howard J., 2019). The Internet of Things (IoT) can be created by connecting any product or device with integrated sensors to the internet and other similar devices (Chui M., et al., 2010). Applications of artificial intelligence are being brought into a wide range of industries, including banking, insurance, criminal justice, healthcare, and national security (West D.M., Allen J.R., 2018). Cutting-edge sensor systems can "sense" their surroundings using deep learning models, much like how humans perceive sound and vision (Howard J., 2019).

2.2.ROBOTIC DEVICES

"Cloud robotics" allows one AI-enabled robotic device to upload its learning experience to all other robots that are linked. (B. Kehoe and others, 2015). All cloud-connected robotic devices can be updated to use the new procedure when a robot's output reveals a safer way to complete a task at work. Robotics can learn more effectively through universal robotic upgradability in a cloud-connected network than through human learning, which is individually dependant (Pratt G.A., 2015).

2.3.DECISION SUPPORT SYSTEMS

A multipurpose informative tool with AI support can be used to extract information from data for applications involving decisionmaking (Howard J., 2019). Utilizing data already recorded in management information systems, technologies are being used to support business decisions as a result of the notion that computers should support decision makers (Bonini C.P., 1963; Pervan G., Willcocks L., 2005). Many industry

sectors, particularly the medical field, use ML-enabled DSSs for decision-making (Kononenko I., 2001; Topol E., 2019). Clinical DSSs are marketed as having the ability to increase diagnostic accuracy and assist physicians in understanding the intricate relationships between clinical variable scores. The healthcare industry generates large amounts of data, which make them ideal learning inputs for ML-enabled DSSs (Ehteshami Bejnordi B., et al., 2017; Obermeyer Z, Emanuel E.J., 2016; Phillips-Wren G., 2012). Several studies that have used ML-enabled DSSs to date include:

Lung cancer screening (Ardila D., et al., 2019),

Detection of pulmonary tuberculosis (Lakhani P., Sundaram B., 2017),

Determination of diabetic retinopathy (Gulsen V., et al., 2016; Kanagasingam Y., et al., 2018),

Skin cancer diagnosis (Esteva A., et al., 2017),

Anticancer medication response prediction in precision oncology therapy (Azuaje F., 2019; Tan M., 2016),

Progress has been made in areas such using retinal pictures to predict cardiovascular risk factors (Poplin R., et al., 2018).

Transforming research findings into clinical advancements is still a difficult undertaking, despite the early research accomplishments using machine learning to huge medical datasets holding significant potential in enhancing the quality of healthcare (Deo R.C., 2015). For instance, an AI-enabled ML image classifier for melanoma skin cancer that is trained solely on fair skin types will reinforce current health disparities rather than serve as a means of eradicating them (Adamson A.S., Smith A., 2018).

3. DRUG DISCOVERY PROCESS AND ARTIFICIAL INTELLIGENCE
3.1. PROCESS OF DRUGS DISCOVERY
3.1.1. DISEASE MODELLING AND TARGET IDENTIFICATION

The success rate of drug development is greatly impacted by disease modeling and target identification, which is a crucial initial phase in the drug discovery process (Pun F.W., et al., 2023). Furthermore, target identification helps researchers understand the mode of action of unknown medications, which makes it a critical step in the discovery and development of new drugs (Schenone M., et al., 2013). Researchers can more effectively tailor a medication for a specific ailment or disease by identifying the molecular target of that medication (McFedries A., et al., 2013; Hughes J.P., et al., 2010). To maximize medication selectivity and minimize possible adverse effects, target identification is also crucial (Schenone M., et al., 2013; Hughes J.P., et al., 2010).

A molecule must be "druggable" in order to have even the remotest chance of being a target for medication. The field of drug development is shifting toward the application of novel design principles to molecules, connecting them to difficult biological targets for novel medications of the future or novel approaches to dosage modification. The conventional pharmaceutical industry concentrates on creating tiny compounds that are orally bioavailable and have specific objectives (Sarkar C., et al., 2023).
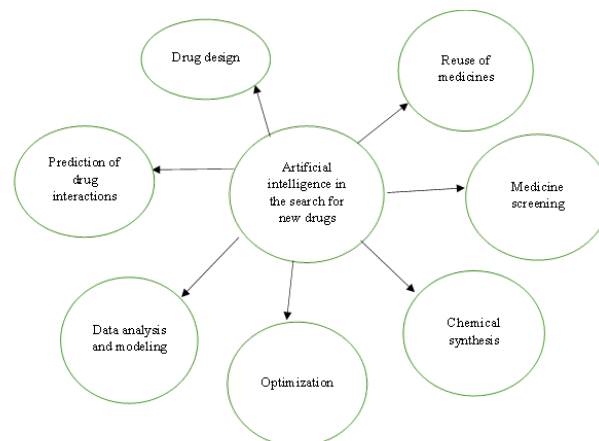
Figure 1. Artificial Intelligence's role in medication discovery. Various steps of drug discovery, including as drug design, chemical synthesis, drug reuse, drug screening, drug interaction prediction, optimization, data analysis, and modeling, can benefit from the application of artificial intelligence.

Millions of molecules may be present in datasets used by pharmaceutical companies for medication research, but conventional machine learning techniques may not be able to handle this volume of data. Though computational models based on the quantitative structure-activity relationship (QSAR) can rapidly predict a large number of compounds or basic physicochemical parameters like logP (partition coefficient), they are not very good at predicting complex biological properties. Additionally, QSAR-based models have issues with experimental data error and insufficient experimental validation on training sets. In order to address these issues, new AI techniques like deep learning (DL) and associated modeling investigations can be used for large data modeling and analysis-based safety and efficacy evaluations of pharmaceutical compounds (Paul D., et al., 2021).

3.1.2. DRUG SCREENING WITH ARTIFICIAL INTELLIGENCE
3.1.2.1. PHYSICAL AND CHEMICAL PROPERTIES PREDICTION

When developing a new drug, physicochemical characteristics like solubility, intrinsic permeability, degree of ionization, and partition coefficient (logP) should be taken into account as they have an indirect impact on the pharmacokinetic characteristics of the drug and its target receptor family (Zang Q., et al., 2017). A variety of AI-based instruments are available for physicochemical property prediction. For instance, ML trains the program using massive data sets produced during prior chemical optimization (Yang X., et al., 2019). Drug design algorithms use chemical descriptors, such as coordinates of 3D atoms, electron density surrounding the molecule, and SMILES sequences, to produce appropriate molecules via DNN and subsequently predict their attributes (Baringhaus K.H., Hessler G., 2018).

3.1.2.2. THE BIOACTIVITY PREDICTION

Drug molecules' ability to generate a therapeutic response is contingent upon their affinity for the target protein or receptor; those that do not exhibit any interaction with the

targeted protein will not be effective. Toxic interactions between produced medication molecules and undesirable proteins or receptors can also occur in certain situations. As a result, drug-target interaction prediction greatly depends on drug target binding affinity (DTBA). AI-based techniques can calculate a drug's binding affinity by considering the characteristics or similarities between the drug and its target. While similarity-based interactions consider the similarity between the drug and the target and presume that similar drugs will interact with the same targets, feature-based interactions identify the chemical moieties of the drug and the target to determine feature vectors (Öztürk H., et al., 2018).

To predict drug-target interactions, a variety of techniques, such as machine learning and deep learning, have been employed. To determine DTBA, machine learning (ML) techniques like Kronecker regularized least squares (KronRLS) assess how similar medicines and protein molecules are. Similarly, SimBoost took into account both feature-based and similarity-based interactions while predicting DTBA using regression trees (Öztürk H., et al., 2018).

3.1.2.3. TOXICITY PREDICTION

Any pharmacological molecule's predicted toxicity can be utilized as a guide to prevent harmful consequences, and cell-based in vitro experiments are frequently employed as pilot research. The expense of drug discovery rises when research on animals are carried out to ascertain a compound's toxicity right after. Cutting-edge AI-based methods either predict a compound's toxicity based on input features or search for commonalities between compounds. By identifying static and dynamic properties like molecular weight and Van der Waals volume within the chemical descriptors of molecules, an ML algorithm named DeepTox outperformed all other methods. It was also able to predict a molecule's toxicity with high efficiency using 2500 predefined toxicophore properties (Mayr A., et al., 2016).

3.2. DESIGN OF DRUG MOLECULES WITH ARTIFICIAL INTELLIGENCE

The necessity of developing novel medications is underscored by the advent of pandemics and epidemics, as well as the growth of grave illnesses like cancer and heart disease. Target selection, validation, high-throughput screening, animal studies, safety and efficacy protocols, clinical trials, and regulatory approval are all necessary steps in the often multi-step process of drug discovery (Vamathevan J., et al., 2019). Certain phases of this process, like finding new targets, assessing drug-target interactions, researching disease mechanisms, and enhancing small-molecule drug design and optimization, can benefit from the application of artificial intelligence-based techniques (Jeon J., et al., 2014; Katsila T., et al., 2016; Lee L., et al., 2019; Nicolaou C.A., Brown N., 2013; Vamathevan J., et al., 2019). These techniques can also be applied to the investigation of pharmacological efficacy, response, and resistance as well as the identification and development of prognostic biomarkers (Qureshi R., et al., 2022).

3.2.1. IDENTIFICATION OF THE TARGET IN DRUG DISCOVERY

Target identification is the process of finding molecules (typically proteins) that have the ability to change a disease state. Numerous data sources, such as gene expression profiles, protein-protein interaction networks, genomic, and proteomic data, can be evaluated using machine learning (ML) methods to find possible targets that may be involved in disease pathways (Sliwoski G., et al., 2014).

Determining the cause of the illness and the target is the first stage in defining a target (Lv B. M., et al., 2014). Tree-based approaches, GNNs, and graphs can be used to determine the causal links between genes and diseases. It was also suggested to identify genes linked to druggable morbidity using a decision tree-based meta-classifier that was trained on a network topology that included protein-protein, metabolic and transcription relationships, tissue expression of proteins, and subcellular localization (Qureshi R., et al., 2023). Key characteristics from the decision tree included regulation by several transcription factors, centrality in metabolic pathways, and extracellular placement. Based on characteristics including protein-protein interaction, gene expression, DNA copy number, and the presence of mutations, ML-based techniques categorized proteins as therapeutic targets or non-targets for particular diseases like lung, pancreatic, and ovarian cancer (Jeon J., et al., 2014).

3.2.2. PREDICTION OF TARGET PROTEİN STRUCTURE

The development of the disease involves many proteins, some of which are overexpressed. Predicting the target protein structure while creating a therapeutic molecule is therefore crucial for the selective targeting of disease. By anticipating the 3D protein structure as the design aligns with the target protein region's chemical environment, artificial intelligence can support structurebased drug discovery by assisting in the prediction of a compound's effect on the target as well as safety concerns prior to synthesis (Wann F., Zeng J.M., 2016). In order to predict the 3D target protein structure, AlphaFold, an artificial intelligence tool based on DNNs, was used to analyze the angles of peptide bonds and the distances between adjacent amino acids. It demonstrated excellent results, correctly predicting 25 out of 43 structures (Paul D., et al., 2021).

3.2.3. DRUG-PROTEIN INTERACTION PREDICTION

The effectiveness of therapy is greatly dependent on drug-protein interactions. Understanding drug efficacy, permitting the bait and switch of medications, and avoiding polypharmacology all depend on the ability to predict how a drug will interact with a receptor or protein. Different AI techniques have improved therapeutic efficacy by accurately predicting ligand-protein interactions (Wann F., Zeng J.M., 2016).

Because AI can anticipate drug-target interactions, it can also be used in Phase II clinical trials to assist minimize polypharmacology and reuse current medications (Mak K.K., Pichika M.R., 2019). This also lowers costs because it is more expensive to relaunch a current drug than to introduce a brand-new medicinal entity (Paul D., et al., 2021). The potential

for polypharmacology—a drug molecule's propensity to bind with many receptors and cause off-target adverse effects—can also be predicted by drug-protein interactions (Li X., et al., 2017). By using polypharmacology logic to design novel molecules, artificial intelligence can contribute to the production of safer pharmaceutical molecules (Reddy A.S., Zhang S., 2014).

4. ARTIFICIAL INTELLIGENCE ALGORITHMS USED IN DRUG DISCOVERY PROCESS
4.1. MACHINE LEARNING (ML) ALGORITHIMS

Supervised and unsupervised learning are the two primary categories of machine learning algorithms. Unsupervised learning detects patterns in a set of instances, frequently without labels for the instances, and the data is frequently transformed to a lower dimension to recognize patterns in high dimensional data using unsupervised learning algorithms before recognizing patterns. Supervised learning learns by training instances with known labels to determine the labels for new instances. Not only is unsupervised learning more effective in a low-dimensional space, but dimensionality reduction also makes the recognized model easier to understand. Semi-experienced and reinforcement learning can be created by combining supervised and unsupervised learning; both functions can be used to different types of data (Rifaioglu A.S., et al., 2019).

ML algorithms are utilized in the drug development process to create a variety of models that forecast the chemical, physical, and biological characteristics of substances (Patel L., et al., 2020). All phases of the drug discovery process, including identifying novel drug uses, forecasting drug-protein interactions, determining drug efficacy, supplying safety biomarkers, and maximizing molecular bioactivity, can benefit from the application of machine learning (ML) algorithms (Patel L. et al., 2020).
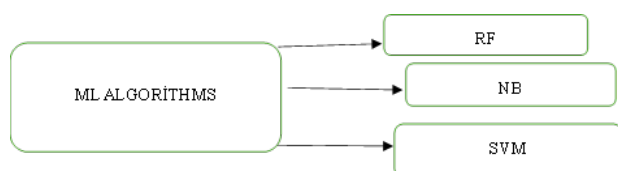
Figure 2. Commonly used ML algorithms.

RANDOM FOREST (RF)

RF is a popular method that is specifically made for big datasets with plenty of characteristics. It makes things easier by eliminating outliers (Outliers are values that deviate significantly from the general trend in the data. They need to be taken into account because they can mislead the ML model, affect its accuracy and cause poor performance. Random forest performs better when predicting variables like the Human Development Index (HDI) when techniques like winsorizing and random oversampling are used to handle outliers and imbalanced data (Notodiputro K.A., Sartono B., Zubedi F., 2022)) and categorizes and identifies datasets according to the relative features that are classified for a certain algorithm. In addition to being trained for accessibility using a variety of huge inputs, variables, and data gathering

from numerous databases, it is helpful in a variety of contexts, including referring to missing data, working with outliers (For instance, the random forest method can be requested to choose the most valuable characteristic out of x attributes. If desired, this information can then be utilized in another desired model), and predicting features for classification (Breiman L., 2001). Many independent decision trees make up the mathematical process that underpins RF as a whole; each tree determines a forecast, and the tree with the greatest number of votes is deemed optimal (Sarica A., et al., 2017). By combining numerous predictions instead of concentrating on just one, multiple decision trees reduce individual errors (Patel L. et al., 2020). Regression, classifiers, and feature selection are the three main uses of RFs in drug discovery. Accelerating the training process, employing fewer parameters, loading missing data, and merging nonparametric data can be added to the list of primary factors that go along with RF in drug development (Cano G., et al., 2017). Multivariate RFs are experts in reducing error by calculating different error estimation methods inside the system. By feeding in data with combinations of genetic and epigenetic characteristics, the computational framework enables the framework to predict the mean and confidence interval of medication reactions. This is a crucial characteristic needed to analyze any medication that will be used in clinical trials (Rahman R., et al., 2017).

NAİVE BAYESİAN (NB)

A subset of supervised learning techniques known as NB algorithms is now a vital tool for classification in predictive modeling. Depending on the input features, factor correlation, and dimensionality of the data, standard NB algorithms can be one of the most effective methods for classifying dataset features. These methods increase the accuracy of retrieved datasets, which frequently come from large, mixed sources (Bielza C., Larrañaga P., 2014; Gilboa E., et al., 2013; Kim S.B., et al., 2006; Ratanamahatana C., Gunopulos D., 2010; Sun H., 2005).

SUPPORT VECTOR MACHINE (SVM)

SVMs are supervised learning algorithms that are used in the drug discovery process to derive a hyperplane and divide classes of compounds according to a feature selector. It creates an endless number of hyperplanes by taking use of commonalities across classes. It trains on linear data by projecting classes of chemicals into chemical feature space, based on features that are chosen. A hyperplane used to categorize data points by establishing decision boundaries is an ideal hyperplane that is obtained by eliminating the largest margin between classes in N (number of features) dimensional space (Heikamp K., Bajorath J., 2013). SVM's capacity to differentiate between active and inactive compounds and rank compounds in each database makes it a crucial tool for drug discovery. Regression models are essential for figuring out how a medicine and ligand interact since they make predictions by running a query against databases. Multiple situations can be associated with SVM when multiple active compounds of interest are screened against a single protein. SVM classification's primary focus is on binary class prediction, which includes a subset that can differentiate between active and inactive chemicals and substances (Patel L. et al., 2020).

SVM is especially made to incorporate ligands and target proteins as an essential part of modeling drug-target interaction (Heikamp and Bajorath, 2013). It can rate compounds from various databases according to their likelihood of being active for any computational screening in the drug discovery process. By training the algorithm with different descriptors for feature selectors, such as target protein and 2D fingerprints, the procedure can be altered. Depending on which way a chemical is positioned relative to the hyperplane, a negative or positive class label is created, resulting in a ranking of compounds from most selective to least selective (Wassermann A.M., et al., 2010; Hinselmann G., et al., 2011). For non-linear data, kernel functions are employed to optimize outcomes. According to Patel L. et al. (2020), kernel functions plot data in a higher dimensional space that allows for class classification.

4.2. DL ALGORITHMS AND ARTIFICIAL NEURAL NETWORKS

The goal of artificial neural networks (ANNs) is to simulate how neurons behave in the natural world. Several artificial neurons arranged in ordered layers make up a common artificial neural network architecture (Yang X., et al., 2019). Its most basic configuration comprises of three layers of neurons that communicate with one another, just like the human brain does. Data input occurs on the first layer, information processing occurs on the hidden layer, and output is the last layer. When every node in one layer of a feed-forward network is connected to every other layer, the neurons in an artificial neural network (ANN) are said to be dense or fully connected. Only these types of networks are referred to as multilayer perceptrons (MLPs; multiple hidden layers), dense neural networks, or complete neural networks. Stated otherwise, a network is deeper the more hidden levels it contains. The depth of the model is determined by the length of the chain connecting the many functions that make up these networks. This idea gives rise to the term "deep learning," which describes learning systems with several information processing layers that may simulate high-level abstractions in data (Lavecchia A., 2019).

In practically every scientific and technological discipline, deep learning algorithms are acknowledged as one of the most advanced areas of development and research. DL algorithms have made it possible for computer models to learn how to represent multidimensional data through abstraction and have helped ML algorithms overcome a number of obstacles (Patel L. et al., 2020).

DL algorithms are now the standard approach for lead molecule, target, and drug activity prediction in the drug discovery process. Neural network systems, which are used to construct systems capable of complicated data recognition, interpretation, and production, are frequently the foundation of deep learning. Deep neural networks (DNNs), recurrent neural networks (RNNs), and convolutional neural networks (CNNs) are the primary subsets of neural networks that are being utilized in drug discovery (Dana D. et al., 2018; Korotcov A., et al., 2017; Ekins S., 2016).
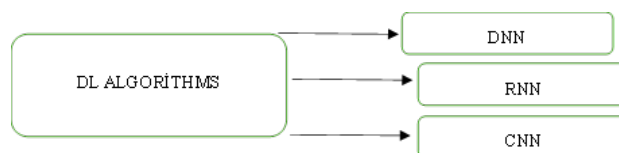
Figure 3. Commonly used DL algorithms.

DEEP NEURAL NETWORKS (DNN)

From the input layer to the hidden layer and finally to the output layer, DNNs operate on a single path data stream. Typically, supervised learning algorithms that have been trained are used to identify the outputs. A DNN may be trained to accomplish complicated tasks using guided reinforcement learning and supervised learning techniques. While a predictive DNN can forecast the chemical characteristics of novel compounds, a generative DNN may create new chemical compounds from preexisting libraries and training sets (D'Souza S., et al., 2020; Baskin I.I., et al., 2016). The correlation between these substances' chemical structure and activity is ascertained by the utilization of QSAR models. One of the most sophisticated applications of deep learning (DL)-based artificial intelligence (AI) in drug discovery and development today is QSAR analysis, which gives scientists access to two-dimensional chemical structures and physicochemical characteristics that are associated with a molecule's activity. Additional research into the geometric structure influencing ligand-target interactions has been made possible by 3D-QSAR (Chen R., et al., 2018; Ghasemi F., et al., 2018).

RECIPIENT NEURAL NETWORKS (RNN)

Sequence prediction was the original purpose of RNN creation. These networks only accept an input stream with varying lengths (Askr R., et al., 2023). Self-iterative or feedback connections between neurons in various levels are what distinguish them. such loops in a network, they feature feedback components to reuse internal information and function especially well with sequential data, such text, phrases, and protein sequence data. To get around the challenges of storing long-term data, they are additionally outfitted with an internal memory.

The chemical synthesis and characterisation phase becomes significant after the initial work on target discovery has been finished and a more effective technique for target-molecule interaction has been created. The majority of algorithms for new drug design and discovery use the descriptive simplified molecular input line input system (SMILES) nomenclature, which is a crucial aspect at this time. The lengthy short-term memory subset of the RNN type has evolved into a dependable, standardized technique for constructing novel chemical structures. When it comes to utilizing neurons connected to the same hidden layer to create an inputoutput processing loop, RNNs are far more beneficial algorithms than DNNs and feed-forward neural networks (Patel L., et al., 2020).

CONVOLUTIONARY NEURAL NETWORKS (CNN)

Developed to handle growing levels of complexity as well as

data preparation and aggregation, CNNs are a high-potential type of artificial neural network (ANN) that receives inputs, weights some of the inputs, and then enhances the ability to distinguish data (Yamashita R. et al., 2018). A convolutional layer with parameters made up of a collection of filters, or kernels, is what distinguishes convolutional neural networks (CNNs) from other types of neural networks. CNNs are designed to resemble the receptive field of the human visual cortex, where neurons react to stimuli. Local filters are what these cells do throughout the input space.

CNNs may process data in four steps and are among the most versatile algorithms for handling both image and non-image data (Askr H., et al., 2023):
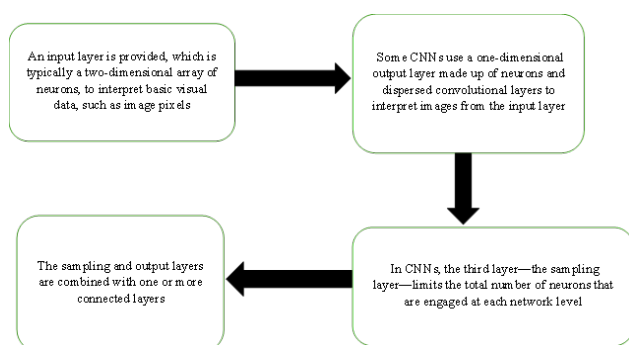
Figure 4. Stages of processing CNNs.

This idea of a network may make it easier to retrieve pertinent visual data in smaller, more manageable pieces. Neurons in a CNN are in charge of the preceding layer's group of neurons (Askr H., et al., 2023).

Four steps are involved in building the CNN when the input data is integrated into the convolutional model (Askr H., et al., 2023):

Convolution: Using the given data, a feature map is created and then put through an objective.

Maximum Pooling: Based on the supplied modifications, this aids CNN in identifying an image.

Flattening: At this point, the data is standardized for CNN's analysis.

Complete Linking: The process of generating a model's loss function is frequently referred to as the "hidden layer".
Image recognition, image analysis, video analysis, picture segmentation (splitting an image into regions with distinct features), and natural language processing (NLP) are among the tasks performed by CNNs (Chauhan et al. 2018; Tajbakhsh et al. 2016; Mohamed et al. 2020).

CNNs are among the most useful tools in the drug development process for target and lead identification and characterisation, protein-ligand scoring, and in silico target-lead interaction screening. Furthermore, CNNs have been utilized in the development of motility models that depict how cancer cells respond to various forms of therapy (Dana D., et al., 2018; Mencattini A., et al. 2020; Ragoza M., et al. 2017; Rathi P.C., et al. 2020; Reher R., et al., 2020).

5. *In Silico* APPROACH
These days, with the aid of modern computers and information technology, the procedures involved in medication development, optimization, and discovery have changed due to the rapid evolution of technology. In the biomedical field, the optimization process from hit detection and hit to routing has been facilitated and accelerated by the use of computer-aided or in silico design utilizing computational tools (Ekins S., et al., 2009).

To find hit and lead compounds, the drug discovery industry often employs one of two models: the phenotype- or target-based method. These vary in ways that help identify therapeutic targets and choose or optimize small molecules (Dodd F.S., 2005; Swinney D.C. and Anthony J., 2011). The phrase "therapeutic target" refers to the location of the substance's binding that will facilitate the substance's biological activity (Andrade E.L. et al., 2016).

The phenotype screening strategy, also known as advanced or classical pharmacology, uses better disease-relevant tests (such as isolated tissue or animal models of the disease, cell-based phenotypic analysis) to identify drugs based on their physiological effects. Through the interaction of several targets (receptors, transcription factors, enzymes, etc.) of a previously undisclosed target, this strategy may lead to the identification of a molecule that modifies the illness phenotype (Dodd F.S., 2005; Swinney D.C., 2012).

The two broad categories of approaches utilized in computer-aided drug design (CADD) are ligand-based and structure-based. Structure-based CADD is recommended when the target protein's structure is known, particularly for soluble proteins that crystallize readily. In the event that target structure information is lacking, ligand-based CADD is utilized by building predictive, quantitative structure-activity relationship (QSAR) models and using the knowledge of known active and inactive compounds through chemical similarity searches (Kapetanovic I.M., 2008; Katsila T., et al., 2016). Drug productivity, speed, and costeffectiveness can all be rationalized and enhanced by using ligand- and structure-based steps in the discovery process, such as compound generation by virtual screening, predicting the binding free energy between a ligand and a receptor, and optimizing high affinities (Sliwoski G., et al., 2014).

5.1. TARGET IDENTIFICATION AND VALIDATION FOR THERAPEUTICS
In target-based drug development, targets are found through a range of molecular techniques and instruments, such as the evaluation of the genome and proteins (proteomics) linked to a disease in humans. Targets related to human pathology can be found by utilizing a variety of molecular techniques, including RNA interference, zinc finger proteins, antisense oligonucleotides, tissue and cell microarrays, nucleic acid microarrays, and protein microarrays (Terstappen G.C., et al., 2007; Wang S., et al., 2004). The target is identified first in the

phenotypic-based approach, which observes the substance's activity beforehand.

Reverse convolution is another term for the target identification procedure in this method. Chemical proteomics-based methods (affinity chromatography, activity-based protein profiling, label-free techniques), expression cloning methods, in silico methods, and others can be used to identify targets (Terstappen G.C., et al., 2007; Lee J., Bogyo M., 2013). Validation of the treatment target is necessary after identification. Here, the objective is to determine whether altering the therapeutic target will result in a believable biological response. To this end, validation methods include altering the target in disease-affected humans as well as using whole animal models and in vitro tools (Hughes J.P., et al., 2010; Terstappen G.C., Reggiani A., 2001).

Three categories comprise the most commonly recognized standards for target validation in drug discovery (Andrade E.L., 2016):
1-Expression of the target protein or mRNA in appropriate cell types, animal models, or patient target tissues
2-Target modulation produces the intended functional effect in cell systems.
3-Prove that the target is responsible for the disease phenotype in patients or animal models.

Typically, in vivo or in vitro experiments are used to get the first steps of therapeutic target validation. These are then followed by the use of immunohistochemistry or in situ hybridization techniques to express messenger RNA or proteins in human samples, respectively. Though the first method that springs to mind is protein characterization, this approach may be hampered by the absence of particular antibodies directed against a particular target; additionally, target validation is rarely, if ever, thought to be achieved solely by the target protein's association with diseased or target tissue (Lindsay M.A., 2003). It's also necessary for the target to have functional significance to disease modification. Using small molecule inhibitors, antisense oligonucleotides, and siRNA, target validation can also be studied in transgenic and gene knockout animals; however, it should be noted that animal models frequently do not exhibit the exact disease phenotype or share the same pathophysiology as observed in patients. Targets frequently result in differing tissue expression and distribution in animal models than in human models. Moreover, pathogenic pathways in humans can have a distinct mechanism of action and differ evolutionarily from those in animal models. It is best to confirm a target using at least two distinct methods before moving on to the rigorous clinical stage of drug development in order to prevent all of these issues (Andrade E.L., 2016).

Like the more widely used biological phrases *in vivo* and *in vitro*, the term "*in silico*" refers to investigations carried out by computers. It explains how data is utilized to build computational models or simulations that can be used to forecast outcomes, put forth theories, and eventually result in new medical discoveries or advancements in therapy. The benefits of in silico investigations are their low cost, quick implementation, and capacity to minimize animal exploitation.

This technique has been employed as a means of expediting the identification of promising novel therapeutics. Toxicology and pharmacokinetic research, as well as the investigation of structure-activity connections, are all included in the construction of *in silico* drug prototypes (Ekins S., et al., 2009). To effectively direct the development of new drugs through the execution of *in vitro* and *in vivo* research, *in silico* studies are crucial.

Homology modeling in the context of in silico pharmacodynamics is predicated on amino acid sequence homology, which offers details on structural and functional similarities. Therapeutic target structures are mapped using this technique, which also covers the three-dimensional structure of the targets (Ekins S., et al., 2009).

Molecular docking, which predicts the bioactive conformation of a small molecule at the binding site of a macromolecule, is another technique frequently employed for pharmacodynamic evaluation. This approach determines the relevant binding affinity after providing a good approximation of the predicted shape and fit of the ligand in the protein cavity (Lengauer T., Rarey M., 1996).

Via the use of three-dimensional macromolecular data on the topological arrangement of biological information as a prerequisite for detailed information, ligand-based virtual screening is based on virtual screening. Target-based virtual screening, which is based on receptor structure, selects compounds for biochemical or biological testing by analyzing vast compound databases using molecular docking techniques to establish an ideal chemical and biological space (Andrade E.L., 2016).

5.3. COMPUTER AIDED DRUG DESIGN (CADD)
Using a variety of computer tools, CADD integrates computational chemistry, molecular modeling, molecular design, and rational drug design to find and create a therapeutic development lead (Muegge et al., 2017). CADD employs two distinct methodologies, namely structure-based drug design (SBDD) and ligand-based drug design (LBDD), contingent upon the accessibility of three-dimensional protein or ligand structures (Vemula D., et al., 2023).

Structure-Based Drug Design (SBDD): Characterizing the binding site cavity and having access to the therapeutic target protein's three-dimensional structure are the two primary components of structure-based drug design (Kawato et al., 2015). SBDD has surfaced as a potential method in the pharmaceutical sector for ligand generation and optimization (Gurung et al., 2021; Jorgensen W.L., 2004; Park H., et al., 2012).

Ligand-Based Drug Design (LBDD): This approach is employed in situations where three-dimensional receptor data is unavailable. Understanding the chemicals that attach to the desired biological target is the foundation of the technique. By using a known ligand as a target, LBDD techniques establish a structure-activity relationship (SAR) between the ligand's activities and physicochemical characteristics. This information can be used to guide the creation of novel

medications with increased activity or to improve currently available ones (Yu and MacKerell, 2017).

6. ARTIFICIAL INTELLIGENCE IN DRUG DOSAGE FORM DESIGN

For biological compartments in the human body system to comprehend the impact of drug delivery, physicochemical barriers are essential. Depending on the route of administration, one of the most crucial parameters for keeping an eye on a successful drug delivery system is the penetration rate. For instance, after entering the stomach, the medication taken orally needs to pass through the intestinal or gastric epithelium. This step is crucial for the drug's continued bloodstream dissemination. The process of delivery involves moving the medication through the bloodstream to a specified tissue or site (Bhhatarai B., et al., 2019; Chavda V.P., 2019; Siepmann J., Siepmann F., 2012; Das P.J., et al., 2016; Colombo S., 2020). The way a medicine interacts with biological components greatly affects how the drug behaves in the body at the end. The drug's molecular characteristics control the process up to the final state. Drugs can either actively or passively aid in their penetration. Drug distribution is predicted via computational analysis using in silico models, which are based on the molecular characteristics of the drug. Passive permeation is ineffective for small, physiologically active compounds and necessitates a specific delivery method. Membrane transport drives the process of active permeation, which is dependent on intricate biological interactions. The pharmacokinetic properties of the drug delivery system can be studied with the aid of numerous specific parameters employed in this intricate process. Research units can be better understood and multi-layered data can be thoroughly analyzed thanks to artificial intelligence. In order to discover the best outcomes with parameter evaluation, the model to be applied methodically is based on a number of criteria, including simulation, scoring, and refinement at each stage of the inquiry. Moreover, AI is used to investigate how a drug delivery method affects the drug's pharmacokinetics in order to improve data prediction for continuous improvement, precise comprehension of the medication's interaction with biology, and efficient comprehension of toxicity and distribution. AI gathers data from many sources and creates indicators according to the chosen drug delivery system's performance. The efficacy of treatment is contingent upon the precision with which AI selects drug delivery devices. The goal of artificial intelligence is to apply current treatments to newly discovered diseases. It is helpful in the drug discovery process in addition to the drug reuse approach. Formulation, pharmacokinetics, and medication development are influenced by the needs of the patient and the condition of the illness (Vora K.L., et al., 2023).

7. ARTIFICIAL INTELLIGENCE IN MEDICINE DISTRIBUTION
7.1. ARTIFICIAL INTELLIGENCE TO DEVELOP ORAL SOLID DOSAGE FORM

Since solid dosage forms are the most convenient to use and promote disease compliance, individuals choose to take them in the form of tablets, granules, and powdered medications (Jiang J. et al., 2022). In the pharmaceutical industry, tablets are one of the most popular formats. Preparing tablets for use entails a number of aspects. The formulator has established these characteristics to fulfill the unique demands of the target patient population. A variety of excipients are put into tablets to manage the intended product outcome, such as tablet disintegration, dissolution, and drug release. Artificial intelligence can be used to forecast drug release in the setting of systemic drug administration and assist in examining the desirable relevant aspects of improved medication formulations. For the purpose of developing solid dosage forms, artificial neural networks and their subfields, such as neural networks and genetic algorithms, are used to improve comprehension of inputs and outputs. Genetic algorithms are employed to forecast outcomes from the usage of input parameters, however artificial neural networks offer superior prediction skills for solid dosage forms (Galata D.L. et al., 2021, Ghourichay M.P. et al., 2021; Navya K. et al., 2022).

7.1.1. Drug Release Prediction Through Formulations

The release of drugs from oral solid dosage forms advances our knowledge of important material characteristics and processing variables. Compression parameters, such as the pressure applied to regulate tablet hardness, the geometric orientation of the tablets, and drug loading properties, are factors that influence drug release. In the formulation of drugs, artificial intelligence is used to predict drug release. As a result, only a small number of runs are needed to optimize the batch, which further reduces labor and expenses during the manufacturing and pilot batch scale-up processes. Artificial intelligence can also be used to predict drug release profiles and dissolution profiles, as well as investigate disintegration time to effectively select the best batch for subsequent scale-up (Vora K.L. et al., 2023).

7.1.2. Applications of Artificial Intelligence for Formulation of Tablet Defects

Tablet photos are analyzed using artificial intelligence algorithms and computer vision techniques, which makes it possible to automatically and effectively detect flaws like cracks, discolorations, or variations in size and shape. The method gains a high degree of accuracy by accurately classifying and identifying various sorts of errors through the training of AI models on massive datasets of annotated photos. The interior structure of tablets has been studied using conventional techniques like Xray computed tomography, however these techniques still take time and interfere with the need for quick tablet production. To find tablet flaws, deep learning and X-ray tomography are combined. Not only does this AI-powered detection increase problem identification speed and accuracy, but it also minimizes human mistake and subjective judgment by reducing the need for manual inspection. AI systems' real-time monitoring capabilities allow for the prompt identification of flaws, which allows for prompt response and can stop faulty tablets from being sold. In the end, incorporating AI into tablet defect detection raises productivity and enhances product quality while guaranteeing the security and effectiveness of pharmaceuticals (Vora K.L. et al., 2023).

7.1.3. Artificial Intelligence for Prediction of Physicochemical Stability

AI can predict the stability of oral formulations by analyzing and interpreting large datasets containing drug properties, formulation parameters, and environmental conditions. AI models can assess factors like drug degradation, interactions with excipients, and environmental influences on formulation stability. These capabilities are achieved by utilizing machine learning algorithms and computational models. With the use of AI's predictive skills, researchers may improve formulation designs, spot any stability problems early in the development process, and make wise decisions that will extend the shelf life and effectiveness of oral dosage forms. Artificial intelligence (AI) integration in stability prediction leads to more economical and effective drug development procedures, which in turn provides patients with safe and effective medications (Vora K.L. et al., 2023).

7.1.4. Contribution of Artificial Intelligence to Dissolution Rate Predictions

The term "dissolution rate" describes how quickly a medicine dissolves in a biological fluid. The drug's bioavailability and therapeutic efficacy are determined by this feature. Because artificial intelligence models can identify important physicochemical properties and molecular characteristics that influence the dissolution process through the analysis of large amounts of experimental data, they have greatly aided in the optimization of drug formulations and dosage forms and helped predict dissolution rates. These models achieve great prediction accuracy by using machine learning algorithms to identify intricate patterns and correlations between drug characteristics and dissolution rates. Artificial intelligence offers valuable insights into the dissolving behavior of various drug formulations. These insights can be utilized to build more efficient drug delivery systems and pick the best formulation techniques for enhanced drug absorption and solubility. Scientists now have useful tools to expedite medication development, improve formulation techniques, and ultimately enhance patient outcomes thanks to artificial intelligence's help for dissolution rate prediction advancements (Mukhamediev R.L. et al., 2022).

CONCLUSION AND DISCUSSION

Technology known as artificial intelligence has been incorporated into pharmaceutical R&D to expedite and lower the cost of the medication development and discovery processes. Owing to the advancement of machine learning theory and the synthesis of pharmacological data, artificial intelligence technology now functions as a potent data mining instrument in several drug design domains, including activity prediction, virtual screening, QSAR analysis, and in silico assessment of absorption, distribution, metabolism, excretion, and toxicity (ADME/T) properties (Çelik İ.N. et al. 2021). It can forecast proteomes, genomes, and patient-specific dosage formulations in addition to enhancing currently available medications. The development of novel compounds with target binding qualities that improve therapeutic efficacy and decrease adverse effects is made possible by systems created in partnership with scientists and artificial intelligence specialists. In order to improve compliance, AI-enabled systems will continuously gather data from wearables, sensors, and remote patient monitoring. They will also use genetic profiles, biomarkers, and electronic

health records to identify eligible patients, lower the cost of trials, and expedite approval. However, this presents ethical questions regarding patient consent. It has a number of benefits over conventional experimental techniques, including lower clinical trial attrition rates, fewer animal studies due to less frequent use of in vivo assays, process and expense control, and labor cost savings. Artificial intelligence (AI) is at the core of cutting-edge technologies because it has the unmatched ability to find novel candidate therapies that can be swiftly made available for clinical trials and, if authorized, integrated into healthcare. Accordingly, AI has promise for the creation of new medications and the repurposing of those already in use to treat human diseases, particularly those that are emerging like Coronavirus Disease 2019 (COVID-19) (Zhou Y., et al. 2016). Despite all of these benefits, artificial intelligence is still viewed as a mystery because it cannot be explained. Features are not well defined throughout the training phase, and the network designer might not know what is being looked at in the intermediate steps or why the model has reached a certain conclusion. Because of this, a lot of work has been done to speed up the drug discovery process and integrate AI tools into the system. However, before the full potential of AI in drug discovery and development can be realized, more successful applications of these tools will be needed (Chan H.C.S., et al. 2019).

REFERENCES

1. Adamson A.S., Smith A. Machine learning and health care disparities in dermatology. JAMA Dermatol. 2018;154(11):1247-1248. https://doi.org/10.1001/jamadermatol.2018.2348
2. Andrade E.L., Bento A.F., Cavalli J. et al. Non-clinical studies required for new drug development - Part I: early in silico and in vitro studies, new target discovery and validation, proof of principles and robustness of animal studies, 2016; 49(11): e5644.
3. Ardila D, Kiralyap, Bharadwaj S, et al. End-to-end lung cancer screening with three-dimensional deep learning on low-dose chest computed tomography. 2019;25(6):954-961.
4. Askr H., Elgeldawi E., Ella H.A. et al. Deep learning in drug discovery: an integrative review and future challenges, 2023;56(7): 5975–6037.
5. Azuaje F. Artificial intelligence for precision oncology: beyond patient stratification. 2019;3(6):6. https://doi.org/10.1038/s41698-019-0078-1
6. Baskin I.I., Winkler D.D., Tetko I.V., A renaissance of neural networks in drug discovery, 2016;11(8):785-95.
7. Bhhatarai, B.; Walters, W.P.; Hop, C.E.C.A. et al. Opportunities and Challenges Using Artificial Intelligence in ADME/Tox. 2019;18(5):418-422.
8. Bielza C., Larrañaga P. Discrete Bayesian Network Classifiers: A Survey, 2014;47(1):1-43. https://doi.org/10.1145/2576868
9. Bonini CP. Simulation of Information and Decision System in the Firm. Englewood Cliffs, NJ: Prentice Hall; 1963.
10. Breiman L., Random Forests, 2001;45:5-32, http://dx.doi.org/10.1023/A:1010933404324
11. Cano G., Rodriguez J.G., Garcia A.G. et al. Automatic selection of molecular descriptors using random forest: Application to drug discovery, 2017;72:151-159.
12. Chan H.C.S., Shan H., Dahoun T. et al. Advancing Drug Discovery via Artificial Intelligence. 2019;40(8):592-604.
13. Chapelle O, Schölkopf B, Zein A. Semi-supervised Learning. Cambridge, MA: MIT Press; 2006.
14. Chauhan R., Ghanshala K.K., Joshi R.C. Convolutional Neural Network (CNN) for Image Detection and Recognition, 2018. First International Conference on Secure Cyber Computing and Communication (ICSCCC). doi:10.1109/icsccc.2018.8703316
15. Chavda, V.P. Chapter 1 - Nanotherapeutics and

Nanobiotechnology, 2019;1-13. https://doi.org/10.1016/B978-0-12-814029-1.00001-6

16. Chen R., Liu X., Jin S. et al. Machine Learning for Drug-Target Interaction Prediction. 2018;23(9):2208.

17. Choy G, Khalilzadeh O, Michalski M, et al. Current applications an future impact of machine learning in radiology. 2018;288(2):318-328.

18. Chui M, Loeffler M, Roberts R. The Internet of Things. McKinsey Quarterly. March 2010. https://www.mckinsey.com/industries/high-tech/our-insights/the-internet-of-things. Accessed June 21, 2019.

19. Colombo, S. Chapter 4 - Applications of artificial intelligence in drug delivery and pharmaceutical development. 2020;85-116. https://doi.org/10.1016/B978-0-12-818438-7.00004-6

20. Çelik İ.N., Arslan F.K., Tunç R. et al. ARTIFICIAL INTELLIGENCE ON DRUG DISCOVERY AND DEVELOPMENT, 2021;45(2): 400-427.

21. D'Souza S., Prema K.V., Balaji S., Machine learning models for drug–target interactions: current knowledge and future directions, 2020;25(4):748-756.

22. Dana D., Gadhiya S.V., Surin L.G.ST. et al. Deep Learning in Drug Discovery and Medicine; Scratching the Surface. 2018;23(9):2384.

23. Das P.J., Preuss C., Mazumder B. Artificial Neural Network as Helping Tool for Drug Formulation and Drug Administration Strategies. 2016;263-276.

24. Deo R.C. Machine learning in medicine. 2015;132(20):1920-1930. https://doi.org/10.1161/CIRCULATIONAHA.115.001593

25. Dodd F.S., Target-based drug discovery: is something wrong?, 2005;10(2):139-147. https://doi.org/10.1016/S1359-6446(04)03316-1

26. Dreyfus S., The numerical solution of variational problems. 1962;5(1):30-45. https://doi.org/10.1016/0022-247X(62)90004-5

27. Bejnordi B.E., Veta M. et al. Diagnostic assessment of deep learning algorithms for detection of lymph node metastases in women with breast cancer. 2017;318(22):2199-2210.

28. Ekins S., The Next Era: Deep Learning in Pharmaceutical Research. 2016;33(11):2594-603. DOI: 10.1007/s11095-016-2029-7

29. Esteva A, Kuprel B, Novoa RA, et al. Dermatologist-level classification of skin cancer with deep neural networks. 2017;542(7639):115-118.

30. Fleming N., How artificial intelligence is changing drug discovery. 2018;557(7707):S55-S57. DOI: 10.1038/d41586-018-05267-x

31. Fukushima K., Neocognitron: a hierarchical neural network capable of visual pattern recognition. 1988;1(2):119–130. https://doi.org/10.1016/0893-6080(88)90014-7

32. Galata D.L., Könyves Z., Nagy B. et al., Real-time release testing of dissolution based on surrogate models developed by machine learning algorithms using NIR spectra, compression force and particle size distribution as input data. 2021;597:120338.

33. Ghasemi F., Mehridehnavi A., Garrido A.P. et al. Neural network and deep-learning algorithms used in QSAR studies: merits and drawbacks. 2018;23(10):1784-1790.

34. Ghourichay M.P., Kiaie S.H., Nokhodchi A. Formulation and Quality Control of Orally Disintegrating Tablets (ODTs): Recent Advances and Perspectives. 2021;24:2021:6618934.

35. Gilboa E., Saatçi Y., Cunningham J.P. Scaling Multidimensional Inference for Structured Gaussian Processes. 2015;37(2):424-36.

36. Goel A.K., Davies J. Artificial intelligence. In: Cambridge Handbook of Intelligence Cambridge. 2019.

37. Goodfellow I, Bengio Y, Courville A. Deep Learning. Cambridge, MA: MIT Press; 2016.

38. Gulsen V, Peng L, Coram M, et al. Development and validation of a deep learning algorithm for detection of diabetic retinopathy in retinal fundus photographs. 2016;316(22):2401-2410.

39. Gupta R., Srivastava D., Sahu M. et al. Artificial intelligence to deep learning: machine intelligence approach for drug discovery. 2021;25(3):1315-1360.

40. Gurung A.B., Ali M.A., Lee J. et al. An Updated Review of Computer-Aided Drug Design and Its Application to COVID-19. 2021; 24:2021:8853056.

41. Hamet P, Tremblay J., Artificial intelligence in medicine, 2017;69:S36-S40. https://doi.org/10.1016/j.metabol.2017.01.011

42. Hassanzadeh P., Atyabi F., Dinarvand R. The significance of artificial intelligence in drug delivery system design. 2019;151-159:169-190.

43. Haugeland J., Artificial Intelligence: The Very Idea. Cambridge, MA: MIT Press; 1985.

44. Heikamp K., Bajorath J. Support vector machines for drug discovery. 2014;9(1):93-104. doi: 10.1517/17460441.2014.866943.

45. Hessler G., Baringhaus K.H., Artificial Intelligence in Drug Design, 2018; 23(10):2520. https://doi.org/10.3390/molecules23102520

46. Hinselmann G., Rosenbaum L., Jahn A. et al. Large-Scale Learning of Structure−Activity Relationships Using a Linear Support Vector Machine and Problem-Specific Metrics. 2011;51(2):203-213.

47. Hinton G, Deng L, Yu D, et al. Deep neural networks for acoustic modeling in speech recognition: the shared views of four research groups. 2012;29(6):82-97.

48. Hinton G., Sejnowski T.J., Unsupervised Learning: Foundations of Neural Computation. Cambridge, MA: MIT Press; 1999.

49. Hirschberg J, Manning C.D. Advances in natural language processing. 2015;349(6245):261-266. https://doi.org/10.1126/science.aaa8685

50. Howard J. Artificial intelligence:Implications for the future of work. 2019; 62(11):917-926. https://doi.org/10.1002/ajim23037

51. Hughes J.P., Rees S., Kalindjian S.B. et al. Principles of early drug discovery. 2011;162(6):1239-49.

52. James G, Witten D, Hastic T, Tibshirani R. An Introduction to Statistical Learning. 2013;87.

53. Jeon J., Nim S., Teyra J. et al. A systematic approach to identify novel cancer drug targets using machine learning, inhibitor design and high-throughput screening. 2014; 6(7):57.

54. Jiang J., Ma X., Ouyang D.et al. , Emerging Artificial Intelligence (AI) Technologies Used in the Development of Solid Dosage Forms. 2022;14(11):2257.

55. Jordan A.M., Artificial Intelligence in Drug Design—The Storm Before the Calm? 2018; 9(12):1150-1152. doi: 10.1021/acsmedchemlett.8b00500.

56. Jordan M.I., Mitchell T.M., Machine learning: trends, perspectives, and prospects. 2015;349(6245):255-260. https://doi.org/10.1126/science.aaa8415

57. Jorgensen W.L., The Many Roles of Computation in Drug Discovery. 2004; 303(5665):1813-8. DOI: 10.1126/science.1096361

58. Kanagasingam Y., Xiao D., Vignarajan J. et al. Mehrotra A., Evaluation of artificial intelligence-based grading of diabetic retinopathy in primary care. 2018;1(5):e182665-e182671.

59. Kapetanovic I.M., Computer-aided drug discovery and development (CADDD): In silico-chemico-biological approach. 2008; 171(2):165-76. https://doi.org/10.1016/j.cbi.2006.12.006.

60. Katsila T., Spyroulias G.A., Patrinos G.P. et al. Computational approaches in target identification and drug discovery, 2016; 14: 177–184.

61. Kawato T., Mizohata T., Shimizu Y. et al. Structure-based design of a streptavidin mutant specific for an artificial biotin analogue. 2015;157(6):467-475.

62. Kehoe B, Patil S, Abbeel P. et al. A survey of research on cloud robotics and automation. 2015;12(2):398-409.

63. Kelley H.J., Gradient Theory of Optimal Flight Paths, 1960;30(10):947-954. https://doi.org/10.2514/8.5282

64. Kim S.B., Han K.S., Rim H.C. et al. Some Effective Techniques for Naive Bayes Text Classification. 2006; 18(11):1457-1466.

65. Knight W. Reinforcement learning: ten breakthrough technologies 2017. MIT Technol Rev. 2017. https://www.technologyreview.com/s/603501/10-breakthrough-technologies-2017-reinforcement-learning/.

66. Kononenko I. Machine learning for medical diagnosis: history, state of the art and perspective. 2001;23(1):89-109. doi: 10.1016/

s0933-3657(01)00077-x.

67. Korotcov A., Tkachenko V., Russo D.P. et al. Comparison of Deep Learning With Multiple Machine Learning Methods and Metrics Using Diverse Drug Discovery Data Sets. 2017;14(12): 4462–4475.

68. Krizhevsky A, Sutskever I, Hinton G. ImageNet classification with deep convolutional networks. Proceedings of Advances in Neural Information Processing Systems. 2012;25:1090-1098.

69. Lakhani P, Sundaram B. Deep learning at chest radiography: automated classification of pulmonary tuberculosis by using convolutional neural networks. 2017;284(2):574-582. doi: 10.1148/radiol.2017162326.

70. Lavecchia A., Deep learning in drug discovery: opportunities, challenges and future prospects, 2019;24(10): 2017-2032, https://doi.org/10.1016/j.drudis.2019.07.006

71. Lee J., Bogyo M., Target deconvolution techniques in modern phenotypic profiling, 2013;17(1):118-126, https://doi.org/10.1016/j.cbpa.2012.12.022

72. Lee I., Keum J., Nam H., DeepConv-DTI: Prediction of drug-target interactions via deep learning with convolution on protein sequences. 2019; 15(6): e1007129.

73. Lengauer T., Rarey M., Computational methods for biomolecular docking, 1996;6(3):402-406.https://doi.org/10.1016/S0959-440X(96)80061-3

74. Li X., Xu Y., Cui H. et al. Prediction of synergistic anti-cancer drug combinations based on drug target network and drug induced gene expression profiles. 2017;83:35-43.

75. Lipinski C.F., Maltarollo V.G., Oliveira P.R. et al. Advances and Perspectives in Applying Deep Learning for Drug Design and Discovery. 2019;5:6:108.

76. Lv B.M., Quan Y., Zhang H.Y. Causal Inference in Microbiome Medicine: Principles and Applications. 2021;29(8):736-746.

77. Mayr A., Klambauer G., Unterthiner T. et al. DeepTox: Toxicity Prediction using Deep Learning. Fronti-ers. 2016.

78. McFedries A., Schwaid A., Saghatelian A. Methods for the Elucidation of Protein-Small Molecule Interactions. 2013; 20(5):667-73.

79. Mencattini A., Giuseppe D.D., Comes M.C. et al. Discovering the hidden messages within cell trajectories using a deep learning approach for in vitro evaluation of cancer drug treatments. 2020; 10(1):7653.

80. Mohamed C., Nsiri B., Abdelmajid S. et al. Deep Convolutional Networks for Image Segmentation: Application to Optic Disc detection. FLORIDA INTERNATIONAL UNIVERSITY, July 24,2020.

81. Muegge I., Bergner A., Kriegl J.M., Computer-aided drug design at Boehringer Ingelheim, 2017;31(3): 275-285.

82. Mukhamediev R.I., Popova Y., Kuchin Y. et al. Review of Artificial Intelligence and Machine Learning Technologies: Classification, Restrictions, Opportunities and Challenges. 2022;10(15):2552.

83. Nag A, Mukhopadhyay SC, Kosel J. Wearable flexible sensors: a review. 2017;17(13):3949-3960.

84. Navya K., Kamaraj R., Bharathi M., The Trending Role of Artificial Intelligence and Its Applications in Formulation of Solid Dosage Forms: A Review. 2022;107(1):20049.

85. Nicolaou C.A., Brown N. Multi-objective optimization methods in drug design. 2013;10(3):e427-e435, https://doi.org/10.1016/j.ddtec.2013.02.001

86. Notodiputro K.A., Sartono B., Zubedi F. Implementation of Winsorizing and random oversampling on data containing outliers and unbalanced data with the random forest classification method. 2022;22(2),108-116.

87. Obermeyer Z, Emanuel EJ. Predicting the future—big data, machine learning, and clinical medicine. 2016;375(13):1216-1219. https://doi.org/10.1056/NEJMp1606181

88. Öztürk H., Özgür A., Ozkirimli E. DeepDTA: deep drug–target binding affinity prediction. 2018; 34(17):i821-i829.

89. Park H., Chien P.N., Ryu S.E. Discovery of potent inhibitors of receptor protein tyrosine phosphatase sigma through the structure-based virtual screening. 2012;22(20):6333-6337.

90. Patel L., Shukla T., Huang X. et al. Machine Learning Methods in Drug Discovery. 2020; 25(22): 5277.

91. Paul D., Sanap G., Shenoy S. et al. Artificial intelligence in drug discovery and development. 2021;26(1):80-93.

92. Pervan G., Willcocks L.,. Introduction to the special issue on decision support systems. 2005;20:65-66.

93. Phillips-Wren G. AI tools in decision support systems: a review. 2012;21(2):1240005.

94. Poplin R, Varadarajan AV, Blumer K, et al. Prediction of cardiovascular risk factors from retinal fundus photographs via deep learning. 2018;2(3):158-164.

95. Pratt G.A. Is a Cambrian explosion coming for robotics? 2015;29(3):51-60. https://pubs.aeaweb.org/doi/pdfplus/10.1257/jep.29.3.51.

96. Pun F.W., Ozerov I.V., Zhavoronkov A., AI-powered therapeutic target discovery. 2023; 44(9):561-572.

97. Qureshi R., Zou B., Alam T. et al. Computational Methods for the Analysis and Prediction of EGFR-Mutated Lung Cancer Drug Resistance: Recent Advances in Drug Design, Challenges and Future Prospects. 2023; 20(1):238-255.

98. Ragoza M., Hochuli J., Idrobo E. et al. Protein–Ligand Scoring with Convolutional Neural Networks. 2017; 57(4):942-957.

99. Rahman R., Dhruba S.R., Ghosh S., Pal R. Functional random forest with applications in dose-response predictions, Scientific Reports. 2019;9 (1):1628.

100. Ratanamahatana C., Gunopulos D. Feature selection for the naive bayesian classifier using decision trees. 2003;17:475-487.

101. Rathi P.C., Ludlow R.F., Verdonk M.L. Practical High-Quality Electrostatic Potential Surfaces for Drug Discovery Using a Graph-Convolutional Deep Neural Network. 2020;63(16):8778–8790,

102. Reddy A.S., Zhang S. Polypharmacology: drug discovery for the future. 2013;6(1):10. doi: 10.1586/ecp.12.74

103. Reher R., Kim H.W., Zhang C. et al. , A Convolutional Neural Network-Based Approach for the Rapid Annotation of Molecularly Diverse Natural Products. 2020;142(9):4114-4120.

104. Rifaioglu A.S., Atas H., Martin M.J. et al. , Recent applications of deep learning and machine intelligence on in silico drug discovery: methods, tools and databases. 2019;20(5):1878-1912.

105. Rosenblatt F (1957) The Perceptron: A Perceiving and Recognizing Automaton, Report 85–60–1.

106. Russel S.J., Norvig P., Artificial Intelligence A Modern Approach Third Edition, 2003.

107. Sarica A., Ceresa A., Quattrone A. Random Forest Algorithm for the Classification of Neuroimaging Data in Alzheimer's Disease: A Systematic Review. 2017; 6:9:329.

108. Sarkar C., Das B., Rawat V.S. et al. Artificial Intelligence and Machine Learning Technology Driven Modern Drug Discovery and Development. 2023; 24(3):2026.

109. Schenone M., Dančík V., Wagner B.K. et al. Target identification mechanism of action in chemical biology and drug discovery. 2013; 9(4):232-40.

110. Siepmann, J., Siepmann, F. Modeling of Diffusion Controlled Drug Delivery. 2012;161(2):351–362. https://doi.org/10.1016/j.jconrel.2011.10.006

111. Sliwoski G., Kothiwale S., Meiler J. et al. Computational Methods in Drug Discovery. 2014;66(1):334-395.

112. Sun H. A Naive Bayes Classifier for Prediction of Multidrug Resistance Reversal Activity on the Basis of Atom Typing. 2005;48(12):4031–4039. https://doi.org/10.1021/jm050180t

113. Sutton R.S., Barto A.G., Reinforcement Learning: An Introduction. 2nd ed. Cambridge, MA: MIT Press; 2018.

114. Swinney D.C. Phenotypic vs. Target-Based Drug Discovery for First-in-Class Medicines. 2013; 93(4):299-301. https://doi.org/10.1038/clpt.2012.236

115. Swinney D.C., Anthony J. How were new medicines discovered? 2011;10(7):507–519. DOI: 10.1038/nrd3480

116. Tajbakhsh N., Shin J.Y., Gurudu S.R. et al. Convolutional Neural Networks for Medical Image Analysis: Full Training or Fine Tuning? 2016;35(5):1299-1312.

117. Tan M. Prediction of anticancer drug response by kernelized multitask learning. Artif Intell Med. 2016;73:70-77. https://doi.org/10.1016/j.artmed.2016.09.004

118. Terstappen G.C., Reggiani A. In silico research in drug discovery. 2001;22(1):23-26. DOI:https://doi.org/10.1016/S0165-6147(00)01584-4

119. Terstappen G.C., Schlüpen C., Raggiaschi R., Gaviraghi G. Target deconvolution strategies in drug discovery. 2007;6(11):891–903. DOI: 10.1038/nrd2410

120. Thorndike E. The Fundamentals of Learning. New York, NY: Teachers College Bureau of Publications; 1932.

121. Topol E. Deep Medicine: How Artificial Intelligence Can Make Healthcare Human Again. New York, NY: Basic Books; 2019.

122. Vamathevan J., Clark D., Czodrowski P. et al. Applications of machine learning in drug discovery and development. 2019;18(6):463-477.

123. Varian H. Artificial Intelligence, Economics, and Industrial Organizations. In: Agrawal A, Gans J, Goldfarb A, eds. The Economics of Artificial Intelligence: An Agenda. Chicago, IL: University of Chicago Press; 2019:399-422.

124. Vemula D., Jayasurya P., Sushmitha V. et al. CADD, AI and ML in drug discovery: A comprehensive review. 2023:181:106324.

125. Vora K.L., Gholap A.D., Jetha K. et al. Artificial Intelligence in Pharmaceutical Technology and Drug Delivery Design. 2023;15(7), 1916.

126. Wang S., Sim T.B., Kim Y.S. et al. Tools for target identification and validation. 2004; 8(4):371-7.

127. Wann F., Zeng J.M., 2016, Deep learning with feature embedding for compound-protein interaction prediction, doi: https://doi.org/10.1101/086033

128. Wann F., Zeng J.M. Deep learning with feature embedding for compound-protein interaction prediction. 2016. doi: https://doi.org/10.1101/086033

129. Waring M.J., Arrowsmith J., Leach A.R. et al. An analysis of the attrition of drug candidates from four major pharmaceutical companies. Nature Reviews Drug Discovery,2015;14(7):475–486.

130. Wassermann A.M., Geppert H., Bajorath J. Application of Support Vector Machine-Based Ranking Strategies to Search for Target-Selective Compounds. Methods Mol Biol. 2011:672:517-30.

131. West DM, Allen JR. How Artificial Intelligence is Transforming the World. Access date: April 24, 2018. Access Adress: https://www.brookings.edu/research/how-artificial-intelligence-is-transforming-the-world/.

132. Yamashita R., Nishio M., Do R.K.G. et al. Convolutional neural networks: an overview and application in radiology. 2018; 9(4):611-629.

133. Yang X., Wang Y., Byrne R. et al. Concepts of Artificial Intelligence for Computer-Assisted Drug Discovery. 2019;119(18): 10520–10594.

134. Yu W., MacKerell A.D., Computer-Aided Drug Design Methods. 2017;1520:85-106. doi: 10.1007/978-1-4939-6634-9_5

135. Zang Q., Mansouri K., Williams A.J. et al. , In Silico Prediction of Physicochemical Properties of Environmental Chemicals Using Molecular Fingerprints and Machine Learning. 2017;57(1):36-49.

136. Zhang L., Tan J., Dan H. et al. From machine learning to deep learning: progress in machine intelligence for rational drug discovery. 2017;22(11):1680-1685.

137. Zhou, Y., Wang, F., Tang, J. et al. Artificial intelligence in COVID19 drug repurposing. The Lancet Digital Health, 2020;2(12): e667–e676.

HİTİT JOURNAL OF SCIENCE

Structural Characterization of Complexes Formed by Cadmium (II) Transition Metal with Schiff Bases

Şenol YAVUZ[1,*] ⓘ | Dursun Ali KÖSE[2] ⓘ

[1]Department of Property Protection and Security, Osmancık Ömer Derindere Vocational School, Hitit University, 19030, Corum, Türkiye.
[2]Department of Chemistry, Science & Arts Faculty, Hitit University, 19030,Corum, Türkiye.

Corresponding Author
Şenol YAVUZ
E-mail: fenol34@msn.com Phone: +90 535 213 6271
RORID: ror.org/01x8m3269

Cite As
Yavuz Ş, Köse D.A. Structural Characterization of Complexes Formed by Cadmium (II) Transition Metal with Schiff Bases. 2024;1(1):22-28.

Peer Review: Evaluated by independent reviewers working in at least two different institutions appointed by the field editor.
Ethical Statement: Not available.
Plagiarism Checks: Yes - iThenticate
Conflict of Interest: The authors have no conflicts of interest to declare.

CRedit Author Statement
1st Author: Writing the article, Synthesis of Schiff base and preparation of metal complexes, Interpretation of FTIR and NMR analyses and characterization study, **2nd Author:** Structural characterization of Cd metal complexes, Investigation of metal complexes' thermal stability, and evaluation of elemental analysis results.

Structural Characterization of Complexes Formed by Cadmium (II) Transition Metal with Schiff Bases

Şenol YAVUZ[1,*] (iD) | Dursun Ali KÖSE[2] (iD)

[1]Department of Property Protection and Security, Osmancık Ömer Derindere Vocational School, Hitit University, 19030, Corum, Türkiye.
[2]Department of Chemistry, Science & Arts Faculty, Hitit University, 19030,Corum, Türkiye.

Abstract

Schiff bases are condensation product compounds obtained from the reaction of carbonyl group compounds with primary amines. The C=N bond formed due to the reaction is called the azomethine bond or imine bond. Coordination compounds formed by Schiff bases with metals have broad application areas and play essential roles as catalysts, biological agents, analytical reagents, materials, and environmental solutions. These compounds' various chemical and physical properties increase their importance in basic science research and industrial applications. In this study, Schiff base ligands (3,5) were synthesized from the reaction of vanillin, an aldehyde compound, with primary amines in an acidic medium. The structure of the synthesized Schiff base ligands was characterized by ^{1}H NMR, ^{13}C NMR, and FTIR spectroscopy, and new metal complexes (6,7) were synthesized from the reaction with cadmium metal salt ($Cd(NO_3)_2$). The structures of the synthesized metal complex compounds were characterized by elemental analysis, FTIR, and thermogravimetric analysis, and their properties were investigated. These findings suggest that it has the potential to be used in various technological and industrial applications.

Keywords: Schiff Base, Cadmium (II), Ligand, Metal Complex, Thermal Stability,

INTRODUCTION

German chemist Hugo Schiff synthesized Schiff bases in 1869[1]. Schiff bases are compounds obtained by condensing carbonyl groups of aldehydes or ketones with imine or azomethine groups under certain reaction conditions of primary amines (Figure 1)[2]. Schiff base reactions are highly efficient and easy reactions. Schiff bases are prone to form complexes by reacting with almost all metals thanks to the nitrogen atom in the imine group, phenoxyl hydrogen in the structure, sulfur atom in the thiol group, and electron-donating atoms of carboxyl groups [3-7].
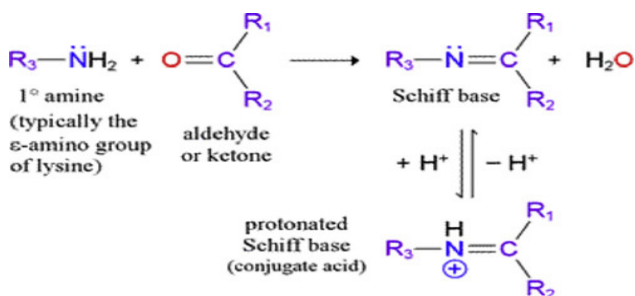
Figure 1. General scheme of Schiff base synthesis

Although there are many aldehyde and amine compounds, the stability of Schiff bases obtained from the reaction of these aldehyde compounds is different [8]. For the synthesized Schiff base ligands to be stable, the presence of a substituted group adjacent to the azomethine group and a second substitutable hydroxyl group increases the stability of the ligand[9]. For Schiff bases to show the best ligand properties, substituted groups such as -OH, $-NH_2$, -SH, and $-OCH_3$ should be attached to the imine group in the ortho state. Due to the structural and biological properties of Schiff bases, they were first studied in coordination chemistry with metal complexes by Pfeiffer in 1933 [10,11,12].

The structure of the complex formed by the ligand with metals is shaped by the metal salt, the mole ratio of the ligand and the metal salt, and the structure of the molecules. The stability of complexes formed by metals with multivalent ligands increases[13]. It is stated that the stability of Schiff bases is due to the Lewis base property due to the unshared electron pair on the nitrogen atom in the imine group, which forms stable

compounds by coordinated covalent bonding with metal salts. Schiff bases are generally shown as RCH=N-Ar. R in the formula is aryl alkyl or alkyl substituents.

Schiff bases and the metal complexes they form have many uses. Metal complexes are pigment dyestuffs in textile dyeing since they show dyestuff properties. Depending on the structure of the groups in the benzene ring in the structure of Schiff bases, ligands showing inhibition properties are also used as inhibitors [14,15]. Schiff base ligands have roles in oxidizing biologically active molecules such as free oxygen, ascorbic acid, catechol, and amino acids by forming coordination compounds with metals[16,17]. Metal complexes of ligand compounds containing heterocyclic thio semicarbazides are used in health treatment due to their antitumor, bacterial, and antiviral properties[17]. In addition, it is known that platinum complexes show antitumoural activity and nitro and halo derivatives show both antimicrobial and antitumoural activity[18,19,20]. In studies with oxo-vanadium(IV) and oxo-vanadium(V) complexes of Schiff base ligands, it was observed that the compounds were particularly influential on plant pathogens Agrobacterium Tumefaciens and Helminthosporium Oryzae [21]. It is also known that ninhydrin and glycine derivative Schiff base metal (Co(II), Ni(II), Zn(II)) complexes are effective on Escherichia coli, Proteus Mirabilis, Staphylococcus Aureus and Streptococcus faecalis [22]. Ferrocene-based metal (II) Schiff base complexes were synthesized from ferrocenyl chalcone in a solvent-free medium and found antibacterial properties [23,24].

The complexes formed by Schiff bases with cadmium metal are important due to the special properties and application potential they provide in various fields. Here are some highlights of these complexes:

Catalytic Activity: Schiff base-cadmium complexes can be used as catalysts in organic synthesis. These complexes show high activity, especially in reactions such as oxidation, hydrogenation, and C-C bond formation [26].

Photophysical and Photochemical Properties: These complexes can be used in optoelectronic devices, photovoltaic cells, and light-emitting diodes (LEDs). Cadmium complexes can exhibit unique properties in light absorption and emission [27].

Therapeutic Applications: Some Schiff base-cadmium complexes are being investigated in the biomedical field as anticancer, antibacterial, and antifungal agents. The biological activity of these complexes allows their use in treating certain diseases [28].

Supermolecular Chemistry: Schiff bases and cadmium can create supermolecular structures and materials. Such structures are essential in molecular recognition, sensors, and materials science [29].

Real-World Environmental Applications: The use of cadmium-containing Schiff base complexes for the removal of heavy metal ions and environmental pollution is not just theoretical. These complexes hold the potential to revolutionize water treatment processes, making a tangible impact on our environment [30].

Coordination Chemistry and Structural Diversity: The complex structures of Schiff base and cadmium show diversity in coordination chemistry and form the basis for synthesizing new complexes. The structural properties of these complexes open the door to new research in chemistry and materials science [31].

For these reasons, the complexes formed by Schiff bases with cadmium metal play an essential role in academic research and industrial applications.
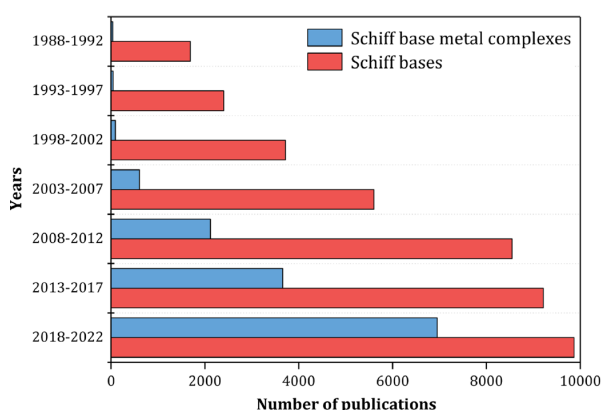
Figure 2. The data of studies with Schiff Bases between 1988 and 2022 [32]

MATERIALS AND METHODS
Materials: The chemicals o-vanillin, 3-amino-4-hydroxy benzene sulphonic acid, and 2-amino-4,5-dimethoxy benzoic acid were used as starting material in the synthesis of Schiff base ligand and metal salt ($Cd(NO_3)_2$) used in the synthesis of the metal complex. Sigma-Aldrich, ethyl alcohol, acetic acid, and methanol solvents used were supplied by Merck. The UV lamp, CAMAG Muttenz-Schweiz 29200, and melting point apparatus, Büchi SMP 20, were used to elucidate the melting points of the synthesized ligands [7]. Infrared spectra were taken from 400 to 4000 cm-1 using a Thermo Scientific Nicolet 6700 FTIR spectrometer. ^{1}H and ^{13}C NMR spectra of the synthesized Schiff bases (**3,5**) were obtained with a liquid Bruker 400MHz AV model NMR spectrometer with a 400 MHz operating frequency. The obtained metal complexes (**6,7**)

were thermally analyzed using the TA Instruments brand and the Q600 SDT (Simultaneous DSC/DTA/TGA) model device. The percentage of elements in the complexes' structures was determined by the Leco brand Truspec Micro Elemental Device.

Metods: In a 100 mL reaction flask, the aldehyde compound was dissolved in 30 mL ethyl alcohol. Then, the amine compound was added at a molar ratio 1:1. The mixture was stirred until completely dissolved. While the reaction mixture was stirred under a cooler, 1-2 drops of acetic acid were added to the reaction flask to maintain the pH around 4-5. The reaction mixture was stirred under a cooler for 12 hours, and after precipitation with water, the solid fraction was obtained by filtration. The solid portion was dried, and FTIR spectroscopy was used to determine whether the reaction occurred [2,7,8]. Schiff base was added to a 100 mL reaction flask and 30 mL of methanol solvent was added to dissolve the Schiff base. $Cd(NO_3)_2$ metal nitrate salt was dissolved in ethanol solvent in a beaker and added to the reaction flask. The reaction mixture was stirred under reflux for 12 hours, and after precipitation with water, the solid was filtered and purified by washing in methanol solvent to obtain cadmium complexes [7,8,10].

SYNTHESIS AND ANALYSIS OF SCHIFF BASE
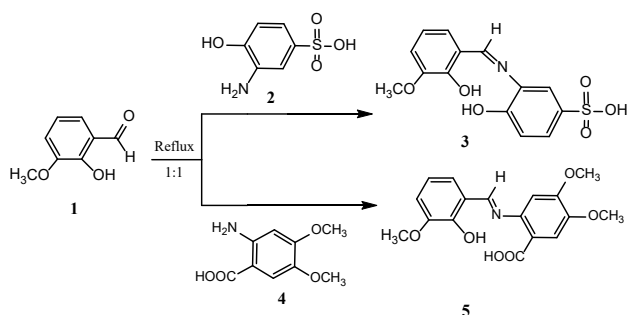4-hydroxy-3-((2-hydroxy-3-methoxybenzylidene)amino) benzenesulfonic acid (3)

4- hydroxy-3-((2-hydroxy-3-methoxybenzylidene)amino) benzenesulfonic acid (**3**) ligand was synthesized from the reaction of o-vanillin (**1**) (0.5g, 3.3 mmol) with 3-amino-4-hydroxybenzenesulfonic acid (**2**) (0.6g, 3.3 mmol) (Scheme 1).

3: Orange solid. E.N: 284.1°C, Yield: 0.6 g (% 56.6); IR (KBr): v = 3665, 3250 (O-H), v = 3159, 3100, 3068 (C-H$_{arom}$), v = 2933, 2846 (C-H), 1644 (HC=N), 1610 (C=C), 1233 (C-O); ^{1}H-NMR (400 MHz, CDCl$_3$): δ = 7.68, 7.57, 7.48, 7.40, 7.32, 7.26, 7.14, 6.92 (m, 6H, CH$_{arom}$), 9.09 (s, 1H, N=CH$_{imin}$), 9.73 (s, 1H, S-OH), 10.28, 10.86 (s, 2H, C$_{fenil}$-OH), 3.86 (s, 3H, -OCH$_3$); ^{13}C-NMR (100 MHz, CDCl3): δ = 162.15 (C=NH), 152.09, 151.17, 148.82, 140.66, 127.33, 124.93, 122.96, 119.67 (C$_{arom}$), 56.55 (OCH$_3$).

(E)-2-((2-hydroxy-3-methoxybenzylidene)amino)-4,5-dimethoxybenzoic acid (5)

(E)-2-((2-hydroxy-3-methoxybenzylidene)amino)-4,5-dimethoxybenzoic acid (**5**) ligand was synthesized from the reaction of o-vanillin (1) (0.5g, 3.3 mmol) with 2-amino-4,5-dimethoxybenzoic acid (4) (0.65g, 3.3 mmol) (Scheme 1).

5: Yellow solid. E.N: 218.2°C. Yield: 0.95g (% 88). IR (KBr): v = 3542, 3136 (O-H), v = 3074, 3008 (C-H$_{arom}$), v = 2985, 2943, 2901 (C-H), 1687 (C=O), 1604 (HC=N), 1513 (C=C), 1215 (C-O); ^{1}H-NMR (400 MHz, CDCl$_3$): δ = 10.28 (s, 1H, COOH), 8.92 (s, 1H, -NCH$_{imin}$), 7.46, 7.20, 7.07, 6.87 (m, 4H, CH$_{phenyl}$), 3.91, 3.87, 3.80 (m, 9H, -OCH$_3$); ^{13}C-NMR (100 MHz, CDCl3): δ = 167.49 (COOH), 162.06 (HC=N), 153.06, 150.98, 148.53, 142.38, 124.01, 120.59, 119.99, 115.76, 99.52 (C$_{arom}$), 56.55 (OCH$_3$).

**Scheme 1.** Synthesis scheme of shiff base ligands

SYNTHESIS AND ANALYSIS OF CD(II) METAL COMPLEXES

bis(4-hydroxy-3-((2-hydroxy-3- methoxybenzylidene)amino)benzenesulfonato -κO,κN,κO')cadmium(II) monoethanol (6)

Bis(4-hidroksi-3-((2-hidroksi-3-metoksibenziliden)amino) benzensulfonato-κO,κN,κO')cadmium (II) mono ethanol (6) complex was synthesized from the reaction of 4-hydroxy-3-((2-hydroxy-3-methoxy benzylidene)amino)benzenesulfonic acid (3) (1g, 3.1 mmol) ligand and Cd(NO3)2 (2) (0.95 g, 3.1 mmol) salt (Scheme 2).

6 : Orange solid. E.N: 372°C. Yield: 0.52g (% 20). IR (KBr): ν = 3542, 3136 (O-H), ν = 3074, 3008 (C-H$_{arom}$), ν = 2985, 2943, 2901 (C-H), 1636 (HC=N), 1494 (C=C), 1220 (C-O).
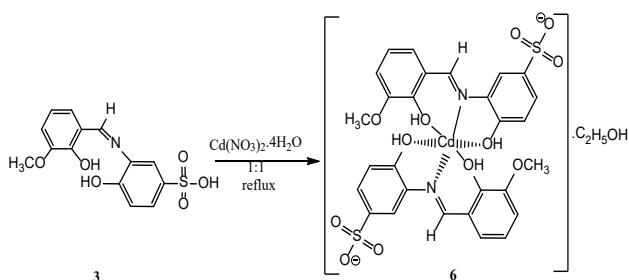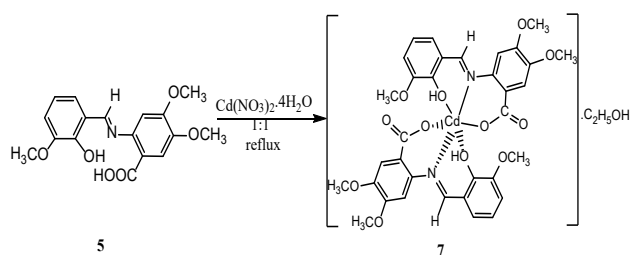

Scheme 2. Synthesis of bis(4-hydroxy-3-((2-hydroxy-3-methoxybenzylidene)amino)benzenesulfonato-κO,κN,κO')cadmium (II) monoethanol (6) complex

bis(2-((2-hydroxy-3-methoxybenzylidene)amino)-4,5-dimethoxybenzoato-κO,κN,κO')cadmium(II) monoethanol (7)

bis(2-((2-hydroxy-3-methoxybenzylidene)amino)-4,5-dimethoxybenzoato-κO,κN,κO') cadmium (II) monoethanol (7) complex was synthesized from the reaction of 4(E)-2-((2-hidroksi-3-metoksibenziliden)amino)-4,5-dimetoksibenzoik acit (5) (1 g, 3.1 mmol) ligand and Cd(NO$_3$)$_2$ (2) (0.96g, 3.1 mmol) salt (Scheme 3).

7 : Red solid. E.N: 219-202°C Yield: 0.56g (% 22). IR (KBr): ν = 3669, 3313 (O-H), ν = 3059, 3007 (C-H$_{arom}$), ν = 2964, 2937, 2835 (C-H), 1628 (C=O), 1543 (HC=N), 1362 (C=C), 1268 (C-O).

Scheme 3. Synthesis of bis(2-((2-hydroxy-3-methoxybenzylidene)amino)-4,5-dimethoxybenzoato-κO,κN,κO') cadmium (II) monoethanol (7) complex

Elemental Analysis of Cd(II) Metal Cation-Centred Complexes

According to the results of elemental analysis of metal-centered complexes formed by 4-hydroxy-3-((2-hydroxy-3-methoxybenzylidene)amino)benzenesulfonic acid (3) and (E)-2-((2-hydroxy-3-methoxybenzylidene)amino)-4,5-dimethoxybenzoic acid (5) ligands with Cd(II) metal cation, the theoretical and experimental results of C, H, N, S data support each other. Although elemental analysis alone is insufficient, it was determined that complexes were obtained when supported by other analyses. Table 1 shows the results of the analyses.

Table 1. Elemental analysis data of Cd(II) metal cation-centred complexes

Complex Molecule	C (%)		H (%)		N (%)		S (%)	
	Exp.	Calc.	Exp.	Calc.	Exp.	Calc.	Exp.	Calc.
(**6**)C$_{30}$H$_{30}$CdN$_2$O$_{13}$S$_2$	45.12	44.87	4.48	3.77	3.40	3.49	8.08	7.98
(**7**) C$_{36}$H$_{38}$CdN$_2$O$_{13}$	52.79	52.01	5.43	4.68	3.50	3.42	-	-

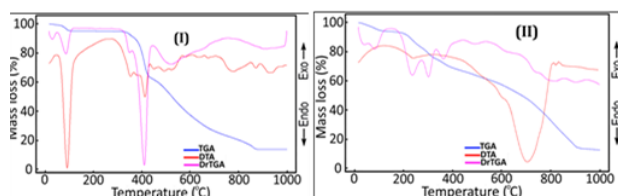## Thermal Analysis of Cd(II) Metal Cation Centred Complexes

Thermal analysis curves (TGA/DTA/DrTG) of the coordination compounds of Shiff base ligands with Cd(II) metal cations as center atoms are given in Figure 3. All data on the thermal decomposition steps and decomposition products generated from the thermal analysis curves are summarised in Table 2. The complex (I) with 4-hydroxy-3-((2-hydroxy-3-methoxybenzylidene)amino)benzenesulfonic acid (3) ligand has five degradation steps, while the complex (II) containing (E)-2-((2-hydroxy-3-methoxybenzylidene)amino)-4,5-dimethoxy benzoic acid (5) ligand was found to degrade in four steps.

It is suggested that ethyl alcohol, used as the synthesis solution in the synthesis of the complexes, binds to the structures by hydrogen bonds and settles outside the coordination sphere. The bonding of ethyl alcohol to the outside of the coordination sphere by hydrogen bonding occurs due to the formation of hydrogen bonds, steric hindrances, solvent interactions, and electron density distribution. These interactions affect the behavior and stability of Shiff base complexes in solution.

Ethyl alcohol can form hydrogen bonds through the hydrogen atom in the -OH group. This hydrogen bond interacts with the appropriate electron pair donors near the Shiff base

complex. These bonds usually form outside the coordination sphere because ethyl alcohol is a solvent that does not bind directly to the coordination center [33-34]. Our suggestion is supported by the fact that the weight losses observed in the first decomposition steps of both complexes (43-120°C and 37-125°C, respectively) are consistent with the theoretical and experimental weight losses of ethyl alcohol (For structure 6, exp.: 5.02%; theo. 5.73% and For structure 7, exp.: 5.10%; theo. 5.62%). The subsequent degradation steps for both structures include data on the thermal degradation of the organic ligands (Table 2).

The conclusion that CdO remains in the reaction vessel as the final residual product of the thermal decomposition of complex six at 881°C is also in agreement with the theoretical and experimental weight losses (exp.: 16.96%; theo.: 15.99%). Similarly, the conclusion that CdO oxide remained as the final decomposition product as a result of the thermal decomposition of complex seven at 912°C was inferred from the agreement between the theoretical and experimental weight losses of the final decomposition product (exp.: 16.58%; theo.: 15.68%). The data that the final decomposition products were CdO were also supported by powder XRD patterns. A difference of approximately 1% was observed between the theoretical and experimental weight losses of both final decomposition products. This was attributed to the lack of sufficient oxygen in the structures during thermal degradation in an inert nitrogen atmosphere and to the fact that the carbon residue of the organic ligand could not complete combustion, and some of it was deposited on the metal oxide residues in the form of carbonized carbon. The black color of the final decomposition products, which were expected to be white, also supports this interpretation.

Figure 3. Thermal curves of Cd(II) metal cation-centered Schiff base complexes.

RESULT AND DISCUSSION

The characteristic structures of the synthesized Schiff base ligands were elucidated by Infrared Spectroscopy and ^{1}H and ^{13}C-NMR spectra. Ligands with an imine group were obtained from the reaction of aldehyde compounds with a carbonyl group in Schiff bases and primary amines in the essential medium. The absorption stretching band of the imine group of 4-hydroxy-3-((2-hydroxy-3-methoxybenzylidene)amino) benzenesulfonic acid (3) ligand was detected at 1644 cm-1 in infrared spectroscopy, while the stretching band of (E)-2-((2-hydroxy-3-methoxybenzylidene)amino)-4,5-dimethoxybenzoic acid (5) ligand was detected at 1604 cm^{-1}. In addition, in the ^{1}H-NMR spectrum, the chemical shift of the imine group proton of 4-hydroxy-3-((2-hydroxy-3-methoxybenzylidene)amino) benzenesulfonic acid (3) was detected at 9.09 ppm and the chemical shift of E)-2-((2-hydroxy-3-methoxybenzylidene) amino)-4,5-dimethoxy benzoic acid (5) at 8.92 ppm. The occurrence of imine groups in different regions between the two ligands is due to the different electron affinity of the sulfonyl and carbonyl groups in the structure of the ligands. The carbonyl group is generally more electronegative than the sulfonyl group because the difference in electronegativity between carbon and oxygen is slightly higher than that between sulfur and oxygen. Therefore, the imine group of the ligand with the sulfonyl group shows a chemical shift in the lower field. The ligand 4-hydroxy-3-((2-hydroxy-3-methoxybenzylidene)amino)benzenesulfonic acid (3) is orange in color and has a higher melting point than E)-2-((2-hydroxy-3-methoxybenzylidene)amino)-4,5-dimethoxy benzoic acid (5) containing a carbonyl group. Since compounds with a sulfonyl group have higher polarity, the sulfonyl group gives the compounds a high dipole moment. Increasing the dipole-dipole interactions between the molecules can raise the melting point. In addition, hydrogen bonds also increase the melting point thanks to groups that can form hydrogen bonds in the compound. The melting point of 4-hydroxy-3-((2-hydroxy-3-methoxybenzylidene)amino)benzenesulfonic acid (3) is 284°C, while the melting point of E)-2-((2-hydroxy-3-methoxybenzylidene)amino)-4,5-dimethoxybenzoic acid (5) is 218°C. When the physical properties of Cd(II) metal cation complexes are examined, metal complex six is orange colored, and metal complex seven is red colored. As in the ligands, the melting point of metal complex six is 372°C due to the presence of a sulfonyl group in its structure. In contrast, the melting temperature of complex seven is lower at 219°C due

Tablo 2. Thermal decomposition data of Cd(II) metal cation-centered Schiff base complexes.

Compounds		Temp. range (°C)	DTA$_{max}$ (°C)	Removing group	Mass Loss (%)				Remaining Product (%)	Colour
					Exp.	Theo.	Exp.	Theo.		
(**6**) [Cd(C$_{14}$H$_{12}$NO$_6$S)$_2$](C$_2$H$_5$OH)										white
C$_{30}$H$_{30}$CdN$_2$O$_{13}$S$_2$	1	43-12	106	C$_2$H$_5$OH	5.02	5.73				
803,1 g/mol	2	310-384	365	2CH$_3$	4.08	3.74				
	3	385-441	393;424	2C$_7$H$_4$O	26.07	25.93				
	4	442-550	501;532	2SO$_2$	16.28	15.96				
	5	552-885	644;680;785;875	C$_6$H$_5$O;C$_6$H$_5$;2NO$_2$	31.59	32.65	16.96	15.99	CdO	black
(**7**) [Cd(C$_{17}$H$_{16}$NO$_6$)$_2$](C$_2$H$_5$OH)										pale-white
C$_{36}$H$_{38}$CdN$_2$O$_{13}$	1	37-125	46;91	C$_2$H$_5$OH	5.10	5.62				
819,11 g/mol	2	169-317	238;302	6CH$_3$O	23.22	22.72				
	3	319-575	364;488	2C$_7$H$_2$O	23.96	24.92				
	4	576-780	618;699;733	C$_7$H$_5$;NO$_2$;NO	31.14	31.04	16.58	15.68	CdO	black

to the presence of a carbonyl group in its structure and the absence of a sulfonyl group. Considering the thermal stability, the thermal stability of compound six is higher as complex six starts to decompose at 43°C while complex seven starts to decompose at 37°C. Experimental and theoretical data of C, H, and O ratios in elemental analyses support the structural characterization of the metal complexes.

The magnetic susceptibility of cadmium metal is shallow and negative, indicating that it is a diamagnetic material. Since the diamagnetic property of cadmium means that magnetic fields weakly repel it, the magnetic susceptibilities of the two metal complexes obtained were not examined. In the literature, magnetic susceptibility analysis of coordination compounds made with Mn^{2+}, Co^{2+}, Ni^{2+}, Cu^{2+}, and Zn^{2+} metal cations is carried out due to their high magnetic susceptibility, but not in coordination compounds formed with Cd^{+2} cation.

The nitrogen atom of the imine group in metal complexes has four bonds. Four bonding of the nitrogen atom in the imine group in metal complexes of Schiff bases can reduce nitrogen's stability by reducing its electron density, but this may vary depending on the complex's overall geometric and electronic properties. Metal-ligand interactions and ligand field effects are important factors determining the effect of nitrogen quadruple bonding on stability. The nitrogen atom usually forms three bonds, each carrying one free electron pair. The formation of a fourth bond requires nitrogen to use this free electron pair, which can affect nitrogen's electron density and, hence, stability. The formation of a fourth bond can cause the formal charge of nitrogen to become positive, reducing the electron density and lowering stability [35,36].

Schiff bases containing a sulfonyl group are generally more stable and chemically resistant. However, Schiff bases containing carboxy groups are more differentiated by specific reactions and complex formation capabilities. Schiff bases containing carboxy groups are primarily used in analytical chemistry and complex formation processes. In contrast, those containing sulfonyl groups are generally more stable, which is a difference in finding a wide range of applications.

CONCLUSION

Schiff base syntheses and coordination compounds formed with metals have different properties and application areas, which increases the importance of Schiff bases. Although there are many coordination compounds made with Mn^{2+}, Co^{2+}, Ni^{2+}, Cu^{2+}, and Zn^{2+} metal cations in the literature, it is an essential study in terms of introducing new coordination compounds to the literature with the new Schiff bases obtained and forming a complex with Cd^{+2}.

When Schiff base ligands are combined with cadmium(II) salt, such as cadmium nitrate, the nitrogen of the azomethine group forms a coordinative bond with the cadmium ion, binding to organic compounds. The stability and high coordination of these complexes are further enhanced if the Schiff base contains additional donor atoms, such as -OH or another nitrogen atom, which also bind to the cadmium ion. This robust bonding pattern instills confidence in the potential of these Schiff bases in forming stable and highly coordinated complexes.

REFERENCES

1. Schiff H. Untersuchungen über salicinderivate, Justus Liebigs Annalen der Chemie, 150 (2), 193-200, 1869.
2. Karaca Ö. Yeni Schiff bazı bileşiklerinin sentezi ve yapılarının aydınlatılması. Politeknik Dergisi 2018; 21(1): 245-249.
3. Abu-Dief AM, Mohamed IMA. A review on versatile applications of transition metal complexes incorporating Schiff bases. Beni-Suef University Journal of Basic and Applied Sciences 2015; 4(2):119-133.https://doi.org/10.1016/j.bjbas.2015.05.004.
4. Taşkın OK, Öztürk ÖF, Canpolat E. Yeni Bir Schiff Bazı ve Geçiş Metalleri İle Oluşturdukları Komplekslerin Sentezi ve Karakterizasyonu, Bitlis Eren Üniversitesi Fen Bilimleri Dergisi 2012; 1(1); 34-39.
5. Silva CM, Silva DN, Modolo LV, Alves RB, Resende MA, Martins CVB, Fatima A. Schiff Bases: a Short Review of Their Antimicrobial Activities 2, Cario University Journal of Advanced Research 2011;1-8.
6. Sılku P, Özkınalı S, Öztürk Z, Asan A., Köse DA. Synthesis of novel Schiff Bases containing acryloyl moiety and the investigation of spectroscopic and electrochemical properties, Journal of Molecular Structure 2016; 1116:72-83. https://doi.org/10.1016/j.molstruc.2016.03.028.
7. Özkınalı S, Yavuz Ş, Tosun T, Köse DA, Gür M, Kocaokutgen H. Synthesis, Spectroscopic and Thermal Analysis and Investigation of Dyeing Properties of o-Hydroxy Schiff Bases and Their Metal Complexes. ChemistrySelect 2020; 5(40): 12624-12634.
8. Koç E. Tripodal Schiff Bazlı Ligandların Sentezi ve Metal Komplekslerinin İncelenmesi. Doktora Tezi, Selçuk Üniversitesi Fen Bilimleri Enstitüsü, Konya ,2006.
9. Patai S. The Chemistry of Carbon-Nitrogen Double Bond. Interscience Publisher, London 1970; 360p.
10. Seçkin T, Köytepe S, Demir S, Özdemir İ, Çetinkaya B. Novel type of metal-containing polyimides for the heck and Suzuki-Miyaura cross-coupling reactions as highly active catalysts. J. Inorg. Organomet P. 2003;13(4): 223-235.
11. Ashraf M, Wajid A, Mahmood K, Maah M, Yusoff I. Spectral Investigation of the Activities of Amino Substituted Bases. Orient. J. Chem. 2011; 27: 363–372.
12. Soroceanu A, Bargan A. Advanced and Biomedical Applications of Schiff-Base Ligands and Their Metal Complexes: A Review. Crystals 2022.
13. Petrucci HR, Harwood SW, Herrıng GF, Qın W, Long S, Panunzıo M, Bıondı S, Schiff Bases: A Short Survey on an Evergreen Chemistry Tool. Molecules 2008; 18: 12264-12289.
14. Agrawal YK, Talati JD, Shah MD, Desai MN, Shah NK. Schiff bases of ethylenediamine as corrosion inhibitors of zinc in sulphuric acid. Corrosion Science 2004; 46(3): 633-651.
15. Desai MN, Desai MB, Shah CB, Desai SM. Schiff bases as corrosion inhibitors for mild steel in hydrochloric acit solutions. Corrosion Science 1986; 26: 827.
16. Niederhoffer EC, Timmons JH, Martell AE. Thermodynamics of oxygen binding in natural and synthetic dioxygen complexes. Chemical Reviews 1984; 84(2): 137-203.
17. Özşahin AD, Bozhan N. Bazı Schiff Bazlarının Saccharomyces cerevisiae BY4741 Kültür Ortamlarında Biyokimyasal Parametreler Üzerine Etkileri. Kahramanmaraş Sütçü İmam Üniversitesi Tarım ve Doğa Dergisi 2018;21(2): 131-140.
18. Karlin KD, Tyekkerz L. Bioorganic Chemistry of Cupper. Chapman and Hill, NewYork 1993.
19. Kuduk J, Trynda L. Impact of K2 PtCl6 on the structure of human serum albumin and its binding ability of heme and bilirubin. Journal of Inorganic Biochemistry 1994;53:4: 249-260.
20. Mohamed GG. Synthesis, characterization and biological activity of bis(phenylimine) Schiff base ligands and their metal complexes. Spectrochim. Acta A 2006; 64: 188.
21. Data S, Banerjee P, Banerjee RD, Sarkar GM, Saha SK, Dey K, Maiti RK, Sen RK, Bhar JK. Antimicrobial, insect sterilizing and ovicidal activity of some oxo-vanadium(IV) and oxo-vanadium(V) complexes. Agents Actions 1982;12(4): 543-51.
22. Rao NS, Reddy MG. Studies on the synthesis, characterisation and

antimicrobial activity of new Co(II), Ni(II) and Zn(II) complexes of Schiff base derived from ninhydrin and glycine. Biol. Met. 1990; 3(1):19-23.

23. Liu Y, Yang L, Yin D, Dang Y, Yang L, Zou Q, Li J, Sun J. Solvent-free synthesis, characterization, biological activity of schiff bases and their metal (II) complexes derived from ferrocenyl chalcone. Journal of Organometallic Chemistry 2019; 899: 120903.

24. Desai S, Desai P, Desai K. Synthesis of Some Schiff Bases,Thiazolidinones and Azetidinones Derived From 2,6-Diaminobenzo[1,2-D:4,5-D'] Bisthiazole and Their Anticancer Activities. Heterocyclic Communications 2001;7(1): 83-90. https://doi.org/10.1515/HC.2001.7.1.83

25. Boulechfar C, Ferkous H, Delimi A, Djedouani A, Kahlouche A, Boublia A, Benguerba, Y. Schiff bases and their metal Complexes: A review on the history, synthesis, and applications. Inorganic Chemistry Communications 2023; 150: 110451.

26. Bhattacharyya R, Roy AS. Catalytic Activity of Schiff Base Complexes in Organic Reactions. Journal of Catalysis and Chemical Engineering 2012; 14(2): 56-63.

27. De Vos DE, Verpoort F. Photophysical Properties of Schiff Base Metal Complexes. Coordination Chemistry Reviews 2003; 245(1-2): 149-160. DOI: 10.1016/S0010-8545(03)00251-5.

28. Da Silva CM, Da Silva DL, Modolo LV, Alves RB, De Resende MA, Martins CVB, De Fátima A. Schiff Bases: A Short Review of Their Antimicrobial Activities. Journal of Advanced Research 2011; 2(1): 1-8. DOI: 10.1016/j.jare.2010.05.004.

29. Atwood JL, Steed JW. Schiff Base Complexes in Supramolecular Chemistry. Supramolecular Chemistry 2004; 16(5): 399-409. DOI: 10.1080/10610270412331334021

30. Mohapatra M, Anand, S. Cadmium Schiff Base Complexes for Environmental Remediation. Journal of Environmental Chemical Engineering 2010; 3(2):89-97. DOI: 10.1016/j.jece.2010.02.005.

31. Sutradhar M. Coordination Chemistry of Schiff Bases: Structural Diversity and Applications. Coordination Chemistry Reviews 2017; 344: 276-299. DOI: 10.1016/j.ccr.2016.01.010.

32. Boulechfar C, Ferkous H, Delimi A, Djedouani A, Kahlouche A, Boublia A, Benguerba Y. Schiff bases and their metal Complexes: A review on the history, synthesis, and applications. Inorganic Chemistry Communications 2023;150:110451.

33. Mohamed G G, Omar MM, Hindy AM. Synthesis, characterization and biological activity of some transition metals with Schiff base derived from 2-thiophene carboxaldehyde and aminobenzoic acid. Spectrochimica Acta Part A: Molecular and Biomolecular Spectroscopy 2005; 62(4-5): 1140-1150.

34. Refat MS. Synthesis and characterization of some transition metal complexes with Schiff base ligand derived from 4,6-diacetylresorcinol. Journal of Molecular Structure 2007; 842(1-3): 24-37

35. Kaim W, Schwederski B, Klein A. Bioinorganic Chemistry--Inorganic Elements in the Chemistry of Life: An Introduction and Guide. John Wiley & Sons ;2013

36. Holleman AF, Wiberg E.Inorganic Chemistry. Academic Press; 2001.

Novel Al(III) and In(III) complexes containing acesulfame and nicotinamide/*N,N*-diethylnicotinamide ligands. Synthesis and structural characterization

Halide KUNDAKÇI[1] | Dursun Ali KÖSE[1,*]

[1]Hitit University, Department of Chemistry, Faculty of Arts and Sciences, Corum 19040, Türkiye.

Corresponding Author
Dursun Ali KÖSE
E-mail: dalikose@hitit.edu.tr Phone: +90 364 227 7000 (1634)
RORID: ror.org/01x8m3269

Cite As
Kundakçı H, Köse D.A. Novel Al(III) and In(III) complexes containing acesulfame and nicotinamide/N,N-diethylnicotinamide ligands. Synthesis and structural characterization. Hitit journal of Science. 2024;1(1):29-38

Peer Review: Evaluated by independent reviewers working in at least two different institutions appointed by the field editor.
Ethical Statement: Not available.
Plagiarism Checks: Yes - iThenticate
Conflict of Interest: Authors approve that to the best of their knowledge, there is not any conflict of interest or common interest with an institution/organization or a person that may affect the review process of the paper.

CRedit Author Statement
1st Author: Conceptualization, Methodology, Software, Validation, Writing-original draft. **2nd Author:** Data curation, Visualization, Investigation.

Novel Al(III) and In(III) complexes containing acesulfame and nicotinamide/*N,N*-diethylnicotinamide ligands. Synthesis and structural characterization

Halide KUNDAKÇI[1] (ID) | Dursun Ali KÖSE[1,*] (ID)

[1]Hitit University, Department of Chemistry, Faculty of Arts and Sciences, Corum 19040, Türkiye.

Abstract

Single-ligand (acesulfame) and mixed-ligand (acesulfame-nicotinamide/N,N-diethylnicotinamide) complexes of Aluminum (Al) and Indium (In) metal cations with 3+ oxidation steps in the 3A group, called earth metals, were synthesized and their structural characterizations were examined. The chemical compositions of the complexes were investigated by elemental analysis method, their binding properties by infrared and solid state UV-Vis spectroscopy, their degradation products analysis by GC-MS spectroscopy and their thermal behavior by TGA/DTA/DrTGA analysis. Acesulfame molecule, which is frequently used in industry, especially as an artificial sweetener, attracts attention as a valuable ligand in terms of coordination chemistry, thanks to the many electron-donating active groups it contains. It is also an easy ligand to work with, as it can form solids by precipitating to obtain a single crystal in coordination compounds. Although complex structures with transition metals are frequently found in the literature, studies on earth elements have not yet been found. It is important that the studies to be carried out in terms of characterization studies of the structures to be obtained and materials that can be used for industry contribute to the literature.

Keywords: Acesulfame, nicotinamide, N,N-diethylnicotinamide, structural characterization, coordination compounds, metal complexes

INTRODUCTION

Acesulfame, potassium acesulfame, a white, odorless, organic and synthetic salt, is a widely used but not metabolizable sweetener in many foods and beverages [1]. In terms of coordination chemistry, acesulfame ligand stands out as a very useful electron donor in the synthesis of inorganic and organometallic molecules [2]. Acesulfame, an oxathiazinone dioxide compound, is systematically named 6-methyl-1,2,3-oxothiazine-4(3H)-one-2,2-dioxide [3]. In addition to its industrial use, acesulfame attracts attention as an interesting ligand in metal complexes with its biological importance and good coordination properties. Discovered by German chemist Karl Clauss in 1967, acesulfame has been studied in fields such as biochemistry, food chemistry, inorganic chemistry, bioinorganic chemistry, analytical chemistry and pharmaceutical chemistry. Its best-known compound is the potassium salt potassium acesulfame (Ace-K) with a similar analogue, 5,6-dimethyl-1,2,3-oxathiazin-4(3H)-one-2,2-dioxide (Figure 1(a)) [4]. It was developed by Karl Clauss and Harald Jensen after the accidental discovery of acesulfame. In the field of inorganic chemistry, the first metal complexes of acesulfame were synthesized in 2005 [5,6]. In the following years, coordination compounds of the acesulfame ligand, especially those containing transition metal cations, were frequently studied [our articles]. Acesulfame is a functional ligand because it has multiple electron-donating groups, such as imine nitrogen, carbonyl oxygen, sulfonyl oxygen, or ring oxygen, on various metal atoms. Although complex structures with transition metal cations are available in the literature [2,3,5,6-12], studies on main group metal cations are quite limited [13-16]. Coordination compounds with earth metals are almost absent. In addition, complexes of some rare earth elements using acesulfame ligand as the electron-donating terminal group have been synthesized and structural studies have been carried out [17-19].

Nicotinamide (or niacinamide) is the amide form of nicotinic acid, or niacin, also known as vitamin B3. Nicotinamide is also called niacinamide, niacin, nicotine acid amide, vitamin PP. Although nicotinamide and nicotinic acid are identical vitamins, their pharmacological effects are very different from each other. Nicotinamide, which has the chemical formula $C_6H_6N_2O$ (Figure 1(b)), has a molecular weight of 122.12 g/mol and a melting point of 128-131°C. The IUPAC name of the compound is 3-pyridine carboxamide. It is a vitamin needed by humans for the production of hydrochloric acid, which is necessary for digestion, as well as for the metabolism of proteins, fats and carbohydrates. While its solubility in water is 100 g/100 ml at 20ºC, its solubility in ethanol is 666 g/100 ml. Moreover, it dissolves very slowly in ether and is insoluble in oils. Nicotinamide is a colorless, crystalline substance with a characteristic odor and taste. Since nicotinamide has a pyridine ring, it gives the same reactions specific to the pyridine ring [20]. It was realized approximately 40 years later that this compound, obtained as a result of the oxidation of nicotine, an alkaloid of tobacco, was a very important vitamin in 1887. The physical and chemical properties of nicotinic acid and nicotinamide, which have the same vitamin value, have been known for a long time [21].

The closed formula of the *N,N*-diethylnicotinamide compound is $C_{10}H_{14}N_2O$ and its molecular weight is 178.12 g/mol. The IUPAC name of the compound is 3-pyridine diethylcarboxamide. This compound, generally called *N,N*-diethylnicotinamide, also has trade names such as cordiamine and nicetamide. Although it has good solubility in water, it is insoluble in oils and ether. Figure 1(c) below shows the structure of *N,N*-diethylnicotinamide. Like nicotinamide, *N,N*-diethylnicotinamide is a colorless, crystalline substance with a unique odor and taste, and gives pyridine reactions due to its pyridine ring. There are many studies in the literature showing that nicotinamide and *N,N*-diethylnicotinamide acts as an electron donor to pyridine nitrogen [22-26]
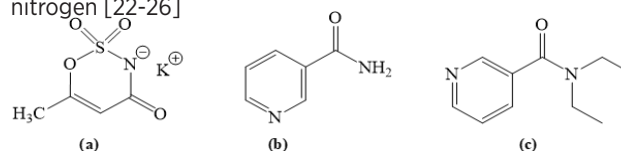
Figure 1. Molecular structures of the ligands of acesulfame anion (a), nicotinamide (b) and N,N-diethylnicotinamide (c).

Mixed ligand complexes containing earth metals (Al^{3+} and In^{3+}), which have not been studied in the literature, and acesulfame-nicotinamide or N,N-diethylnicotinamide were synthesized. The structures of the collected complexes were tried to be characterized by FT-IR spectroscopy, elemental analysis, thermal

analysis (TG-DTG and DTA) and mass spectroscopy techniques.

MATERYAL METOD

Synthesis

The synthesis reagents, ClO_4^- salts of Al^{3+} and In^{3+} metal cations, potassium acesulfame, nicotinamide and N,N-diethylnicotinamide ligands were obtained from Sigma-Aldrich. Pure water and absolute ethanol mixtures (50%:50%) were used as reaction media. For the synthesis, firstly, 1 mmol of potassium acesulfame was dissolved in 50 ml of distilled water in a beaker, and then 3 mmol of Al^{3+} and 3 mmol of In^{3+} were added to perchlorate salt to react. In the reaction, 1:3 (metal:acesulfame) ratio was taken as basis according to charge balance (Scheme 1). With the ethyl alcohol added to the reaction vessel, the potassium perchlorate salt was completely separated from the solution and precipitated. The potassium perchlorate salt precipitate was removed from the total solution by filtration. Care was taken to thoroughly wash the white potassium perchlorate precipitate with distilled water to prevent substance loss. 2 mmol of nicotinamide and N,N-diethylnicotinamide ligands solutions formed in ethyl alcohol were added separately to the acesulfame solutions of Al^{3+} and In^{3+} metal cations (Scheme 2).

The resulting final reaction solution was stirred on a magnetic stirrer for approximately 4 hours at 60 °C. Afterwards, the crystals that precipitated in approximately 3-5 weeks at room temperature with the lid closed were collected by filtration. The crystals were washed with pure water and dried in a vacuum oven at room temperature for analysis.
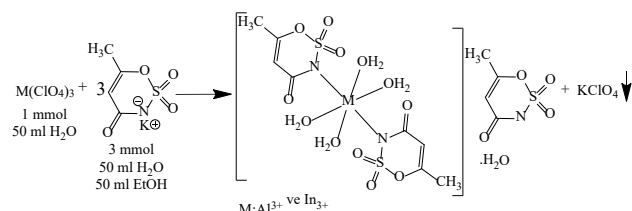
Scheme 1. Synthesis reaction of Al^{3+} and In^{3+} metal cations salts of acesulfame ligand.
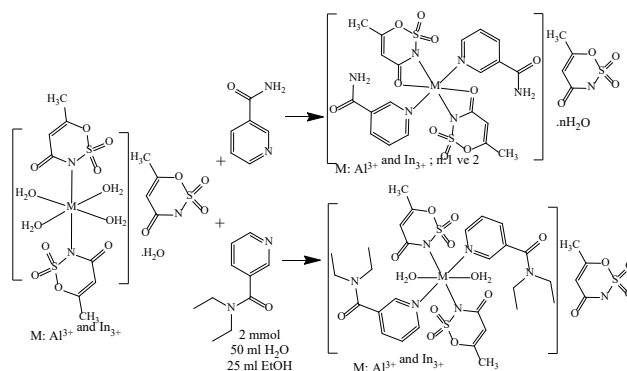
Scheme 2. Synthesis reaction of Al^{3+} and In^{3+} metal cation center complexes containing acesulfame and nicotinamide / N,N-diethylnicotinamide ligands.

Elemental Analysis

Elemental analysis results of metal-acesulfame-nicotinamide / N,N-diethylnicotinamide mixed ligand coordination compounds using Al^{3+} and In^{3+} earth metal cations as electron acceptors are summarized in Table 1. The colors of the complex molecules were determined as pale/off-white, as expected, depending on the electronic configurations of the central atoms in the 3+ oxidation state. Since the "d" orbitals of metal cations are filled, electronic transitions that cause color formation are prohibited. For this reason, color formation is not observed. However, slight impurity colors can be detected due to electronic transitions caused by charge transfer from the ligand to the metal. The agreement of experimental and theoretical results obtained from elemental analysis supports the molecule formulations proposed by us.

Infrared (FT-IR) Spectroscopy Studies

According to the FTIR spectra (Figure 2) recorded in the range of 4000 cm^{-1} – 400 cm^{-1}, it was found that -OH stretching bands originating from H_2O molecules appeared in the regions of approximately 3650 cm^{-1}-2850 cm^{-1} in all structures. While N-H stretches originating from nicotinamide were detected in the 3521 cm^{-1} and 3517 cm^{-1} bands in structures only I and II, the absence of any stretch peak belonging to this group in structures III and IV is evidence of the ionized coordination of the acidic N-H group in the ring of acesulfame ligands in all structures. The bending peaks of the N-H bonding of the amide group were also observed at 1586 cm^{-1} and 1588 cm^{-1}

Table 1. Chemical composition data of for mixed-ligand metal-acesulfame-nicotinamide and N,N-diethylnicotinamide complexes

Complex	M.A. (g/mol)	Yield	Content (%) exp. (theo.)				Colour	Decomp Temp. (°C)
			C	H	N	S		
$[Al(C_6H_6N_2O)_2 (C_4H_4NO_4S)_2](C_4H_4NO_4S).2H_2O$ $C_{24}H_{28}AlN_7O_{16}S_3$ **(I)**	793.68	85	36.12 (36.32)	3.87 (3.56)	12.21 (12.35)	12.39 (12.12)	White	77
$[In(C_6H_6N_2O)_2 (C_4H_4NO_4S)_2](C_4H_4NO_4S).H_2O$ $C_{24}H_{26}InN_7O_{15}S_3$ **(II)**	863.50	83	33.07 (33.38)	3.67 (3.03)	11.55 (11.35)	11.41 (11.14)	pale-white	88
$[Al(C_{10}H_{14}N_2O)_2(C_4H_4NO_4S)_2 (H_2O)_2](C_4H_4NO_4S)$ $C_{32}H_{44}AlN_7O_{16}S_3$ **(III)**	905.90	72	42.88 (42.43)	4.67 (4.90)	10.96 (10.82)	10.87 (10.62)	White	135
$[In(C_{10}H_{14}N_2O)_2(C_4H_4NO_4S)_2(H_2O)_2](C_4H_4NO_4S)$ $C_{32}H_{44}InN_7O_{16}S_3$ **(IV)**	993.74	70	39.75 (38.68)	4.63 (4.46)	9.98 (9.87)	9.47 (9.68)	pale-white	141

for complexes I and II, respectively. The presence of v(C-N-C)$_{ace}$ stretching peaks for acesulfame and pyridinic v(C-N-C)$_{pyrd}$ group observed in all structures support the existence of ligands in coordination compounds as in the proposed structural formulas. The fact that the numerical difference between the symmetric and asymmetric stretching vibrations of the -SO$_2$ groups is compatible with the difference in the potassium salt of acesulfame is evidence that coordination does not occur through this group. The most important evidence of the molecular formulations we propose is the presence of binding peaks in which the ligands coordinate with metal cations. Accordingly, v(M-N)$_{ace}$ stresses are 649 cm^{-1}-620 cm^{-1}, v(M-N)$_{pyrd}$ stresses are 673 cm^{-1}-648 cm^{-1}, v(M-O)$_{ace}$ stresses (only in structures I and II) 507 cm^{-1}-509 cm^{-1} and finally v(M-O)$_{aqua}$ stresses (only in structures III and IV) were detected in the 545 cm^{-1}- 543 cm^{-1} regions, respectively. Data on binding peaks showing the characteristic binding properties of all structures are summarized in Table 2.
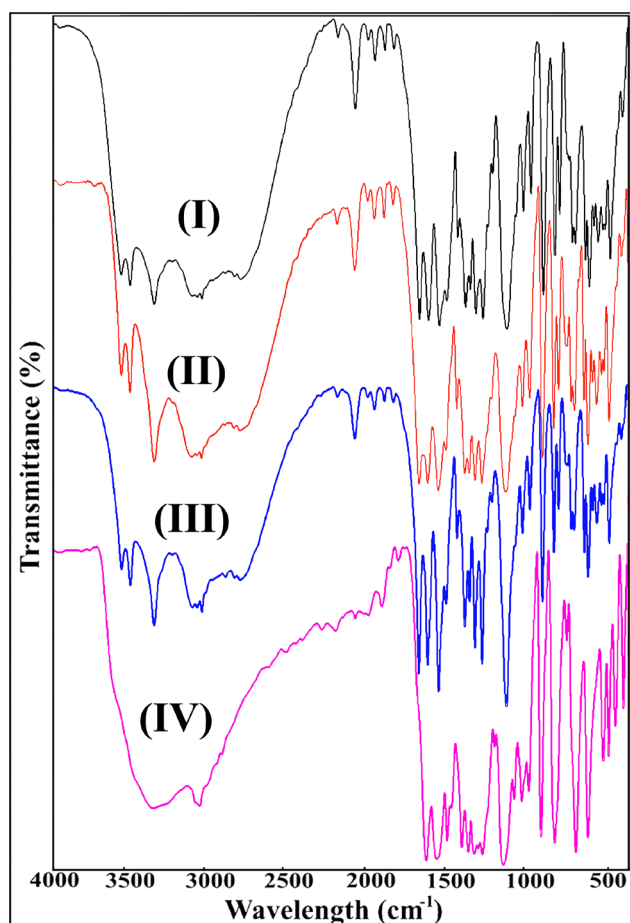
Figure 2. FTIR spectra of mixed-ligand metal-acesulfame-nicotinamide and *N,N*-diethylnicotinamide complexes

Table 2. Important infrared peak data for mixed-ligand metal-acesulfame-nicotinamide and *N,N*-diethylnicotinamide complexes

Groups	(I)	(II)	(III)	(IV)
v(OH)$_{H2O}$	3650-2850	3650-3150	3550-3150	3600-3050
v_{ger}(N–H)	3521	3517	-	-
v(=C–H)	3372	3370	3406	3401
v(C=O)$_{ace}$	1655	1654	1652	1650
v_{eg}(N–H)	1586	1588	-	-
v(C=C)	1540	1540	1554	1549
v(C-N-C)$_{ace}$	1357	1357	1363	1364
v(C-N-C)$_{pyrd}$	1393	1393	1394	1394
v_{as}(SO$_2$)/ v_s(SO$_2$)	1314/1162	1314/1165	1319/1173	1321/1175
v_{as-s}	152	149	146	146
v(ring)	1061-834	1060-833	1090-840	1093-842
v_s(CNS)/ v_{as}(CNS)$_{ace}$	1323/935	1321/934	1309/938	1310/938
v(C-N)	1013-735	1014-734	1014-723	1016-721
v(M-N)$_{ace}$	649	649	620	621
v(M-N)$_{pyrd}$	673	673	645	648
v(M-O)$_{aqua}$	-	-	545	543
v(M-O)$_{ace}$	507	509	-	-

Thermal Analysis Studies

Thermal analysis curves recorded in an inert nitrogen atmosphere in the temperature range of 25-1000 ºC are shown in Figure 3. The synthesized four different mixed ligand coordination compounds were classified as nicotinamide and N,N-diethylnicotinamide (III and IV) according to their secondary ligands. While the degradation characteristics of Al^{3+} (I) and In^{3+} (II) complexes containing nicotinamide are similar to each other, it has been determined that the degradation characteristics of Al^{3+} (III) and In^{3+} (IV) complexes containing N,N-diethylnicotinamide ligand are also similar. The decomposition of complexes I and II begins with the dehydration of the hydrate waters present in the structures. In complex I containing two hydrated waters, primary decomposition occurs with an experimental weight loss of 4.80% (theoretically 4.54%) in the temperature range of 48-101 ºC. In Structure II, the removal of hydrated water with a weight loss of 2.29% experimentally (2.09% theoretically) occurred in the temperature range of 68-140 ºC. In the secondary degradation step, the organic ligands for both structures begin to decompose. While the SO$_2$ groups of the three acesulfame ligands present in complex II are separated (142-241 ºC), the nicotinamide ligands in structure I are degraded. For structure I, the removal of SO$_2$ groups took place in the temperature region of 290-386 ºC. For structure I, the degradation of organic derivatives occurs via nicotinamide, while for structure II, this occurs via acesulfame ligands. The internal compatibility of the experimental and theoretical weight losses of the organic derivatives proposed for the degradation steps of organic ligands for both complexes supports the proposed degradation products (Table 3). While complex I completes its decomposition in six steps, structure II transforms into its oxide in five steps. The decompositions of

Novel Al(III) and In(III) complexes containing acesulfame and nicotinamide/N,N-diethylnicotinamide ligands. Synthesis and structural characterization

coordination compounds with N,N-diethylnicotinamide ligands (III and IV) are characteristically more similar to each other. While both complexes decompose in four steps, the first step indicates the removal of two ligand water and one SO$_2$ group each located in the coordination spheres. In complexes that become dehydrated, it is recommended to separate one SO$_2$ group as a secondary step. The third degradation step of both structures is interpreted as the step in which the acesulfame ligands are completely disintegrated and removed from the reaction environment, and the consistency of experimental and theoretical weight losses supports this claim (Table 3). The last degradation steps of the structures were attributed to the degradation of N,N-diethylnicotinamide ligands. The proposed final decomposition products of all complexes were thought to be oxides of the relevant metal cations, and the experimental and theoretical weight losses found also support the existence of metal oxides. It has been determined that the experimental weight losses of the final residue products are approximately 1% higher than the theoretical weight losses. The reason for this has been shown to be that during thermal decomposition in an inert nitrogen atmosphere, complete combustion does not occur due to the lack of sufficient oxygen in the environment, and some carbonized coal residue accumulates on the surface of

the metal oxides. The fact that metal oxides, which are expected to be white in color, are collected in black color is also evidence supporting our suggestion. Detailed degradation properties of all complexes are summarized in Table 3.
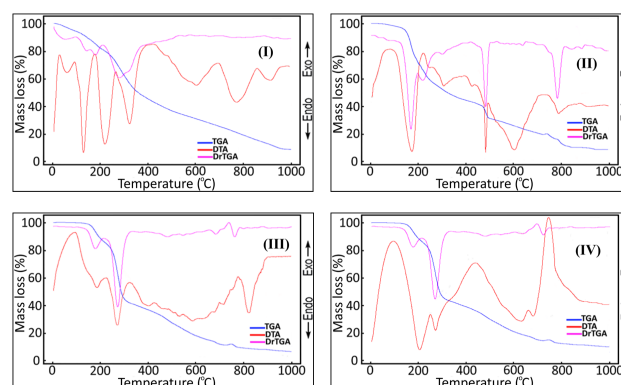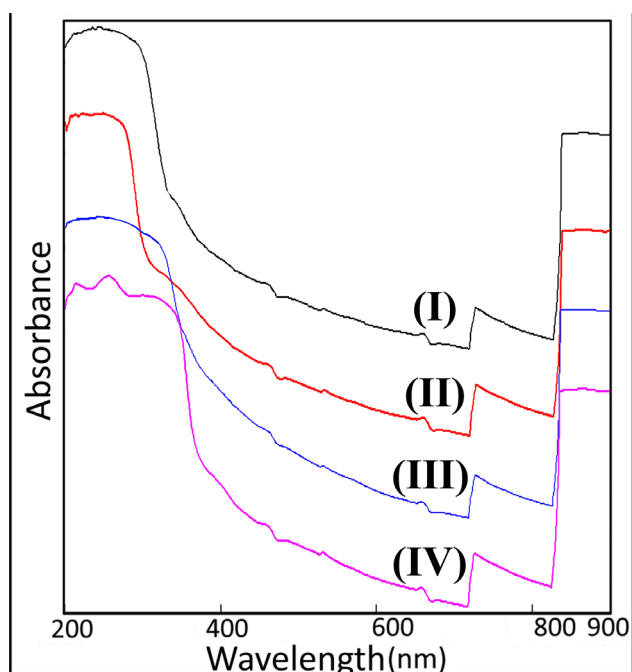

Figure 3. Thermal decomposition curves (TG/DTA) of Al^{3+} and In^{3+} mixed ligand complexes with acesulfama-nicotinamide and *N,N*-diethylnicotinamide.

Table 3. Thermal analysis data of Al^{3+} and In^{3+} mixed ligand complexes with acesulfama-nicotinamide and *N,N*-diethylnicotinamide.

Compounds		Temp. range (°C)	DTA$_{max}$ (°C)	Removing group	Mass Loss (%) Exp.	Mass Loss (%) Theo.	Remaining Product (%) Exp.	Remaining Product (%) Theo.	Decomp. Product	Colour
[Al(C$_6$H$_6$N$_2$O)$_2$(C$_4$H$_4$NO$_4$S)$_2$](C$_4$H$_4$NO$_4$S).2H$_2$O										white
C$_{24}$H$_{28}$AlN$_7$O$_{16}$S$_3$	1	48-101	79	2H$_2$O	4.80	4.54				
793,69 g/mol	2	102-193	147	2CH$_2$NO	10.97	11.09				
	3	194-288	235	2C$_5$H$_5$N	19.12	19.65				
	4	290-386	336	3SO$_2$	24.62	24.22				
	5	388-940	611;771;916	3C$_4$H$_4$NO;3/2O	33.77	34.18	5.79	6.43	1/2Al$_2$O$_3$	black
[In(C$_6$H$_6$N$_2$O)$_2$(C$_4$H$_4$NO$_4$S)$_2$](C$_4$H$_4$NO$_4$S).H$_2$O										pale-white
C$_{24}$H$_{26}$InN$_7$O$_{15}$S$_3$	1	68-140	130	H$_2$O	2.29	2.09				
863,51 g/mol	2	142-201	183	3SO$_2$	22.62	22.26				
	3	202-343	221; 295	2C$_6$H$_6$N$_2$O	28.24	28.29				
	4	344-481	430	3CO	9.86	9.73				
	5	482-512	491	C$_2$H$_3$	8.95	9.38				
	6	513-931	607;739;871	CHN;3/2O	11.77	12.27	15.12	16.08	1/2In2O3	black
[Al(C$_{10}$H$_{14}$N$_2$O)$_2$(C$_4$H$_4$NO$_4$S)$_2$(H$_2$O)$_2$](C$_4$H$_4$NO$_4$S)										white
C$_{32}$H$_{44}$AlN$_7$O$_{16}$S$_3$	1	103-198	190	2H$_2$O;SO$_2$	10.82	11.05				
905,90 g/mol	2	200-231	218	SO$_2$	6.52	7.07				
	3	232-306	285	3C$_4$H$_4$NO$_2$;SO$_2$	38.92	39.55				
	4	308-903	401;512;596;810	2C$_{10}$H$_{14}$N$_2$; 2C$_{10}$H$_{14}$N$_2$O$_{1/2}$	36.89	36.69	6.85	5.63	1/2Al$_2$O$_3$	black
[In(C$_{10}$H$_{14}$N$_2$O)$_2$(C$_4$H$_4$NO$_4$S)$_2$(H$_2$O)$_2$](C$_4$H$_4$NO$_4$S)										pale-white
C$_{32}$H$_{44}$InN$_7$O$_{16}$S$_3$	1	110-196	185	2H$_2$O;SO$_2$	9.81	10.07				
993,74 g/mol	2	198-241	214	SO$_2$	6.78	6.45				
	3	242-302	281	3C$_4$H$_4$NO$_2$;SO$_2$	37.05	36.06				
	4	305-897	-426;615;680;-731	C$_{10}$H$_{14}$N$_2$; C$_{10}$H$_{14}$N$_2$O$_{1/2}$	31.51	33.35	14.85	13.97	1/2In$_2$O$_3$	black

Ultraviolet-Visible Spectroscopy Studies

The UV-Vis spectra recorded in the 200-900 nm range of the structures of the mixed ligand complexes containing synthesized metal-acesulfame-nicotinamide / *N,N*-diethylnicotinamide are as follows. When the recorded solid-state UV-VIS spectroscopic curves of metal ions with group IIIA 3+ cationic charge valence were examined, no significant peak was observed in the 750-400 nm range, which corresponds to the band transition regions of the metals. Since the "*d*" orbitals of earth elements, which undergo splitting under UV light in the 3+ cationic oxidation state, do not undergo any splitting, the "*d-d*" transitions seen in transition metals are not observed. The most obvious result of this effect is the colors of the synthesized complexes, and the color of all complexes is either colorless or close to pale white. When the spectra of all metal complexes are examined, it is assumed that the high intensity but numerically evaluable peaks (M-L) occurring in the 300-200 nm region may belong to electron transitions from the metal to the ligands.


Figure 4. Solid State UV-Vis spectra of Al^{3+} and In^{3+} mixed ligand complexes with acesulfama-nicotinamide and *N,N*-diethylnicotinamide.

Mass Spectroscopy (GC-MS) Studies

When the thermal analysis curves of metal-acesulfame-nicotinamide and metal-acesulfame-N,N-diethylnicotinamide mixed ligand complexes are examined, it is seen that the degradation of the complexes is similar. Decomposition begins with deaquatation and continues with the formation of SO_2 by acesulfamate ligands. Similar results are seen when the mass spectra of these complexes are examined. There are also peaks resulting from the removal of nicotinamide and N,N-diethylnicotinamide ligands from mixed ligand complexes. Although multiphase distortions are generally observed in the mass spectra, the most prominent peaks in the spectra have been tried to be explained. The mass spectra of complexes I and II are given in Figures 5 and 6. Peaks whose m/z ratio corresponds to the removal of acesulfamate ions are seen at 161.22 and 161.02 m/z, respectively. The peaks corresponding
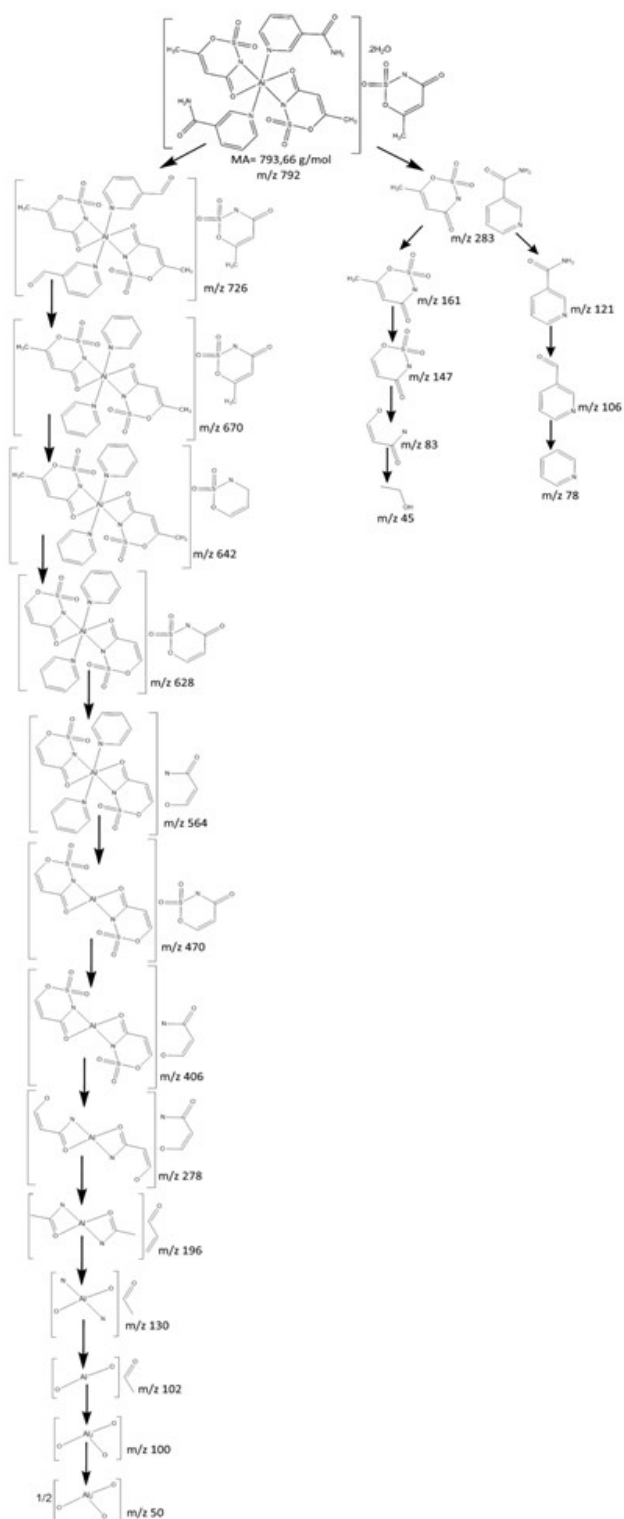
to the removal of nicotinamide ions were detected at m/z 121.01- 121.20, respectively. Formulations that can be attributed to possible degradation products of the breakdown of the complexes, taking into account the molecular ion peaks, are shown in Figures 7 and 8.
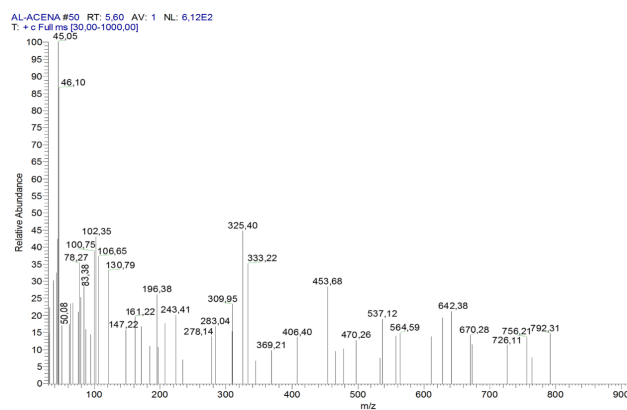
Figure 5. Mass spectrum pattern of complex I.
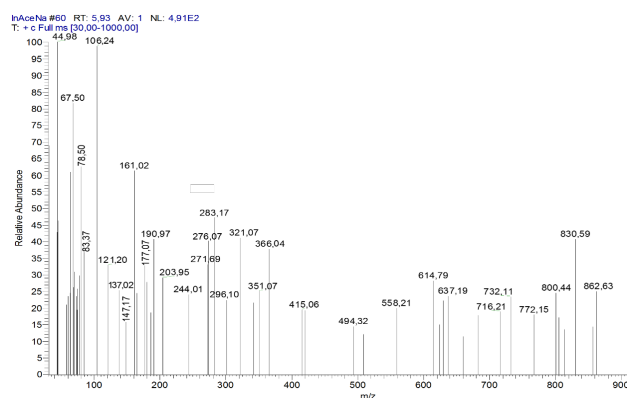
Figure 6. Mass spectrum pattern of complex II.

Figure 7. Possible molecular ion formulations and degradation schematics of the degradation products of complex I.

Figure 8. Possible molecular ion formulations and degradation schematics of the degradation products of complex II.

Figures 9 and 10 show the mass spectra of complexes III and IV, respectively. Peaks whose m/z ratio corresponds to the removal of acesulfamate ions are seen at 161.22 and 161.12 m/z, respectively. The peaks corresponding to the removal of N,N-diethylnicotinamide ions appeared at 177.24 and 177.17 m/z,

respectively. Formulations that can be attributed to possible degradation products of the breakdown of the complexes, taking into account the molecular ion peaks, are also shown in Figures 11 and 12.
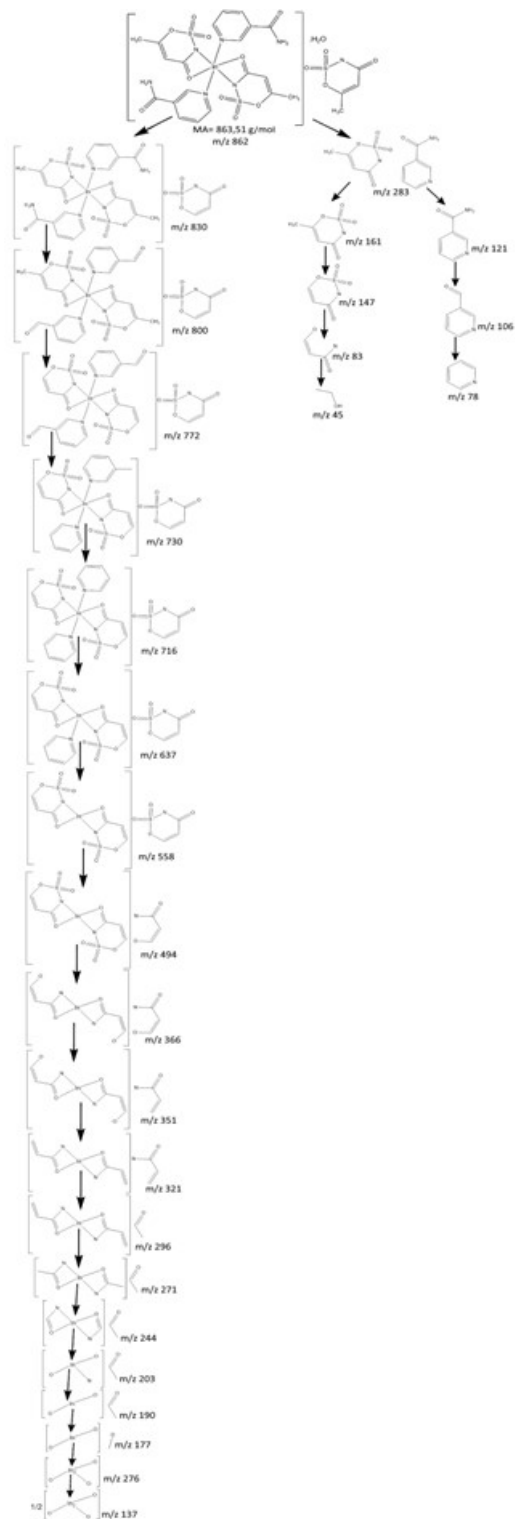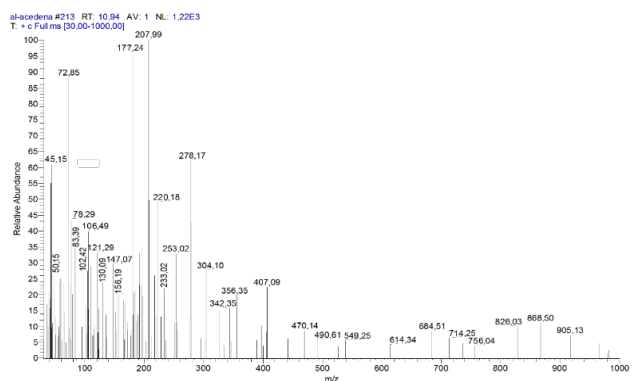

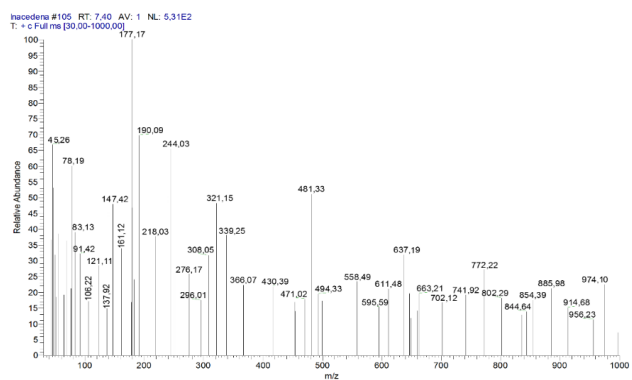**Figure 9.** Mass spectrum pattern of complex III.

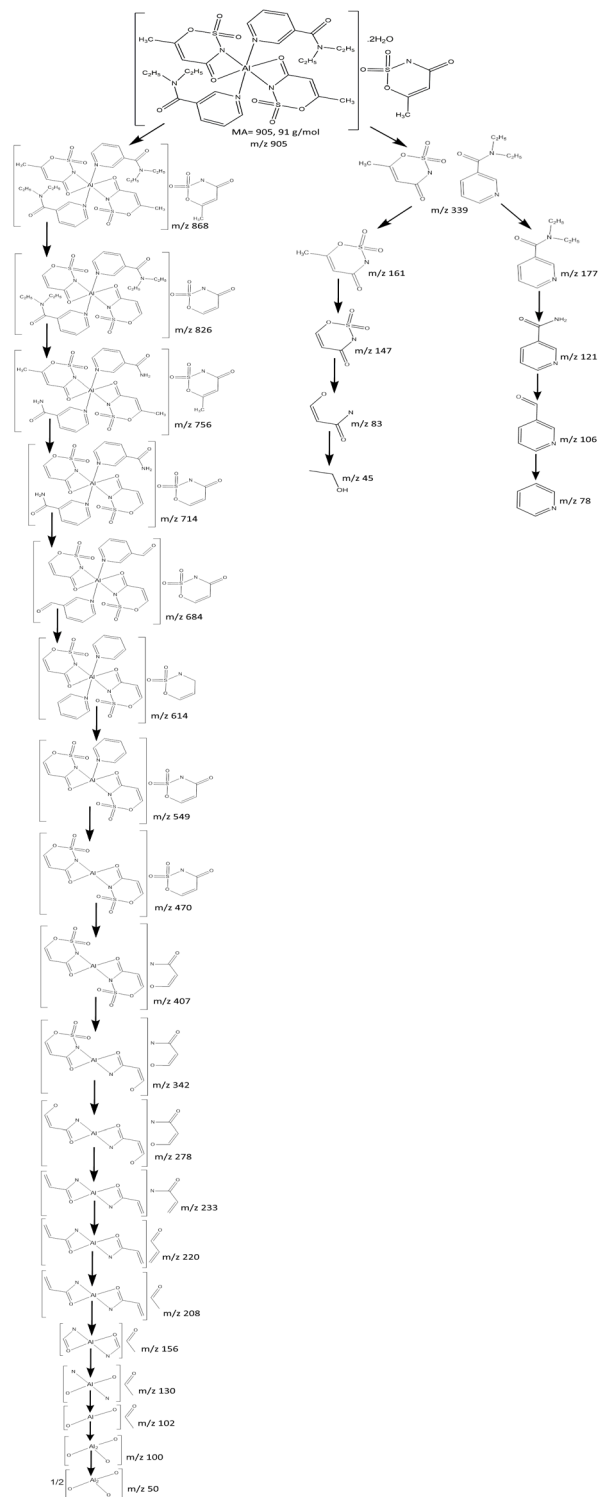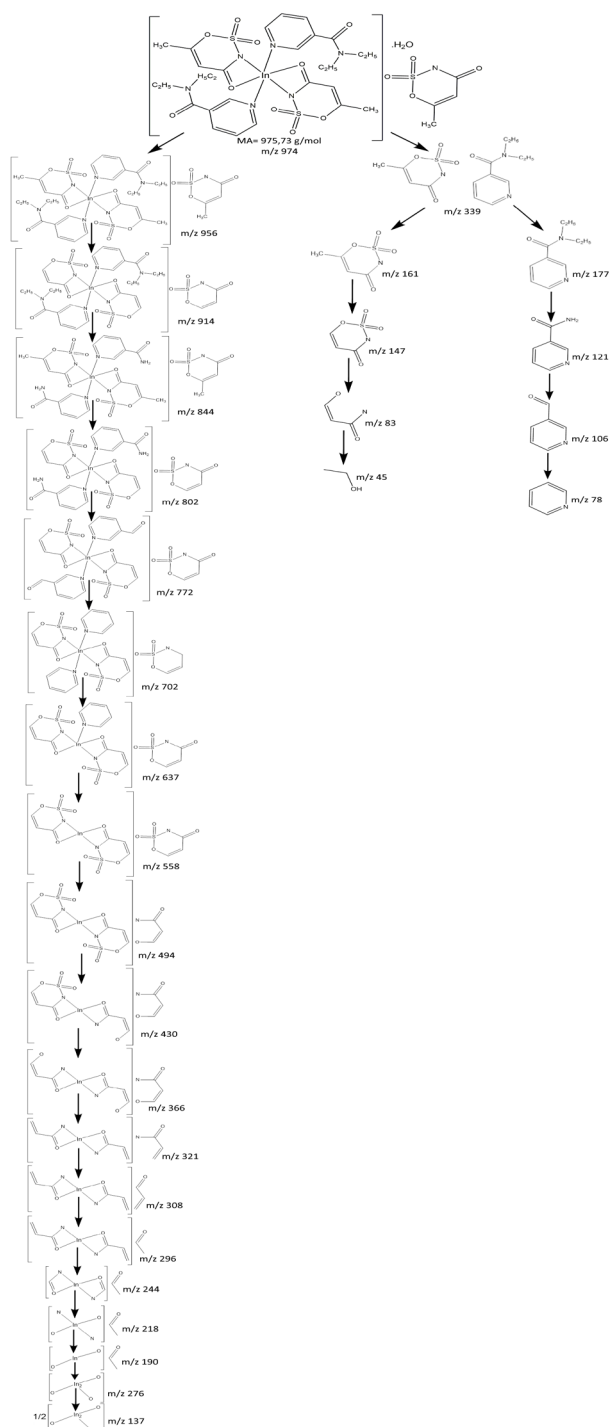**Figure 10.** Mass spectrum pattern of complex IV.

Figure 11. Possible molecular ion formulations and degradation patterns of the degradation products of the complex III.

Figure 12. Possible molecular ion formulations and degradation pattern of the degradation products of the complex IV.

the complexes, it was determined that the metal:ligand1:ligand2 ratios in mixed ligand complexes were 1:3:2. While hydrate waters are located outside the coordination sphere in complexes I and II, it has been suggested that there may be two ligand waters each inside the coordination sphere in structures III and IV. In all structures, it is predicted that two monoanionically acesulfame ligands are involved in coordination, while one of each is located outside the coordination sphere to ensure charge balance. For this reason, we can say that all complexes are cationic salt-like structures. It has been claimed that the coordination of metal cations is six and the geometries of the structures may also be decomposed octahedral. It was determined by infrared analysis that the neutral ligands nicotinamide and N,N-diethylnicotinamide molecules bind to the metal cation through the nitrogen atom of pyridine. While it has been suggested that acesulfame ligands provide monoanionic-bidentate coordination in complexes I and II, acesulfame ligand is in monoanionic-monodentate coordination in structures III and IV. Proposed explicit structural formulas for metal-acesulfame-nicotinamide and metal-acesulfame-N,N-diethylnicotinamide mixed ligand complexes are shown in Figure 13(a) and (b).
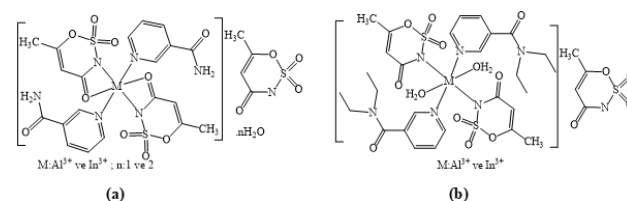
Figure 13. Molecular structure formulations of acesulfame-nicotinamide and *N,N*-diethylnicotinamide mixed ligand complexes of Al^{3+} and In^{3+} metal cations.

CONCLUSIONS

In this thesis, new complexes of group 3A Al^{3+} and In^{3+} metals with acesulfame-nicotinamide and acesulfame-N,N-diethylnicotinamide mixed ligands were synthesized for the first time. The structures of these synthesized complexes were elucidated by elemental analysis, infrared spectroscopy, thermogravimetric analysis, solid ultraviolet-visible region spectroscopy, mass analysis and melting point determination methods. According to the results of the elemental analysis of

REFERENCES

1. Yalamanchi S, Srinath R, Dobs A. Encyclopedia of Food and Health Acesulfame – K. Amsterdam: Elsevier Inc.; 2015.
2. Yıldırım T, Köse DA, Avcı GA, and et al. Novel Mixed Ligand Complexes of Acesulfame / N,N-diethylnicotinamide with Some Transition Metals. Synthesis and Crystal Structural Characterization, Journal of Coordination Chemistry 2019;72(22-24):3502-3517. doi:10.1080/00958972.2019.1705970
3. Clauss K, Jensen H. Oxathiazinone dioxides – A new group of sweetening agents. Angewandte Chemie International Edition in English 1973;12(11):869-942. doi:10.1002/anie.197308691
4. İçbudak H, Heren Z, Uyanık A, and et al. Prediction of the decomposition pathway of diaquabis(N,N′-dimethyl-1,2-ethanediamine) nickel(II) acesulfamate by thermal and mass spectroscopic data. Journal of Thermal Analysis and Calorimetry 2005;82(2):303-306. doi:10.1007/s10973-005-0894-0
5. Bulut A, İçbudak H, Sezer G, and et al. Bis(acesulfamato-κ^2N^3,O^4)bis(2-aminopyirimidine-κN^1)copper(II). Acta Crystallographica 2005;C61:228-230. doi:10.1107/S0108270105008188
6. İçbudak H, Adıyaman E, Çetin N, and et al. Synthesis, structural characterization and chromotropism of a Ni(II) and a Co(II) compound with acesulfamate as a ligand. Transition Metal Chemistry 2006;31:666-672. doi:10.1007/s11243-006-0045-x
7. Yurdakul Ö, Köse DA, Şahin O, and et al. Two novel mixed-ligand zinc-acesulfame compounds: Synthesis, spectroscopic and thermal characterization and biological applications. Journal of Molecular Structure 2020;1203:127265. doi:10.1016/j.molstruc.2019.127265
8. Yurdakul Ö, Köse DA, Şahin O, and et al. Novel Mn(II) and Co(II) mixed-ligand coordination compounds with acesulfame and 3-aminopyridine: Synthesis and structural properties. Journal of Coordination Chemistry (2021;74(7):1168-1180. doi:10.1080/00958972.2021.1888083
9. Çetin N. Synthesis, Structure, Spectroscopic, Thermal and Chromotropic Properties of Some Acesulfame-Transition Metal Complexes, Master's Thesis, Ondokuz Mayıs University, Institute of Science and Technology, Samsun, 2005.
10. Şahin ZS, Demir M, Yıldırım T, and et al. Novel Mixed Ligand Complexes of Co(II), Ni (II), Cu(II), and Zn(II) with 1,10-Phenanthroline and Acesulfame. Synthesis, Structural Analysis and Hydrogen Adsorption Study. International Journal of Hydrogen Energy 2021;46(54):27631-27642. doi:10.1016/j.ijhydene.2021.06.026
11. Yıldırım T, Köse DA, Avcı E, and et al. Novel mixed ligand complexes of acesulfame / nicotinamide with some transition metals. Synthesis, crystal structural characterization, and biological properties. Journal of Molecular Structure 2019;1176:576-582. doi:10.1016/j.molstruc.2018.08.099
12. Sahin O, İçbudak H, Buyukgungor O. Synthesis and Crystal Structure of Trans-bis (acesulfamato-O) tetraaquazinc (II). Chinese Journal of Structural Chemistry 2010;29(7):1047-1050.
13. Yurdakul Ö, Köse DA. Mixed Ligand Complexes of Acesulfame/Nicotinamide with Earth Alkaline Metal Cations MgII, CaII, BaII and SrII. Synthesis and Characterization. Hittite Journal of Science and Engineering 2014;1(1):51-57. doi:10.17350/HJSE19030000008
14. Yurdakul Ö, Demirtaş G, Dege N, and et al. Crystal Structure, Thermal Analysis, Spectroscopic Studies and DFT Calculations on Hexaaquamagnesium(II) Acesulfamate. Hacettepe Journal of Biology & Chemistry 2016;44(1):95-106.
15. Demirtaş G, Dege N, İçbudak H, and et al. Experimental and DFT Studies on Poly[di-μ3-acesulfamato-O,O:O′;O′:O,O-di-μ-acesulfamato-O,O; N-di-μ-aqua-dicalcium(II)] Complex, Journal of Inorganic and Organometallic Polymers and Materials 2012;22:671-679. doi:10.1007/s10904-012-9679-7
16. İçbudak H, Demirtaş G, Dege N. Experimental and theoretical (DFT) studies on poly[octa-μ3-acesulfamato-O,O:N,O′;O′,N:O,O-tetraaquatetrabarium(II)] and poly[octa-μ3-acesulfamato-O,O:N,O′;O′,N:O,O-tetraaquatetrastrontium(II)] complexes. Macedonian Journal of Chemistry and Chemical Engineering 2015;34(1):105-114.
17. Zeybel L, Köse DA. Acesulfame complex compounds of some lanthanide group metal cations. Synthesis and characterization, Journal of Molecular Structure 2021;1226:129399. doi:10.1016/j.molstruc.2020.129399
18. Zeybel L, Köse DA. Novel mixed ligand coordination compounds of some rare metal cations containing acesulfame/N,N-diethylnicotinamide. Journal of Turkish Chemistry 2021;45:1004-1015. doi:10.3906/kim-2012-47
19. Zeybel L, Köse DA. Novel mixed ligand complexes of rare earth metal cations containing acesulfame / nicotinamide. Synthesis and structural characterizations. Journal of Molecular Structure 2023;1290:135979. doi:10.1016/j.molstruc.2023.135979
20. Edebalı S. Synthesis and Properties of Nicotinamide, Isonicotinamide and N,N-Diethylnicotinamide Complexes of Zinc p-Fluoro and p-Bromobenzoates, Master's Thesis, Kafkas University, Institute of Science and Technology, Kars 2007.
21. Köse DA. Synthesis and Structure Investigation of Nicotinamide and Diethylnicotinamide Complexes of Copper(II), Nickel(II), Cobalt(II) and Zinc(II) Acetylsalicylates, Master's Thesis, Kafkas University, Institute of Science and Technology, Kars 1999.
22. Icbudak H, Heren Z, Köse DA, and et al. Bis(Nicotinamide) and Bis(N,N-Diethyl Nicotinamide) P-Hydroxybenzoate Complexes of Ni(II), Cu(II) and Zn(II)– Spectrothermal Studies. Journal of Thermal Analysis and Calorimetry 2004;76(3):837-851.
23. Öztürkkan EF, Köse DA, Necefoglu H, and et al. Synthesis and Characterization of bis(N,N-Diethylnicotinamide) p-Halogenobenzoate Complexes of Co(II). Asian Journal of Chemistry 2007;19(6):4880-4888.
24. Köse DA, Kaya A, Necefoğlu H. Synthesis and Characterization of bis(N,N-Diethylnicotinamide) m-Hydroxybenzoate Complexes of Co(II), Ni(II), Cu(II) and Zn(II). Russian Journal of Coordination Chemistry (2007;33(6):422-427. doi:10.1134/S1070328407060073
25. Köse DA, Necefoğlu H, Icbudak H. Synthesis and Characterization of N,N-Diethylnicotinamide-Acetylsalicylato Complexes of Co(II), Ni(II), Cu(II), and Zn(II). Journal of Coordination Chemistry 2008;61(21):3508-3515. doi:10.1080/00958970802074555
26. Köse DA, Gökçe G, Gökçe S, Uzun İ. Bis(N,N-Diethyl nicotinamide)p-Chlorobenzoate Complexes of Ni(II), Zn(II) and Cd(II), Synthesis and Characterization. Journal of Thermal Analysis and Calorimetry 2009;95:247-251. doi:10.1007/s10973-008-9150-8

Toxicity Assessments of Carbon-Based Nanomaterials: A mini review

Selma NACAK (iD)

Department of Chemistry, Hitit University, 19030, Corum, Türkiye.

Corresponding Author
Selma NACAK
E-mail: selmanacak@hitit.edu.tr Phone: +90 364 227 7000
RORID: ror.org/01x8m3269

Cite As
Nacak S. Toxicity Assessments of Carbon-Based Nanomaterials: A mini review. Hitit journal of Science. 2024;1(1):39-43

Peer Review: Evaluated by independent reviewers working in at least two different institutions appointed by the field editor.
Ethical Statement: Not available.
Plagiarism Checks: Yes - iThenticate
Conflict of Interest: The author declares no competing financial interest.

CRedit Author Statement
Selma Nacak, declare that I am the sole author of this review article titled "Toxicity Assessments of Carbon-Based Nanomaterials: A mini review." I confirm that I have contributed to all aspects of the manuscript, including the conceptualization, data collection, analysis, and writing of the article. Additionally, I assure that this manuscript is an original work and has not been previously published, nor is it under consideration for publication elsewhere.

Toxicity Assessments of Carbon-Based Nanomaterials: A mini review

Selma NACAK [iD]

Department of Chemistry, Hitit University, 19030, Corum, Türkiye.

Abstract

Carbon-based nanomaterials (CNMs) are materials with exceptional properties that play an important role in the development of new technologies. Their widespread use, however, has raised concerns about their possible harmful effects on the environment and human health. Safe use of CNMs can be possible by performing toxicity tests and determining an attitude based on the test results. To date, researchers have conducted toxicology tests with carbon-based nanomaterials such as carbon nanotubes, fullerene, graphene, carbon dot and nanodiamond. According to the results of the researches, it has been revealed that these materials can cause toxic effects such as DNA damage, inflammation, protein stress and oxidative stress, depending on factors such as concentration, surface charge and material size. There are different types of toxicity tests currently used. However, a uniform international protocol is still a requirement. This study will present various research on the toxic effects of CNMs and provide an overarching perspective.

Keywords: Carbon-based nanomaterial, Toxicity, Biomedical

INTRODUCTION

In recent years, research on carbon-based nanomaterials has been increasing exponentially. These nanomaterials offer a wide range of application due to their large surface areas, exceptional optical properties, high electrical and thermal conductivities, and outstanding mechanical properties. These properties enable the successful use of carbon-based nanomaterials in solar energy systems, flexible electronics production, molecular recognition applications, as well as in areas such as bio-imaging, biosensing, super-resolution imaging and nanoscale temperature sensing.(1)

Carbon, with an atomic number of six, has an average atomic mass of 12 amu (2). As one of the most abundant elements on Earth, carbon is a key component in many macromolecules vital for life, including sugars, proteins, and DNA (3). Pure carbon exists in several forms, such as allotropes including diamonds and graphite, which come from variations in the arrangement of carbon atoms (2)(3). Amorphous allotropes of carbon include coal, lampblack, and charcoal (3)(4). CNMs encompass a variety of carbon forms as shown in Figure 1. These include sp^2 carbon nanomaterials (like graphene, carbon nanotubes, fullerene), amorphous carbon nanoparticles (like carbon dots, ultrafine carbon particles and carbon nanoparticles), and nanodiamonds (3).
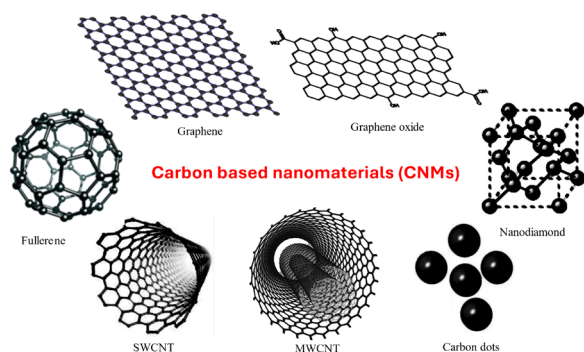
Figure 1. Structures of various types of carbon-based nanomaterials.

Carbon nanotubes (CNTs) possess cylindrical tubular structures with a nanometer diameter, formed by rolling graphene sheets (5). These are classified into two basic types. One of them is single-walled carbon nanotubes (SWCNTs) and the other is multi-walled carbon nanotubes (MWCNTs).

SWCNTs are formed from a single layer of a graphene sheet, whereas MWCNTs comprise several concentric layers of graphene (6).

Fullerene is named after architect Buckminster Fuller, who in the 1960s constructed a cagelike lightweight dome made of carbon atoms. These molecules consist only of carbon atoms arranged in various shapes like hollow, tube, sphere, or ellipsoid, in which carbon atoms interconnect in pentagonal and hexagonal rings (2).

Graphene, the main structure of graphite, is one of the most researched CNMs (7)(8)(9). This material consists of two-dimensional, single, or few sheets of sp^2 arranged carbon atoms (7). Graphene serves as the structural precursor to various carbon allotropes including carbon nanorings, carbon nanotubes, carbon fibers, graphite, and graphyne (8)(9).

Carbon dots (CDs) are carbon nanoparticles, which are found in spherical-like shape and in a size less than 10 nm. CDs show tunable and efficient photoluminescence properties. Furthermore, they are cost-effective and environmentally-friendly type of nanomaterials (10).

Diamond is a metastable allotrope of carbon with an unstable face-centered cubic crystal structure. It is known for its exceptional hardness and thermal conductivity. Nanodiamonds (ND) were first made in 1963 by detonating an oxygen-deficient trinitrotoluene and hexogen composition. They consist of a diamond core covered an amorphous carbon shell. The average size of NDs is 4-5 nm, which allows for their existence in colloidal suspensions (2)(11)(12).

BIOMEDICAL APPLICATION OF CARBON-BASED NANOMATERIALS

Biosensors identify disease biomarkers, enabling diagnosis and monitoring. Biomarkers are key molecules like proteins, hormones, glucose, and others, found in body (3). CNMs are widely employed in biosensing due to their conductivity, catalytic activity, and biocompatibility. Various carbon-based nanomaterials, including CNTs, graphene oxide (GO), and fullerene, are utilized for optical and electrochemical biosensor development (13).

The rising prevalence of cancer worldwide imposes significant

emotional, physical and financial burdens on individuals and families. Therefore, it's crucial to develop new technologies that effectively treat cancer (14). Barahuie et. al. synthesized GO to investigate its potential use as a nanocarrier for chlorogenic acid (CA) known as one of the active anticancer agents. The study confirmed the successful conjugation of CA onto GO through π–π interaction and hydrogen bonding. The CA loading in the nanohybrid was around 13.1%. The release profiles exhibited favorable, sustained, and pH-dependent release of CA from the CA-GO nanocomposite. This aligned well with the pseudo-second order kinetic model. Additionally, the designed anticancer nanohybrid proved to be thermally more stable than its counterpart (15). Recent research has highlighted the potential of quasi-freestanding bilayer epitaxial graphene for detecting SARS-CoV-2 in body fluids or exhaled breath, offering rapid, cost-effective, and efficient alternatives to conventional detection methods (16). Gene therapy holds significant promise as a therapeutic approach for treating a wide range of diseases. Wu et. al. have synthesized a new multifunctional theranostic folate conjugated-reducible polyethyleneimine-carbon nanodots/small interference RNA (fc-rPEI-Cdots/siRNA) nanoagent. The fc-rPEI-Cdots act as a siRNA carrier, releasing siRNA in a reducing environment, with enhanced accumulation in lung cancer cells. Viability of H460 treated with the fc-rPEI-Cdots/ pooled siRNA complex for three days is reduced to nearly 30%. Furthermore, clear inhibition of cyclin B1 and epidermal growth factor receptor (EGPR) expression was determined. Hence, this novel nanoagent has potential for targeted lung cancer treatment (17). Monitoring cholesterol levels is clinically significant, and both enzymatic and nonenzymatic methods are employed for this purpose. Multiwalled carbon nanoparticle electrodes in a metal-carbon-polymer nanocomposite functionalized with cholesterol oxidase enzymes were utilized as an enzymatic method with good selectivity, sensitivity and reproducibility (18). Glucose monitoring is integral in diabetes diagnosis and management. CNMs, including nanotubes, graphene, and graphene dots, modified with glucose oxidase exhibit high sensitivity and selectivity in glucose detection. These nanosensors have been evaluated for interference from substances like acetaminophen, uric acid, and ascorbic acid (19).

TOXICITY ASSESSMENTS
CNMs have gained significant importance in various fields, including biomedicine, due to their unique properties such as high conductivity, structural diversity, and ease of functionalization. However, the increasing use of CNMs has also raised concerns about their potential toxicity and impact on human health and the environment. The toxicity assessment of CNMs is crucial for their safe application in biomedicine. Key findings from toxicity studies suggest that the toxicity of CNMs depends on their physicochemical properties like size, shape, surface area, and metal impurities (20)(21). The most common methods used to assess the toxicity of carbon-based nanomaterials in biomedicine include in-vitro cell culture assays, physicochemical characterization, flow cytometry, comprehensive toxicological studies (20) (21)(22) (23) (24).

Garriga et. al. studied the in-vitro toxicity of carbon nanotubes (CNT), graphene oxide (GO), carbon nanoplatelets (CNP),

carbon nanohorns (CNH), nanodiamonds (ND) and reduced graphene oxide (RGO) on human breast adenocarcinoma (MCF-7) cells and human epithelial colorectal adenocarcinoma (Caco-2) cells, after 24 h and 72 h incubation. After the CNMs treatment, the cell viability shown by toxicity assessments is in the order: CNP < CNH < RGO < CNT < GO < ND. The fast-dividing Caco-2 cells were more effected from the CNMs treatment. The lowest toxicity was exhibited by ND and GO because of the functional groups with oxygen on the surface of nanomaterials. Researchers of the study emphasized that the long-term toxicity assessments remain an important requirement (23).

When MWCNTs are inhaled, alveolar macrophages and pulmonary alveolar epithelium are activated. This may result in a pro-inflammatory response or even chronic pathology. Sweeney et. al investigated the bioreactivity of MWCNT length by utilizing primary human alveolar type-II epithelial cells (ATII) and alveolar macrophages (AMs) as well as a human alveolar type-I-like epithelial cell line (TT1) to find the role that the length of MWCNTs plays in pulmonary toxicity. Bioreactivity caused by MWCNTs of different lengths (MWCNT 0.6 μm, MWCNT-3 μm and MWCNT-20 μm) resulted in negative effects. TT1 and ATII epithelial cells exhibited higher reactivity when exposed to shorter MWCNTs. This phenomenon was observed even at very low concentrations. Long MWCNTs exhibited high reactivity with alveolar macrophages. It also caused a high rate of cell death. For this reason, it has been reported that inhalation of MWCNTs will cause serious health problems (25).

Montes-Fonseca et. al studied the cytotoxicity of functionalized carbon nanotubes dependent on the functionalization grade. They functionalized CNTs with different concentration of 46 kDa surface protein, P46, (6 mg/L, 0.6 mg/L, 0,006 mg/L). Then they investigated toxic effect CNTs with various functionalization grade on J774A macrophages. The study revealed that CNTs functionalized with high concentration of P46 were more toxic to J774 macrophages than CNTs functionalized with low concentration of P46 (26).

Hiraku et al exposed RAW 264.7 macrophages and A549 lung epithelial cells to carbon black (CB) with primary diameters of 56 nm (CB56) and 95 nm (CB95). They comparatively investigated whether these nanomaterials could form 8-nitroguanine on DNA. Both nanomaterials induced the formation of 8-nitroG in the nucleus of the cells examined. Flow cytometry showed that CBs with a diameter of 95 nm generated higher amounts of reactive oxygen species in RAW 264.7 cells and caused more 8-nitroguanine formation than CBs with a diameter of 56 nm. As a result of the research, it was revealed that DNA damage may occur in lung epithelial cells exposed to CBs and that these CNMs may contribute to carcinogenesis (27).

Jiang at. al. revealed in their article published in 2020 the results of the study on the toxic effects of 6 SWCNT samples with different lengths, functional groups and electronic structures. Quantitative toxicogenomic assay endpoint protein expression level index (PELI) examination revealed that short SWCNTs (0.5–2 μm) caused a higher toxicity and

oxiditive stress than long SWCNT (5–30 µm). Carboxylated SWCNTs caused higher genotoxicity, protein damage, chemical stress, and overall toxicity than hydroxylated SWCNTs. While semiconductor SWCNTs exhibited almost no toxicity, metallic SWCNTs showed more toxic behavior. In conclusion, these materials exhibited molecular toxicity dependent on their physicochemical properties (28).

Adamson et. al. investigated cellular uptake, cell viability, mitochondrial membrane potential, and macrophage responses in graphene nanoplates-exposed mice. Different exposure times (1, 3 and 6 hours) and different graphene nanoplate (GNP) concentrations (0, 25, 50 or 100 µg/ml) were used in the study. They also evaluated the effect of CD36 on responses to GNPs. This study revealed that GNPs increased mitochondrial potential and were easily internalized by macrophages. However, by blocking CD36 using an antibody, internalization of GNPs by macrophages was reduced. The study revealed that exposure time and GNP concentration affected macrophage responses in different ways. Additionally, data explaining the metabolic pathways disrupted due to exposure and the role of CD36 in GNP-macrophage interaction were obtained (29).

CONCLUSION
Carbon-based nanomaterials and their hybrid nanocomposites exhibit excellent properties, making them useful across various fields. New products containing carbon-based nanomaterials emerge every year. Therefore, the society is increasingly interested in their reliability. Scientists use various in vivo and in vitro methods to investigate the toxic effects of carbon-based nanomaterials and try to reveal their toxic effects related to their various properties. However, these studies lack of a standard methodology which leads to confusion the scientific community. Toxicity tests developed in accordance with internationally accepted proficiency standards should be used as soon as possible. These tests should consider factors like the physicochemical properties of the CNMs, environmental interferences, nano-bio interactions, and the type and concentration of the solution for easy evaluation.

ACKNOWLEDGEMENT

REFERENCES
1. Maria Diez-Pascual A. Carbon-Based Nanomaterials. Int J Mol Sci. 2021;22(7726).
2. Mostafavi E, Zare H. Carbon-based nanomaterials in gene therapy. OpenNano [Internet]. 2022;7(June):100062. Available from: https://doi.org/10.1016/j.onano.2022.100062
3. Holmannova D, Borsky P, Svadlakova T, Borska L, Fiala Z. Carbon Nanoparticles and Their Biomedical Applications. Appl Sci. 2022;12(15):1–21.
4. Sharma M. Understanding the mechanism of toxicity of carbon nanoparticles in humans in the new millennium: A systemic review. Indian J Occup Environ Med. 2010;14(1):3–5.
5. Ali E, Hadis D, Hamzeh K, Mohammad K, Nosratollah Z, Abolfazl A, et al. Carbon nanotubes: properties, synthesis, purification, and medical applications. Nanoscale Res Lett. 2014;9(1):393.
6. Karimi M, Solati N, Amiri M, Mirshekari H, Mohamed E, Taheri M, et al. Carbon nanotubes part I: Preparation of a novel and versatile drug-delivery vehicle. Expert Opin Drug Deliv. 2015;12(7):1071–87.
7. Imani R, Mohabatpour F, Mostafavi F. Graphene-based Nano-Carrier modifications for gene delivery applications. Carbon N Y [Internet]. 2018;140:569–91. Available from: https://doi.org/10.1016/j.carbon.2018.09.019
8. Tiwari SK, Kumar V, Huczko A, Oraon R, Adhikari A De, Nayak GC. Magical Allotropes of Carbon: Prospects and Applications. Crit Rev Solid State Mater Sci [Internet]. 2016;41(4):257–317. Available from: http://dx.doi.org/10.1080/10408436.2015.1127206
9. Lu H, Li SD. Two-dimensional carbon allotropes from graphene to graphyne. J Mater Chem C. 2013;1(23):3677–80.
10. De Medeiros T V., Manioudakis J, Noun F, Macairan JR, Victoria F, Naccache R. Microwave-assisted synthesis of carbon dots and their applications. J Mater Chem C. 2019;7(24):7175–95.
11. Zhang Y, Rhee KY, Hui D, Park SJ. A critical review of nanodiamond based nanocomposites: Synthesis, properties and applications [Internet]. Vol. 143, Composites Part B: Engineering. Elsevier Ltd; 2018. 19–27 p. Available from: https://doi.org/10.1016/j.compositesb.2018.01.028
12. Rehman A, Houshyar S, Wang X. Nanodiamond in composite: Biomedical application. J Biomed Mater Res - Part A. 2020;108(4):906–22.
13. Purohit B, Vernekar PR, Shetti NP, Chandra P. Biosensor nanoengineering: Design, operation, and implementation for biomolecular analysis. Sensors Int [Internet]. 2020;1(July):100040. Available from: https://doi.org/10.1016/j.sintl.2020.100040
14. Sharma G. Biogenic carbon nanostructured materials for detection of cancer and medical applications: A mini review. Hybrid Adv [Internet]. 2024;5(February):100166. Available from: https://doi.org/10.1016/j.hybadv.2024.100166
15. Barahuie F, Saifullah B, Dorniani D, Fakurazi S, Karthivashan G, Hussein MZ, et al. Graphene oxide as a nanocarrier for controlled release and targeted delivery of an anticancer active agent, chlorogenic acid. Mater Sci Eng C [Internet]. 2017;74:177–85. Available from: http://dx.doi.org/10.1016/j.msec.2016.11.114
16. Kim S, Ryu H, Tai S, Pedowitz M, Rzasa JR, Pennachio DJ, et al. Real-time ultra-sensitive detection of SARS-CoV-2 by quasi-freestanding epitaxial graphene-based biosensor. Biosens Bioelectron [Internet]. 2022;197(November 2021):113803. Available from: https://doi.org/10.1016/j.bios.2021.113803
17. Wu YF, Wu HC, Kuan CH, Lin CJ, Wang LW, Chang CW, et al. Multi-functionalized carbon dots as theranostic nanoagent for gene delivery in lung cancer therapy. Sci Rep [Internet]. 2016;6(October 2015):1–12. Available from: http://dx.doi.org/10.1038/srep21170
18. Alagappan M, Immanuel S, Sivasubramanian R, Kandaswamy A. Development of cholesterol biosensor using Au nanoparticles decorated f-MWCNT covered with polypyrrole network. Arab J Chem [Internet]. 2020;13(1):2001–10. Available from: https://doi.org/10.1016/j.arabjc.2018.02.018

19. Lin Y, Lu F, Tu Y, Ren Z. Glucose Biosensors Based on Carbon Nanotube Nanoelectrode Ensembles. Nano Lett. 2004;4(2):191–5.

20. Malina T, Poláková K, Hirsch C, Svoboda L, Zbořil R. Toxicity of carbon nanomaterials—towards reliable viability assessment via new approach in flow cytometry. Int J Mol Sci. 2021;22(14).

21. Yuan X, Zhang X, Sun L, Wei Y, Wei X. Cellular Toxicity and Immunological Effects of Carbon-based Nanomaterials. Part Fibre Toxicol. 2019;16(1).

22. Jiang T, Lin Y, Amadei CA, Gou N, Rahman SM, Lan J, et al. Comparative and mechanistic toxicity assessment of structure-dependent toxicity of carbon-based nanomaterials. J Hazard Mater [Internet]. 2021;418(March):126282. Available from: https://doi.org/10.1016/j.jhazmat.2021.126282

23. Garriga R, Herrero-Continente T, Palos M, Cebolla VL, Osada J, Muñoz E, et al. Toxicity of carbon nanomaterials and their potential application as drug delivery systems: In vitro studies in caco-2 and mcf-7 cell lines. Nanomaterials. 2020;10(8):1–21.

24. Côa F, Bortolozzo L de S, Ávila DS, Souza Filho AG, Martinez DST. Toxicology of carbon nanomaterials in the Caenorhabditis elegans model: current status, characterization, and perspectives for testing harmonization. Front Carbon. 2023;2(September):1–13.

25. Sweeney S, Berhanu D, Misra SK, Thorley AJ, Valsami-Jones E, Tetley TD. Multi-walled carbon nanotube length as a critical determinant of bioreactivity with primary human pulmonary alveolar cells. Carbon N Y [Internet]. 2014;78:26–37. Available from: http://dx.doi.org/10.1016/j.carbon.2014.06.033

26. Montes-Fonseca SL, Sánchez-Ramírez B, Luna-Velasco A, Arzate-Quintana C, Silva-Cazares MB, González Horta C, et al. Cytotoxicity of protein-carbon nanotubes on J774 macrophages is a functionalization grade-dependent effect. Biomed Res Int. 2015;2015.

27. Hiraku Y, Nishikawa Y, Ma N, Afroz T, Mizobuchi K, Ishiyama R, et al. Nitrative DNA damage induced by carbon-black nanoparticles in macrophages and lung epithelial cells. Mutat Res - Genet Toxicol Environ Mutagen [Internet]. 2017;818(March):7–16. Available from: http://dx.doi.org/10.1016/j.mrgentox.2017.04.002

28. Jiang T, Amadei CA, Gou N, Lin Y, Lan J, Vecitis CD, et al. Toxicity of single-walled carbon nanotubes (SWCNTs): effect of lengths, functional groups and electronic structures revealed by a quantitative toxicogenomics assay. Environ Sci Nano. 2020;7(5):1348–64.

29. Adamson SXF, Wang R, Wu W, Cooper B, Shannahan J. Metabolomic insights of macrophage responses to graphene nanoplatelets: Role of scavenger receptor CD36. PLoS One. 2018;13(11):1–30.